2016

Energy Resources Use Metrics

Rahul Y. Nehete
University of Kentucky, rahulynehete@gmail.com
Digital Object Identifier: http://dx.doi.org/10.13023/ETD.2016.025

STUDENT AGREEMENT:

I represent that my thesis or dissertation and abstract are my original work. Proper attribution has been given to all outside sources. I understand that I am solely responsible for obtaining any needed copyright permissions. I have obtained needed written permission statement(s) from the owner(s) of each third-party copyrighted matter to be included in my work, allowing electronic distribution (if such use is not permitted by the fair use doctrine) which will be submitted to UKnowledge as Additional File.

I hereby grant to The University of Kentucky and its agents the irrevocable, non-exclusive, and royalty-free license to archive and make accessible my work in whole or in part in all forms of media, now or hereafter known. I agree that the document mentioned above may be made available immediately for worldwide access unless an embargo applies.

I retain all other ownership rights to the copyright of my work. I also retain the right to use in future works (such as articles or books) all or part of my work. I understand that I am free to register the copyright to my work.

REVIEW, APPROVAL AND ACCEPTANCE

The document mentioned above has been reviewed and accepted by the student's advisor, on behalf of the advisory committee, and by the Director of Graduate Studies (DGS), on behalf of the program; we verify that this is the final, approved version of the student's thesis including all changes required by the advisory committee. The undersigned agree to abide by the statements above.

Rahul Y. Nehete, Student

Dr. Dusan P. Sekulic, Major Professor

Dr. Haluk Karaca, Director of Graduate Studies

ENERGY RESOURCES USE METRICS

THESIS

A thesis submitted in partial fulfillment of the
requirements for the degree of Master of Science in
Mechanical Engineering in the College of Engineering
at the University of Kentucky

By

Rahul Nehete

Lexington, Kentucky

Director: Dr. Dusan P. Sekulic, Professor of Mechanical Engineering

Lexington, Kentucky

2016

ABSTRACT OF THESIS

ENERGY RESOURCES USE METRICS

Energy resources use has been considered as a key component of sustainable development. Data related to global, regional, state, sector, industry and process demonstrate that a significant reduction of energy resources for a given production rate in manufacturing processes requires an introduction of transformational technologies at the process level, propagating the impact to higher scales, leading not just to a gradual improvement of traditional technologies but to more sustainable development.

The study offers two approaches to the formulation of the limits of energy use in the context of sustainable development. The first is to construct a map of key selected sustainable development metrics that would include energy use, economic and social aspects of the individual economy. The second view offers a close-up insight into an energy use at a process level, at the technical domain where actual energy transformations take place. Case study for a Controlled atmosphere brazing process is provided to investigate the gap between the theoretical minimum and actual energy used for the process. It has been demonstrated that the energy use, associated with a manufactured product is number of orders of magnitude smaller than the actual energy resources use for the actual process under consideration.

KEYWORDS: Controlled Atmospheric Brazing, Sustainable Manufacturing, Thermodynamics Metrics, Energy Resource use, Material Processing.

Rahul Nehete

February 4th, 2016

ENERGY RESOURCES USE METRICS

By

Rahul Nehete

Dr. Dusan P. Sekulic

(Director of Thesis)

Dr. Haluk Karaca

(Director of Graduate Studies)

Date: February 4th 2016

This work is dedicated to my parents Yashwant and Lalita Nehete. I appreciate all of the sacrifices you have made so that I could succeed.

ACKNOWLEDGEMENTS

First and foremost, I would like to thank my thesis director and academic advisor, Dr. Dusan P. Sekulic for providing me the opportunity and mentoring throughout my course of study. I have been motivated by his encouragement and I am thankful that he was a major influence in my graduate studies. This research work has been supported in part through the US NSF CBET Grant # 1235759. I would like to acknowledge the Research Assistantship from University of Kentucky.

I would like to extend my regards to Dr. Lawrence Holloway and Dr. Kozo Saito for agreeing to be on my advisory committee. I acknowledge the assistance of late Mr. Charles Arvin for his help with the experimentation setup. I would also like to extend my gratitude to my colleagues in Dr. Sekulic' s research team, Mr. Cheng-Nien Yu, Mr. Jonathan Gasser and Mr. Hai Fu for their support with the experimentation and their valuable suggestions.

Above all, I would like to thank my parents Mr. Yashwant Nehete and Mrs. Lalita Nehete, and my sisters Anjali Nehete and Anuja Nehete and my wife Vinita Nehete for their unconditional support. I am ever indebted for their motivation and encouragement, which made every hurdle surmountable and every task achievable. I dedicate each and every achievement to them and consider myself to be blessed to have such a family.

TABLE OF CONTENTS

LIST OF TABLES

LIST OF FIGURES

Chapter 1: INTRODUCTION

1.1 Background and Motivation

Energy resources became an economically important commodity shortly after invention of steam engine and the beginning of industrialization. Prior to that, slavery was one of the main fuels in the society. Since slavery was abolished, energy resources have replaced it to power the economic growth. The article by Cobb K.[1] provides an insight into a unique distinction between slaves of 18th century and energy resources today powering the economy. It is interesting to note that it would take an equivalent of 100 slaves to supply the energy used by each American at the present time. [2]

Importance of Energy resources management within the sustainability realm has been a hot topic of discussion. However, sustainability remains a mysterious field of knowledge, especially as it relates to underlined energy systems. Definitions of sustainability and sustainable development are still vague and do not offer a universally accepted means of measurement [3]. Especially in the realm of Energy resource utilization and energy efficiency, which are two of the central aspects in environmental and economic debates, there is a lack of widely accepted, all encompassing “metrics” for associated measurements.

There are many institutional advocates of the promotion of sustainability metrics, which include prominent groups such as

- United Nations Conference on Sustainable Development (UNCSD)
- Global Footprint Network - Ecological Footprint[4]
- United Nations Development Programme – Human Development Index (HDI)[5]

- Yale University Environmental Performance Index (EPI)[6]

Some of these metrics, HDI for example, are more or less sophisticated but comprehensive indicators by themselves. However these current metrics generally focus on particular aspects of sustainability and fail to present a complete transdisciplinary picture. There is a need for evaluating the relationship between these metrics so that sustainable development can be assessed considering all the main aspects; environmental, economic, societal, resource use etc.

Current studies on sustainable development either focus on large scale macro levels (Global / National) or at small scales (Process levels). The multiple order of magnitude of the difference between these two scales warrants a need to assess the impact of process level inefficiencies or improvements on the large global scales. That is, to evaluate the impact of technological interventions executed at the small scale on the large (e.g., global) scale[7]. Additionally, there is a need for a consistent metric which can be used to describe the efficiency of a manufacturing process for the perspective of energy resource utilization.

The goals that the present study encompasses are as follows:

- Offer a means of assessing the transdisciplinary aspects of sustainable development as it relates to the central idea of Energy Resource use

- Offer a focused discussion and analysis to understand the state of sustainability and energy resource use at a manufacturing process level, and provide a general commentary on its relation to the global scale.

- The process level analysis is facilitated by assessing the order of magnitude difference between the energy resource utilization for state of the art manufacturing process and the theoretical minimum energy resources needed to accomplish the same task; presented as a case study. Also under this analysis, one of the major goals of this study is to create a case study involving a material and energy flow evaluation for a typical controlled atmosphere brazing facility.

1.2 Research Objectives

This research study presents two views on the formulation of the limits of energy use in the context of sustainability. The two views are connected through social, economic and environmental frameworks, all within the realm of sustainable development.

The first view discussed is a global level presentation of the energy resources use as a driver of social progress. This is accomplished through construction of a novel "metrics quadrant plot." It offers an interrelation between selected, broadly accepted metrics such as: (i) the primary energy use (E), (ii) GDP per capita, and (iii) the human development index, HDI. The objective is to provide an answer on whether the rate of change of these metrics and their interrelations may offer an insight into the state of sustainability of a global, regional, country, sector, etc., realm considered. It is certainly clear that this representation does not pretend to offer an ultimate solution to the difficult problem of selecting The Sustainability Metric. It rather offers an insight into possible interrelations at large scale levels.

The second view offers a close-up insight into an energy use at a process level, at the domain where actual energy transformations take place. The objective is to conduct a detailed study of energy flows involved in executing a particular task of a manufacturing process in order to determine the specific energy use. A state-of-the-art manufacturing process, a metal bonding executed by using a controlled atmosphere brazing, is considered in great detail to evaluate the difference between the actual energy resources utilized for the task and the theoretical minimum energy needed to accomplish the task.

The objective is to assess the energy flows in and out of the system in order to evaluate the margin for improvement of the existing technology.

This can also provide an insight on whether (in a larger global context) it is sufficient to improve the existing process or if there is a need for radical thinking and introduction of new transformational technologies.

1.3 Thesis layout

The thesis is organized into five main sections. It starts with an introduction which presents the overview of the content in brief; the background and motivation for the work described and provides the organization of the thesis.

The second chapter contains the literature review. This section summarizes the work done in the field of study as related to this work, and provides a brief but in-depth coverage of the sources used and material consulted for the thesis. The contents are classified into three sub segments. The first provides an overview of research related to broader aspects of sustainability and global energy flows. The second sub-segment highlights the research initiatives at a process level specifically targeting manufacturing processes. The third segment provides information about the case study process of Controlled atmosphere brazing.

The third chapter presents a novel concept for evaluating multiple transdisciplinary metrics (Environmental, Energy, Economic, Societal) for assessing the sustainability at global level. “Metrics quadrant plots” are presented for three world economies, viz. USA, China and India, each representing a different level of development. Further analysis of sub-levels (i.e., scales) such as Process level, Sectors, Industry etc. creates a need for further analysis at a process level which is then presented in the next sections.

The fourth chapter narrows down the scope from a broad level of energy flows (related to the key world economies) to energy resource use and associated losses at a manufacturing process level. A case study for a state of the art aluminum brazing process (Controlled atmosphere brazing) is provided. This section presents the experimental setup

and procedure followed for measuring the energy inputs and losses for a laboratory level equipment.

The fifth chapter focuses on the details of the results for the experimental case study and discussion related to the associated energy flows and inherent process inefficiencies. A detailed Sankey diagram for the flows is constructed. Figure 1-1 shows a simplified energy flow diagram (Sankey diagram) for the CAB process. The material is presented such that only essential information is provided in the main body of the text for the chapter and all other relevant work, calculations, and auxiliary discussions are given in a series of Appendices.

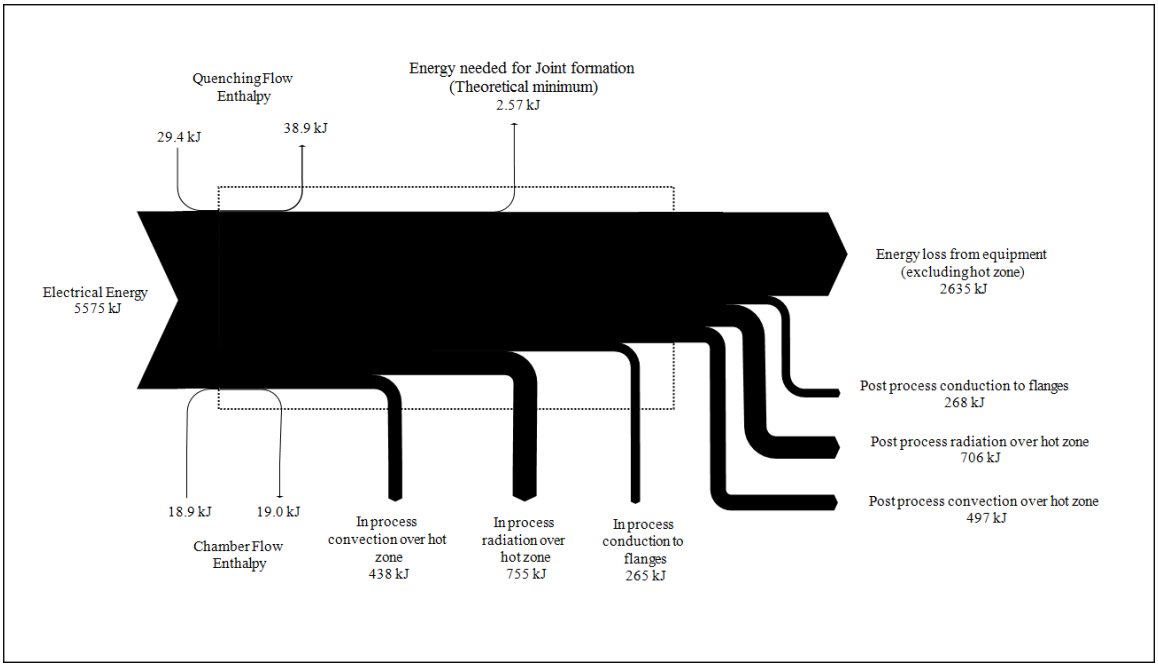

Figure 1-1: Simplified energy flow diagram for CAB process

Note that process requires 5575 kJ for its execution while the theoretical minimum for the task is 2.57 kJ!

The last chapter summarizes the outcomes of the study and concludes the work presented in the previous chapters. Additionally, suggestions are provided regarding some of the areas for further exploration.

Chapter 2: LITERATURE REVIEW

2.1 Sustainability and Energy Resource Use

One of the first and widely accepted definitions for Sustainable Development was offered in the report “Our Common Future” published in 1987 by the World Commission on Environment and Development, known as Brundtland Commission. In this report, the Commission defined Sustainable Development as “Development that meets the needs of the present without compromising the ability of future generations to meet their own needs.”[8]

The terms “Sustainability” and “Sustainable Development” have become commonplace since then. Numerous alternate, more detailed definitions of Sustainable Development and Sustainability have been proposed to reflect different scopes depending on their focus on Individuals, Companies, National Governments, Natural resources, etc. In the area of engineering, there have been theories proposed on sustainable manufacturing, sustainable products, sustainable designs etc. Although they may differ in scope, most definitions of sustainability/sustainable development share the same foundation. This foundation consists of three fundamental principles[9]:

1. **Availability of Resources** – Resources can be further categorized into Material, Ecological/Environmental, Social, Economic, and Political.
2. **Limits of Resources** – The resources being analyzed under the sustainability framework have imposed limitations. These can be direct such as fossil fuel reserves or indirect such as economic stability.
3. **Interdependence of Systems** – The interaction between the various systems, i.e. Environmental, Social, Economic etc. is a complex and plays a major role in

analyzing the effects on other systems. Note that a well-defined system is essential in any such analysis.

Most definitions of Sustainability agree that regardless of the entity being considered, Sustainability involves ensuring that there are sufficient supplies of resources to meet the needs and enable continued development and existence and that the access to the resources is equitable both inter-generational and intra-generational (future generations). Systems can only be sustainable if they can continue indefinitely, without depleting the resources required to maintain the system.

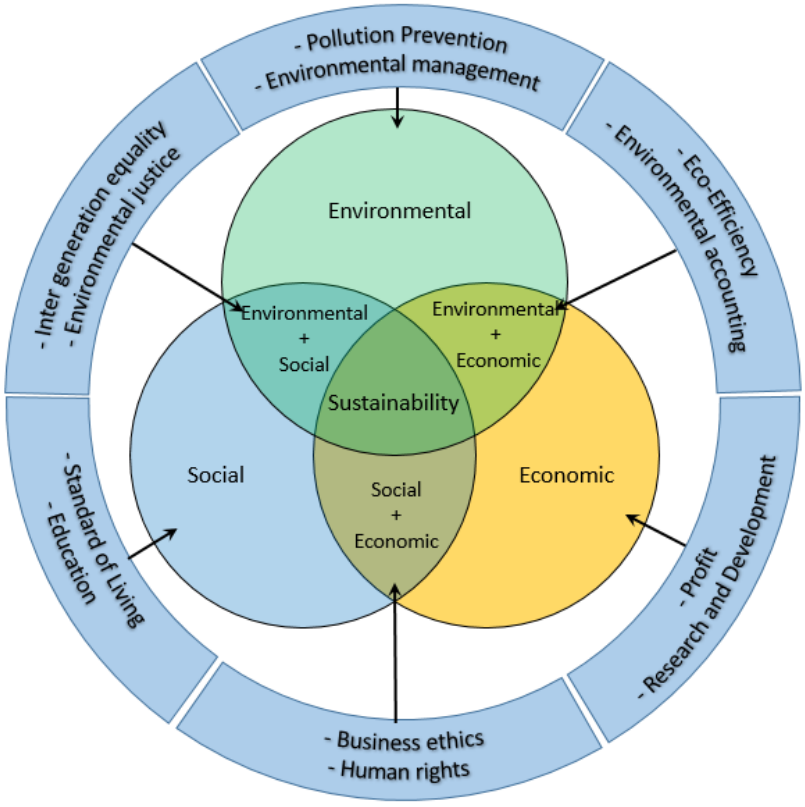

Figure 2-1: Three Spheres of Sustainability (Adapted from [9])

The spheres of sustainability as shown in figure above depict the interrelationship between the three main realms of sustainability[10].

Social: Social sustainability is the ability of a social system, such as country, organization etc. to function at a defined level of social wellbeing and harmony. Problems like war, poverty, low education rates are systems of a socially unstable system.

Environmental: Environmental sustainability is the ability of the environment to support a defined level of environmental quality and natural resource extraction rate on a continuous and indefinite basis.

Economic: Economic Sustainability is the ability of an economy to support a defined level of economic production indefinitely.

The recent past has seen multiple instances of economic instability, The Recession of 2008 being one of the most noticeable one. In instances like these, Environmental sustainability generally gets a low priority, with nations cutting back on stricter environmental laws and investments to focus on improving the economic stability. However, the well-being of environmental aspect is interlinked with the other two systems and has a counter effect, generally slow and unnoticeable at first, but creating a further imbalance.

Generally, the focus of most national and international agencies lies on one aspect at a time. UNEP (United Nations Environmental Programme)[11], EPA (Environmental Protection agency)[12] and Environmental NGO's focus primarily on the environmental aspect.

WTO (World Trade Organization)[13] and OECD (Organization for Economic Cooperation and Development)[14] focus mostly on economic growth, thought the OECD gives some attention to social sustainability, like war reduction and justice.

UN (United Nations)[15] does attempt to strengthen all three aspects of sustainability; however its focus shifts mostly towards the economic aspect since economic growth is given higher priority by its members, especially developing nations.

In terms of sustainable development, the growth in use of natural resources has been a topic of interest.[16] Some of this increase reflects higher resource demands from a growing world population. It also reflects a growth of per capita output and consumption. The last 100 years has shown an increase in world energy resources use by a factor of 16. Energy resources have become an economically important commodity shortly after invention of the steam engine and the beginning of industrialization. As technology advanced, especially since the Industrial Revolution, an increasing variety of energy resources and use patterns emerged that have allowed human societies to "consume"[1] energy on a much larger scale. However, the uncontrolled growth regimen is resulting in various ill effects, with environmental depletion effects being a major concern.

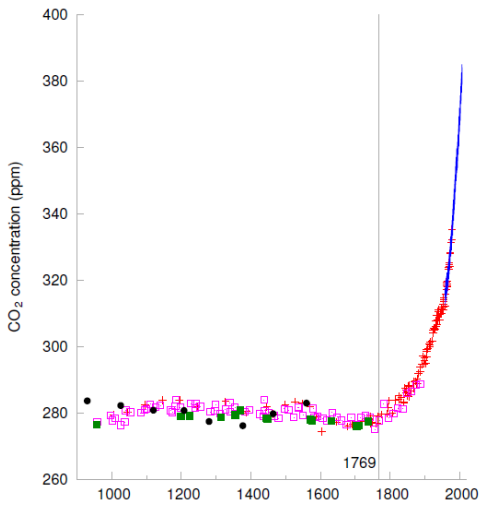

Figure 2-2: CO_2 concentrations (ppm) for last 1100 years[17]

[1] Note that the term "consume" signifies the process of energy conversion to produce goods and services. In a thermodynamics context energy is a conserved quantity and the processes involved merely alter the quality/usefulness of the available energy.

The CO_2 concentrations depicted in Figure 2-2 present a convincing argument for environmental degradation. Carbon Dioxide is a primary greenhouse gas emitted through human activities. Historically, the CO_2 concentrations have been hovering around the 280 ppm levels. However, the year 1769 marks the inception of a drastic exponential growth of the CO_2 concentrations. This marks the year in which James Watt patented his steam engine, an important event which fueled the growth of the Industrial Revolution.[17] One of the main applications of the steam engine was to pump water from the coal mines, and coal was a major contributor to the early stages of industrial development. The main human activity that emits CO_2 is the combustion of fossil fuels (coal, natural gas, and oil) for energy and transportation, industrial processes, electricity generation etc. It is obvious from the graph that there has been an unprecedented exponential growth in the concentrations which presents a strong case against the skepticism and disagreements on environmental degradation.

As shown above, the CO_2 concentration metric provides valuable insight on the issue of sustainable development. However, as indicated earlier in this document, studies like these generally present hypothesis based on single metrics at a time. Means of addressing the multi domain effects of these metrics can provide further insight which can then be used to quantitatively build a sustainable development model. The study presented as a part of this thesis proposes one such way to assess the multidisciplinary aspects of sustainability.

The preliminary drive for understanding the energy resource use on a global scale initiated with the primary energy resource use data presented in Figure 2-3, which clearly indicates dependence on fossil fuels as the primary energy sources on a global scale. One

of the first thoughts about energy resource use for economies started with the need to understand how different economies/nations used energy, and what the sources were.

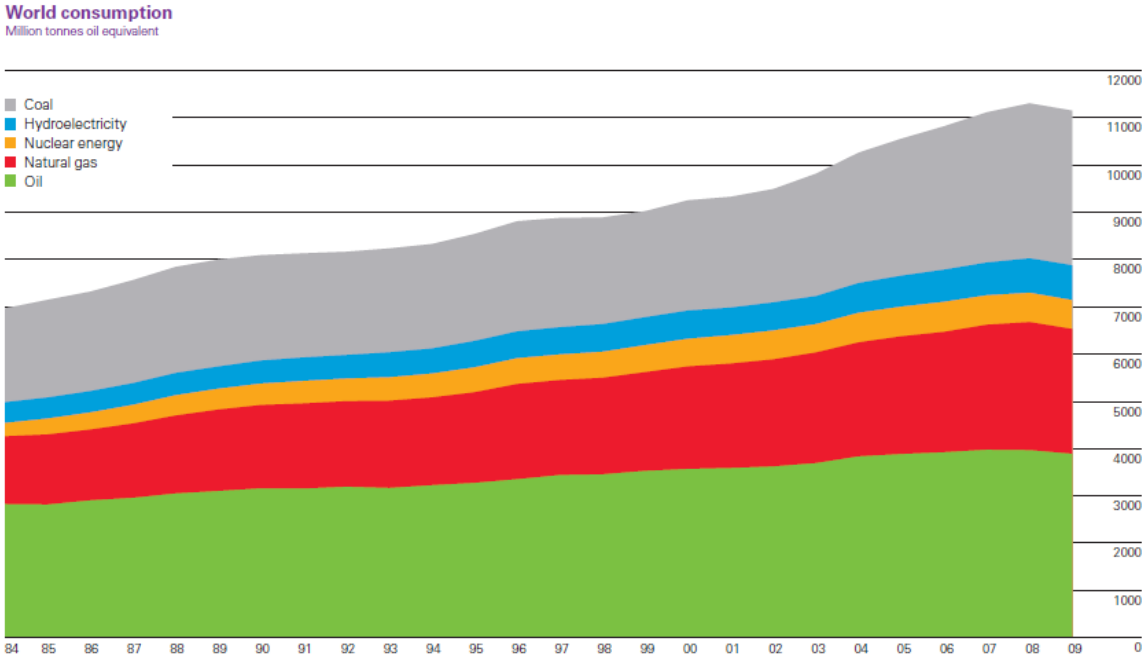

Figure 2-3: World Energy Consumption. Adopted from [18]

After initial research, 3 world economies were chosen such as to represent highly developed nation (USA), a nation which is at the point of transition from a developing to a developed economy (China), and a nation which is in the inception stage of development (India). The mappings for each of these economies are presented below by constructing Sankey Diagrams.

A Sankey diagram is a specific type of flow diagram, in which the width of the arrows is shown proportionally to the flow quantity. Sankey diagrams put a visual emphasis on the major transfers or flows within a system and are typically used to visualize energy or material or cost transfers at process, regional, national levels etc.

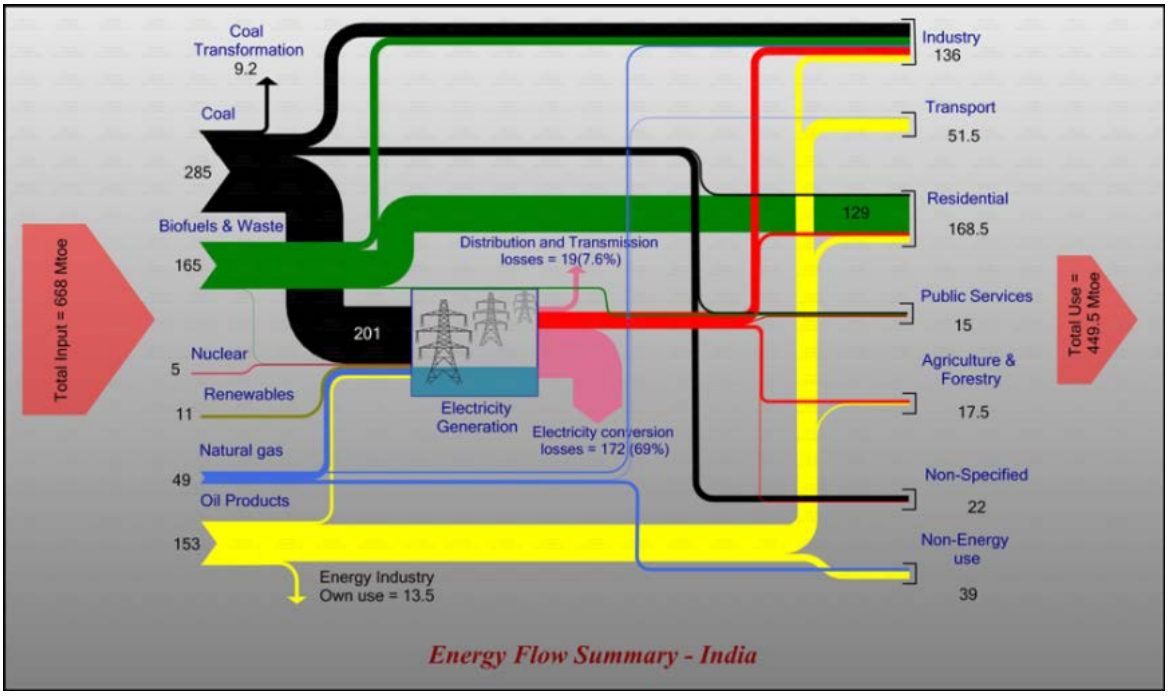

(a) India

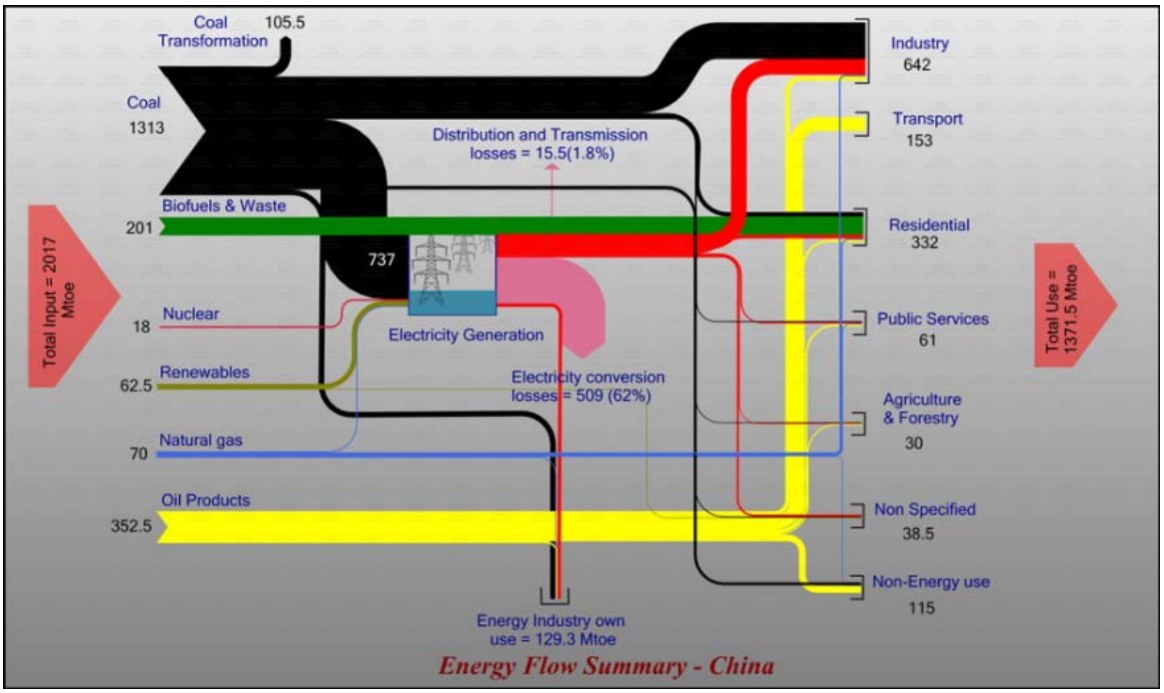

(b) China

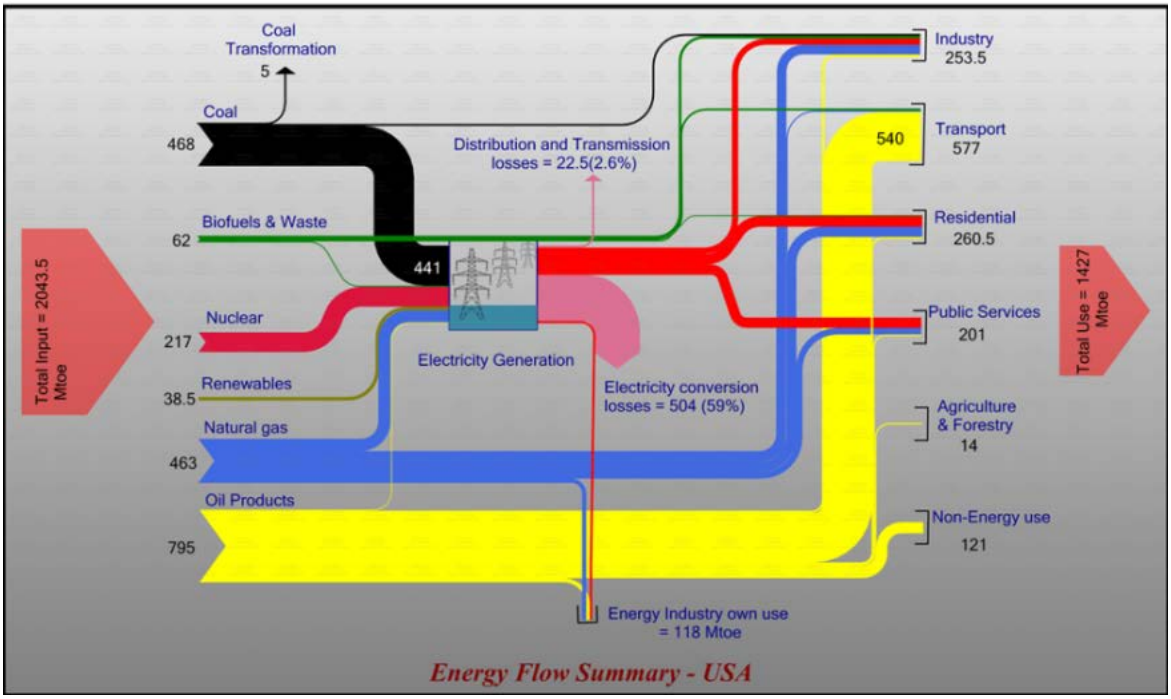

(c) USA

Figure 2-4: Energy Flow Sankey Diagrams – India, China, and USA

Figure 2-4 presents the Sankey diagrams for energy flows of the three nations selected for this study. The data for construction of these Sankey diagrams was obtained from International Energy Agency's (IEA) Statistical database for the respective economies, for the year 2009[19]. The Sankey diagrams have been constructed using the e!Sankey Software[20].

Each economy presented has a different usage pattern when compared to other; however, fossil fuels are still the main sources for development. Considering the diagram for USA, the transportation sector seems to be the largest energy consumer and indicates a huge petroleum products usage to provide for it. China on the other hand has made rapid social and economic progress by being the world manufacturing hub over the recent decades. The manufacturing sector however is fueled primarily by Coal which is reflected in the

diagram. India, which is still in the early stages of development, has a higher focus on infrastructure development. It is interesting to observe the huge amount of losses associated with the energy conversion systems which generate electrical energy from fossil fuels and other sources.

For all three economies considered, and in general for any other nation, the industry sector is one of the major consumers of energy resources. This sector also in turn plays a crucial role in the economic and social development of the economy and hence has been a topic of interest.

This study will present novel 4 quadrant plots which aid in the analysis of multiple sustainability metrics simultaneously. Additionally a process level case study for energy resource utilization metric at a manufacturing process level is presented, and its aggregated effect on the higher global energy flows is briefly presented.

2.2 Energy use in manufacturing processes

Manufacturing processes involve transformation of raw materials using labor, machines, processes, into finished goods which are used to cater to the social and economic requirements and progress. In doing so, energy resources are consumed and the material is transformed. This energy resource consumption, especially on large scales can have a significant impact on the environment and sustainable development and thus presents a need for detailed evaluation.

Any manufacturing process can be modelled as an open thermodynamic system which has work, heat and material flow interactions over a system boundary. Additionally the processes involve interaction with the environment resulting in losses by virtue of irreversibility[21]. All the material flows; temperature and pressure changes associated with a manufacturing process can hence be evaluated as energy interactions.

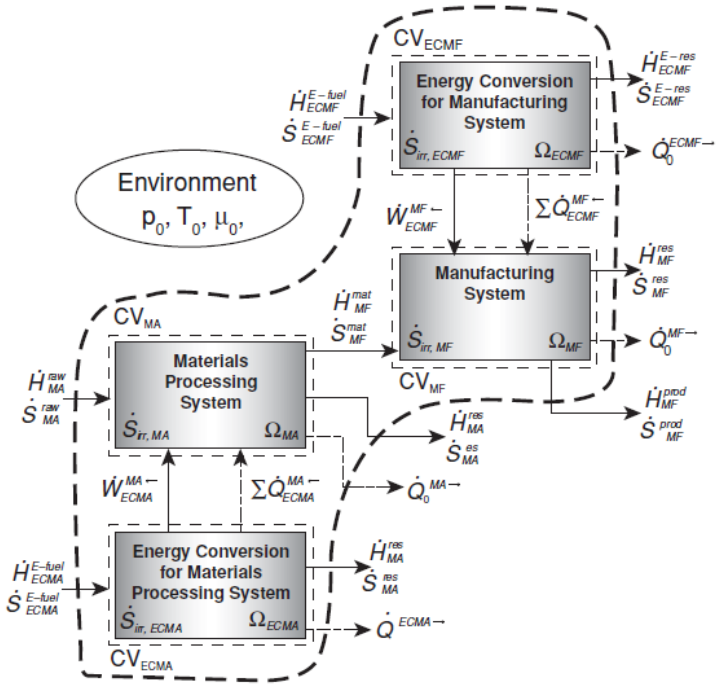

Figure 2-5: Generalized Model of a Manufacturing system(Adopted from[22])

Figure 2-5 depicts a generalized model of a manufacturing system[21]. The manufacturing sub-system which is the system in focus is denoted by Ω_{MF}. It receives work and heat inputs from the system Ω_{ECMF}, which are utilized for executing the task. The material inputs to the manufacturing system Ω_{MA} are depicted crossing the system boundary including the interactions with the conversion system Ω_{ECMA}. As shown in Figure 2-5 each subsystem has materials and energy interactions with other systems in terms of heat, work and material inputs and outputs. Additionally each subsystem interacts with the environment and involves inherent losses due to the irreversibility of processes, resulting in entropy generation. Representing a manufacturing process this way can thus be used to analyze the process using mass, energy and entropy balances. Considering the manufacturing subsystem (Ω_{MF}) the three equations [23] can be described as follows:

Mass Balance

Equation 2-1

$$\frac{dM_{MF}}{dt} = \left(\sum_{i=1} \dot{N}_{i,in}\widetilde{M}_i\right)_{MF} - \left(\sum_{i=1} \dot{N}_{i,out}\widetilde{M}_i\right)_{MF}$$

The Equation above represents the rate of change of mass in a system, where $\dot{N}_i$ represents the amount of matter of the *i*th component entering or leaving the manufacturing system per unit time. $\widetilde{M}_i$ represents the molar mass of the *i*th component.

Energy Balance

Equation 2-2

$$\frac{dE_{MF}}{dt} = \sum_{k} \dot{Q}_{ECMF,k}^{MF\leftarrow} - \dot{Q}_{0}^{MF\rightarrow} + \dot{W}_{ECMF}^{MF\leftarrow} + \dot{H}_{MF}^{mat} - \dot{H}_{MF}^{prod} - \dot{H}_{MF}^{res}$$

The Equation above represents the rate of change of energy for the manufacturing system. $\dot{Q}_{ECMF,k}^{MF\leftarrow}$ represents the rate of energy interactions between the manufacturing subsystem (Ω_{MF}) and its energy supplying sub system (Ω_{ECMF}) in form of heat. Similarly $\dot{W}_{ECMF}^{MF\leftarrow}$ represents the work interaction between Ω_{MF} and Ω_{ECMF}. The sums of enthalpy rates of all materials, products and residue bulk flows into or out of system are denoted by $\dot{H}_{MF}^{mat}, \dot{H}_{MF}^{prod}$ and $\dot{H}_{MF}^{res}$ respectively. The heat interaction between manufacturing subsystem Ω_{MF} and the surroundings is denoted by the term $\dot{Q}_{0}^{MF\rightarrow}$. This accounts for the losses to the surroundings at the local ambient temperature T_0.

Entropy Balance

Equation 2-3

$$\frac{dS_{MF}}{dt} = \sum_{k} \frac{\dot{Q}_{ECMF}^{MF\leftarrow}}{T_k} - \frac{\dot{Q}_{0}^{MF\rightarrow}}{T_0} + \dot{S}_{MF}^{mat} - \dot{S}_{MF}^{prod} - \dot{S}_{MF}^{res} + \dot{S}_{gen,MF}$$

The entropy balance is an expression of the second law of thermodynamics (through the closing the balance with entropy generation term). The term $\frac{\dot{Q}_{ECMF}^{MF\leftarrow}}{T_k}$ represents the entropy flow accompanying the heat transfer rate exchanged `between the manufacturing

subsystem (Ω_{MF}) and its energy supplying sub system (Ω_{ECMF}). Similarly $\frac{\dot{Q}_0^{MF\rightarrow}}{T_0}$ represents the entropy flow associated with Ω_{MF} and the surroundings. The terms$\dot{S}_{MF}^{mat}$, $\dot{S}_{MF}^{prod}$ and $\dot{S}_{MF}^{res}$ represent the entropy rates for material inputs, products and residual waste materials respectively. The $\dot{S}_{gen,MF}$ term represents the entropy generation caused by irreversibilities generated in the manufacturing system.

Exergy analysis

Generally, material processing of any kind involves heat exchange between the material and a heat source/sink. For a typical controlled atmosphere brazing manufacturing process (details discussed in Chapter 4 and 5), heat is provided to form a joint by converting electrical work input to heat transfer via a radiant heater. During the process, portion of the heat supplied is utilized towards the joint formation, while a sizable portion is dissipated to the environment as heat losses by means of convection and radiation. This process of heat transfer to the surroundings continues until the time the brazing furnace's hot zone reaches a temperature equal to the ambient temperature and is in equilibrium with the surroundings. As per the first law of thermodynamics, energy is a conserved property. Hence for the system under discussion, the energy balance targets the quantity of energy required for a process. However, from second law of thermodynamics, we know that all manufacturing processes are irreversible. i.e. it requires more resources to run the process in reverse than is required for running it forward. The analysis of transformation of energy resource use requires an additional consideration of energy "quality" beyond energy "quantity"[23]. This quality of energy depends of the process of transformation and the temperature levels encountered during the process and accounts

for the inherent irreversibilities. In thermodynamics the measure of the quality of energy quantity is called Exergy, and it is also expressed in units of energy.

Exergy of a material flow represents the maximum amount of work that could be extracted from the flow as it is reversibly brought to equilibrium with a well-defined environmental reference state. One of the most commonly used reference environment is the Szargut reference environment.[24]

The Energy and Entropy balance equations presented above can algebraically be modified to yield the following Exergy balance equation[23]

Equation 2-4

$$\dot{E}x_{in} + \dot{E}x_{W,in} + \dot{E}x_{Q,in} = \dot{E}x_{out} + \dot{E}x_{W,out} + \dot{E}x_{Q,out} + \dot{E}x_{destruction}$$

The exergy flows in the above equation consist of physical and chemical exergies. The physical is that portion of exergy that can be extracted from a system by bringing the system from its given state to a “restricted dead state” at reference temperature and pressure (To, po). The chemical exergy represents the additional energy that can be extracted from system at the restricted dead state by bringing the chemical potentials at that state to equilibrium with its surroundings at the “ultimate dead state”. In addition to requiring equilibrium at the reference temperature and pressure, the definition of chemical exergies also requires equilibrium at reference state with respect to a specified chemical composition. This reference state is typically representative of the compounds in the Earth’s upper crust, atmosphere, and oceans.[23]

As a consequence of so defined exergy, in exergy analysis, work and heat are not equivalent as is the case in terms of the first law analysis. The available energy in the

form of heat is reduced by the Carnot factor$\left(1-\frac{T_0}{T}\right)$, i.e., the exergy value of a quantity of heat is equal to the product of that quantity of heat and the Carnot's coefficient.[23]

The term $\dot{E}x_{destruction}$ represents exergy destruction during the process.

Considering the above constitutive terms, the exergy balance can be represented as follows:

Equation 2-5

$$\dot{E}x_{in}^{ph}+\dot{E}x_{in}^{ch}+\dot{W}_{in}+\left(1-\frac{T_0}{T}\right)\dot{Q}_{in}=\dot{E}x_{out}^{ph}+\dot{E}x_{out}^{ch}+\dot{W}_{out}+\left(1-\frac{T_0}{T}\right)\dot{Q}_{out}+T_0\dot{S}_{gen}$$

For the manufacturing subsystem (Ω_{MF}) under consideration, the exergy balance can be reduced to the following.

Equation 2-6

$$\dot{W}_{ECMF}^{MF\leftarrow}=\dot{E}x_{MF}^{prod,ph}+\dot{E}x_{MF}^{res,ph}-\dot{E}x_{MF}^{mat,ph}+\dot{E}x_{MF}^{prod,ch}+\dot{E}x_{MF}^{res,ch}-\dot{E}x_{MF}^{mat,ch}-\sum_{k>0}\left(1-\frac{T_0}{T_k}\right)\dot{Q}_{ECMF}^{MF\leftarrow}+T_0\dot{S}_{gen,MF}$$

The minimum amount of work necessary for any manufacturing process is represented by the term $\dot{W}_{ECMF}^{MF\leftarrow}$ when the term $T_0\dot{S}_{gen,MF}$ in the equation above is zero. I.e. Irreversibilites are zero. Hence $T_0\dot{S}_{gen,MF}$ represents the difference between the actual amount of resources consumed to complete a task and the theoretical minimum amount of work needed to complete the same task.

With the objective of understanding the margin for improvement in current state of the art technologies, it can (in theory) be proposed that the energy resource utilization for a

current technology may be smaller than a technology of the past to attain the same objectives. As technology progresses, the resource utilization to accomplish the same task may further reduce, however with a physical limit under which no future technology would be able to reduce the resource use. Utilizing entropy generation as a metric may be beneficial in determining the absolute margin for improvement.

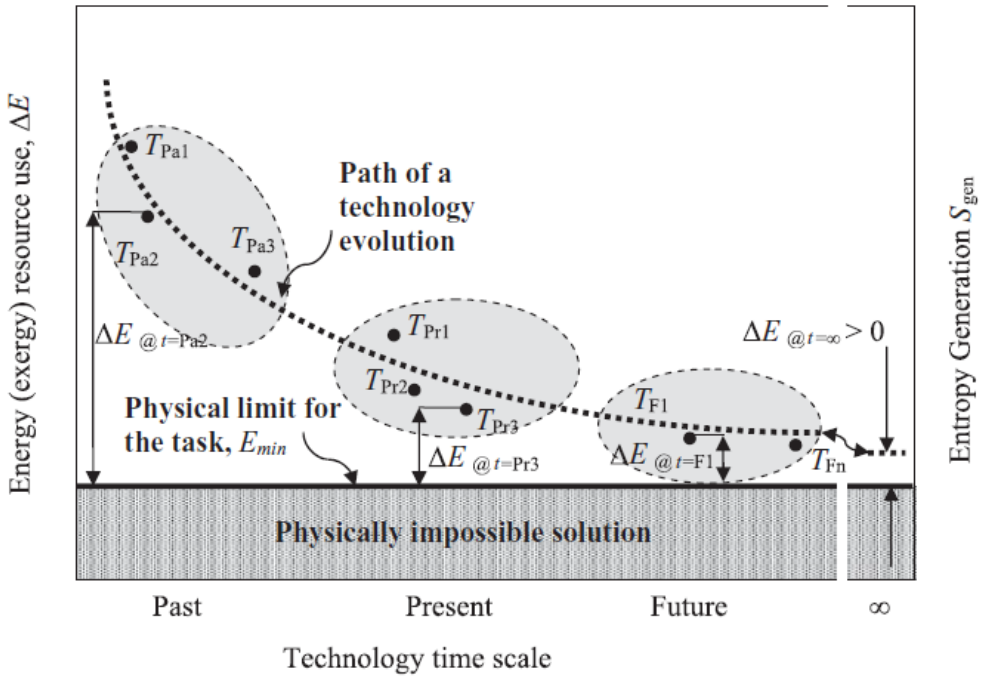

Figure 2-6: Technology evolution[25]

Figure 2-6 presents a technology evolution scale which depicts the margin between the energy resources needed to complete a given task and the physical minimum required to complete this task with respect to the generic timescale of past, present, and future technologies. Additionally, the secondary vertical axis displays entropy generation change w.r.t time.[23]

From a sustainability standpoint, for any manufacturing process, it is essential to understand the margin for improvement with technology improvements. For example, if a

state-of-the-art technology used to complete a given task presently is Tpr1, it is obvious that this technology uses less energy than the most efficient technology of the past, Tpa1, but still more than a technology of the future, TF1. The important point to note is that these improvements are incremental and their rate of improvement is decreasing with time as indicated by the formation of the horizontal asymptote. However, as presented, the horizontal axis extends infinitely, and that the margin for improvement ΔE must always be greater than zero as the second law of thermodynamics mentions that the entropy generation for any real process will always be greater than zero. Although a hypothetical technology which can complete a given task with the smallest margin of energy resources used may not be available currently or in the near future, it is valuable to know the physical limit to which any future technology would be constrained with respect to energy resource usage. Ultimately, this advocates the fact that a metric to facilitate an assessment of a margin for improvement of energy resources use should be related to a theoretical limit of energy resources use for a given task, irrespective of technology.[23]

This thesis promotes the idea of calculating the theoretical minimum amount of energy needed to accomplish the desired task of a metal joining process and a compares this theoretical minimum to present technology energy resource utilization [26]. This comparison provides an assessment that may assist us in defining a need for a novel transformational technology.

2.3 Controlled Atmosphere Brazing

As indicated in chapter 1, in addition to the global outlook for energy flows this thesis also presents a process level study and its aggregated effect on global levels. Controlled atmosphere brazing, which is a process widely used for mass production of aluminum heat exchangers, was selected as a case study in the context of determining energy resources demand from a sustainability standpoint. This section presents the review of industrial Controlled atmosphere brazing process.

Brazing is a metal joining process whereby a molten filler metal is heated above its melting point and is thus drawn into the gap between materials to be joined (parent materials) by capillary forces[27]. A metallurgical bond is formed on solidification of the filler metal. The composition of the filler material used is such that its melting point is appreciably lower than that that of the base metals to be joined.

Aluminum brazing is the preferred process for mass production compact heat exchangers use as radiators, condensers, evaporators and heater cores in the automobile industry.[28] Due to the recent developments in the process technology the application of aluminum heat exchangers has extended to commercial and residential air conditioning, refrigeration and household and electrical appliances due to the benefits such as lower costs, smaller sizes, higher heat transfer efficiencies, recyclability etc.

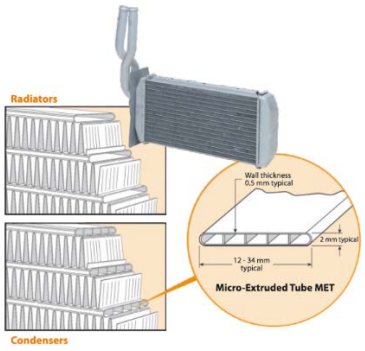

Figure 2-7: Typical aluminum heat exchanger construction[29]

Aluminum brazing involves joining of components with an Al-Si brazing alloy whose melting point is lower than that of the base alloy material. The cladding is placed in between or adjacent to the components to be bonded. The assembly is then heated to a temperature in between the melting points for the cladding and the base metal, such that the cladding melts and the parent material does not. Upon cooling the cladding forms a metallurgical bond between the joining surfaces of the component.

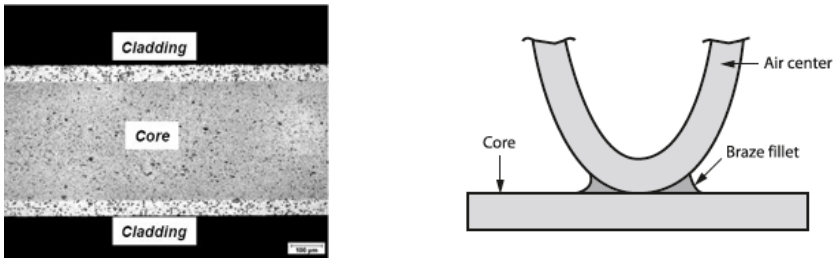

Figure 2-8: Brazing sheet and fillet configuration[29]

In automotive heat exchanger applications, the cladding is supplied via a thin layer, metallurgically attached to the base alloy in form of the brazing sheets. The base alloy provides the structural integrity while the low melting point cladding melts to form the brazed joints. A typical sheet and fillet geometry for a heat exchanger joint as shown in

Figure 2-8; may be manufactured using a base aluminum alloy such as AA 3003 with a cladding of AA 4343, 4045, or 4047. While the base alloy melts at about 630ºC, the clad material melts between 577ºC and 613ºC. Therefore, the ideal furnace temperature is somewhere in the middle of the melting range of the cladding material (depending on whether the clad Si composition is eutectic or hypo-eutectic) [27]. In controlled atmosphere brazing process, flux needs to be applied to the surfaces to disrupt the oxide film present on the surfaces and allow for free flow of the molten clad material. One of the most commonly used flux is the NOCOLOK® flux which is a non-hygroscopic, non-corrosive fine white powder consisting primarily of potassium fluroaluminate salts.[30] At the elevated brazing temperatures this flux breaks down the oxide layer thus providing a capillary action to draw the molten metal into the joint. A controlled atmosphere that has an oxygen content of less than 100 ppm and a dew point of up to –40ºC must be provided. These atmospheric conditions are accomplished through the use of pure nitrogen, which is readily available.

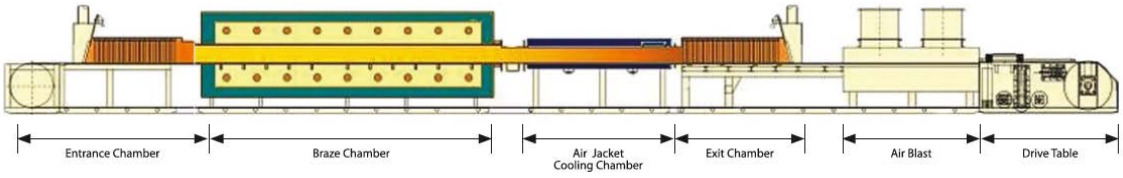

Figure 2-9: Industrial CAB furnace configuration[29]

A typical configuration of an industrial controlled atmosphere brazing furnace is presented in Figure 2-9. These continuous operation furnaces provide a high volume throughput. The aluminum brazing process under controlled atmosphere in industry usually has the following process parameters.[31]

- Operating Temperature 853 K to 893 K
- Part Temperature Uniformity ± 3K
- Nitrogen atmosphere with dew point -35 through -40 ºC at the onset of ramp-up and oxygen content <100 ppm
- Flux surface density 5-15 g/m^2

A radiation heating CAB furnace is an ideal facility for brazing similar size products in a continuous flow environment such as radiator, condenser mass production. The heat input into the furnace chamber is controlled through electric heating elements or natural gas fired burners to a stainless steel heat muffle which in turn heats the products.[32] The process in most brazing operations includes the following steps:

- Component forming and assembly
- Cleaning and Flux Application
- Brazing
- Post Brazing Procedures

The typical process steps involved in aluminum brazing are the furnace bake-out, continuous ramp-up heating till the peak temperature of brazing, dwell period and the quench. The bake-out is done by allowing the inert gas (nitrogen) to flow through the hot zone continuously. This helps in removing out all the water vapor and oxygen content present in the chamber. In general practice, the start of the brazing is prompted by monitoring the oxygen level and the dew-point temperature in the chamber.

Chapter 3: SUSTAINABILITY METRICS: A GLOBAL PERSPECTIVE

3.1 Metrics for Sustainable Development

The developing countries of the world are striving to reach the level of development, social and economic, something that the developed nations take for granted. With the current technologies, these demands present a scenario which is not sustainable by any means. The rate at which human race is using scarce and limited resources it appears that, unless measures are taken now, the future of civilization, as we understand it is uncertain[33].

It is a necessity to express the state of a considered system in terms of relevant properties (metrics), inevitably involving multiple trans-disciplinary aspects of sustainability such as its social, environmental and economic. As initiated in the previous chapter (Section 1.1), the current state of findings related to sustainable development metrics are inadequate and lack a comprehensive unified approach. A variety of widely accepted metrics focus on social, environmental, economic, realms rather separately[23]. However, note that metrics are still essential to measure and calibrate progress towards sustainable development goals. At a process level, metrics have a well-defined meaning. However at a higher hierarchical scale level, such as an industry, sector, economy, system boundary shift is required, the concept of sustainability is more meaningful, and the analysis becomes more complex. Even though this study is focused on energy resource use, the metric is interrelated to economic and social metrics. Metrics related to the different transdisciplinary aspects are defined next.

Energy Metrics (Primary energy Consumption)

The most common means of quantifying energy use at a global scale is Primary energy consumption. Multiple agencies define primary energy in different ways such as

1. Primary energy is the energy embodied in sources where human induced extraction or capture, with or without separation from contiguous material, cleaning or grading, must be undertaken before the energy can be traded, used or transformed.[34]

Or

2. Energy in the form that it is first accounted for in a statistical energy balance, before any transformation to secondary or tertiary forms of energy. For example, coal can be converted to synthetic gas, which can be converted to electricity[35]

In common terms, Primary energy is a quantity to be converted from an energy source found in nature that has not yet been subjected to any conversion or transformation process.

Economic Metrics (GDP and GDP per capita)

In terms of economic aspects of sustainable development, GDP, GNI, Total reserves, Inflation etc. have been used widely. GDP (Gross Domestic Product) at purchaser's prices is the sum of gross value added by all resident producers in the economy plus any product taxes and minus any subsidies not included in the value of the products. It is calculated without making deductions for depreciation of fabricated assets or for depletion and degradation of natural resources. GDP per capita is gross domestic product divided by midyear population.[36]

On the other hand, GDP has often been criticized as an inadequate metric as a measure of economic welfare.[37-39]. It has been proposed that GDP is a measure of economic activity and not economic well-being. Over the past years GDP has erroneously been used to measure economic progress and quality of life, as it ignores changes in the natural, social, and human components of capital on which a community relies for continued existence and well-being. [38]. One of the prime concerns raised is that GDP measurement encourages the depletion of natural resources at a faster rate in order to fuel economic growth.

Some of the alternative indicators of economic well-being, that use GDP as the foundation but address its inefficiencies include Index of Sustainable Economic Welfare (ISEW), Genuine Progress Indicator (GPI)[40], Human development Index (HDI) [37, 41]

While GDP is a measure of income, GPI is a measure of the sustainability of that income. By accounting for aspects such as income inequality, environmental degradation, etc., GPI is designed to measure sustainable economic welfare rather than economic activity alone.[38]

Societal Metrics (Human development index (HDI))

Of all the various metrics related to sustainable development, the societal development domain is the most difficult to assess. Employment rates, Life expectancy, School enrollment etc. are generally referred to, but do not provide a means of an aggregated all-inclusive factor. The human development index seems to bridge the gap to an extent, at least in principle. It is a composite statistic published by U.N.D.P (United Nations

Development Programme) used to rank countries into four tiers of human development. It is a summary of measure of average achievement in key dimensions of human development namely Life expectancy, Education and Standard of living[5]. The health dimension is assessed by life expectancy at birth component of the HDI is calculated using a minimum value of 20 years and maximum value of 85 years. The education component of the HDI is measured by mean of years of schooling for adults aged 25 years and expected years of schooling for children of school entering age. The standard of living dimension is measured by gross national income per capita. The HDI is the geometric mean of normalized indices for each of the three dimensions. Note that the HDI does not reflect on inequalities, poverty, human security, empowerment, etc. HDI is reported on a 0-1 scale with 0.8 being the threshold for high human development.

Although HDI is often used as indicator of well-being, there have been views which have criticized its validity. It has been argued that the HDI sensitivity for each of its components is different and equal increase in any of the one dimension may bring different changes in HDI. Further it has also been argued that the HDI values for most developed countries are very high and close, thus making it redundant to compare them based on HDI alone.[41] Also, its strong correlation to the GDP has been criticized. It has been highlighted that some of the largest improvements in HDI since 1990 have been reported for nations such as China and India, primarily due to the high GDP gains for these growing economies.[37]

Some of the alternative metrics proposed in lieu of HDI include Social progress Index[42], Weighted Index of Social Progress (WISP)[37], Genuine progress Indicator (GPI)[40], Happy planet index (HPI)[43] etc.

Environmental Metrics (CO_2 Emissions)

Environmental degradation due to human activity has been one of the most actively debated aspects in the past decades. Some of the metrics used commonly are EPI (Environmental Performance Index)[6], CO_2 emissions[44], Environmental footprint[4] etc. As the primary focus of this study is energy resource use, the metric CO_2 emission was shortlisted for analysis. CO_2 is a greenhouse gas emitted through human activities. It is naturally present in the atmosphere as part of the Earth's carbon cycle. However, human activities are altering the carbon cycle—both by adding more CO_2 to the atmosphere and by influencing the ability of natural sinks, like forests, to remove CO_2 from the atmosphere. CO_2 emission is a metric which has been widely accepted as a measure for environmental degradation.

The World Bank Indicators database defines CO_2 emissions as the emissions stemming from the burning of fossil fuels and the manufacture of cement. They include carbon dioxide produced during consumption of solid, liquid, and gas fuels and gas flaring.

Apart from the major approaches such as improvement in energy efficiency and increasing of non-carbon energy sources, “Carbon Sequestration” has developed into an approach which provides significant contributions towards reduction in greenhouse gas emissions[45]. Carbon sequestration strategy uses engineering techniques to capture CO_2 from power plant flue gases and industrial process effluents and transfer it to long lived pools underground, or deep into ocean.[46]

The next section of this chapter provides a novel methodology using 4 quadrant plots for simultaneously analyzing multiple metrics related to sustainable development. The study presented will focus the metrics described in this section above. However, the similar approach can be utilized with many sets of metrics to gain insight into aspects of sustainability.

Energy flow analysis regardless of the scale of the system follows the conservation of energy principle. The total energy for a higher global hierarchical level can be presented as

$$E_{total} = \sum_{j=1}^{k} \dots \sum_{n=1}^{p} E_{j,\dots,n}$$

Where,

E_{total} is energy at a higher (or highest) level e.g. Global scale.

and Ej…n energy at lower hierarchical levels such as at a manufacturing process level such as machining, welding, etc.

Also, it can be hypothesized, and will be proved in the case study, that the actual energy resources at the lowest hierarchical level of process energy use are still often multiple orders of magnitude higher than the theoretical minimum energy required for the same task. The energy resource levels will often consist of flows which are multiple orders of magnitude lower than for the higher levels. From equation above, it is implied that energy resources related study must be considered by starting analysis at the process level, and then gradually moving across the hierarchy sequence to see the impact on a higher level. Such an analysis at a process level can be done within the thermodynamic framework.

3.2 Sustainability analysis for key world economies

Analysis of the state of sustainability for a considered system at a large scale necessitates, in principle, evaluating multiple trans-disciplinary aspects such as societal, environmental and economic features. Furthermore, for better analysis of these aspects, there is a need for quantitative metrics in transdisciplinary domain, not just a qualitative assessment in a single domain.

Although this study is focused primarily on the energy resource use, considering the state of sustainability for a nation, this metric is interrelated to the corresponding economic and social metrics. An example of such interdependence is presented in this section.

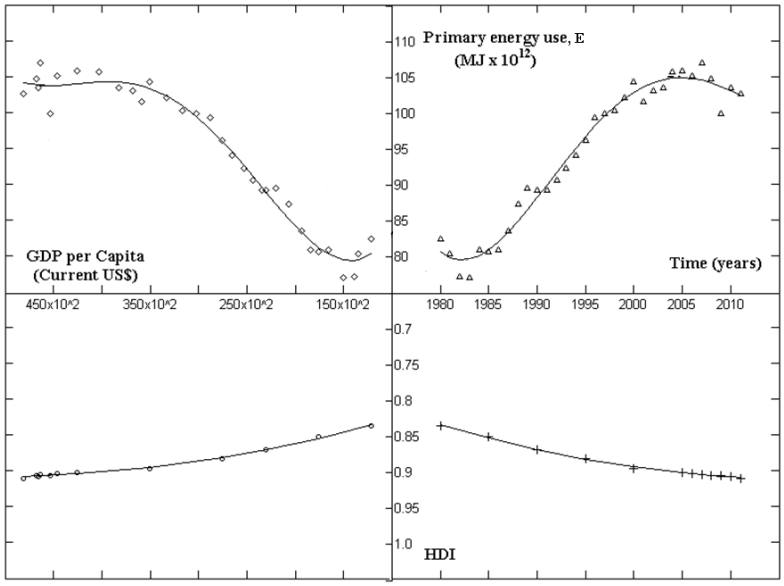

Figure 3-1: Metrics Quadrant sustainability Plot – U.S.A

Consider the sets of plots presented in Figure 3-1, Figure 3-2 and Figure 3-3 representing different countries/nations. The novel metrics-quadrant plot provides means of presenting multiple metrics (three) on one single diagram, thus enabling the analysis of the interdependence between those metrics.

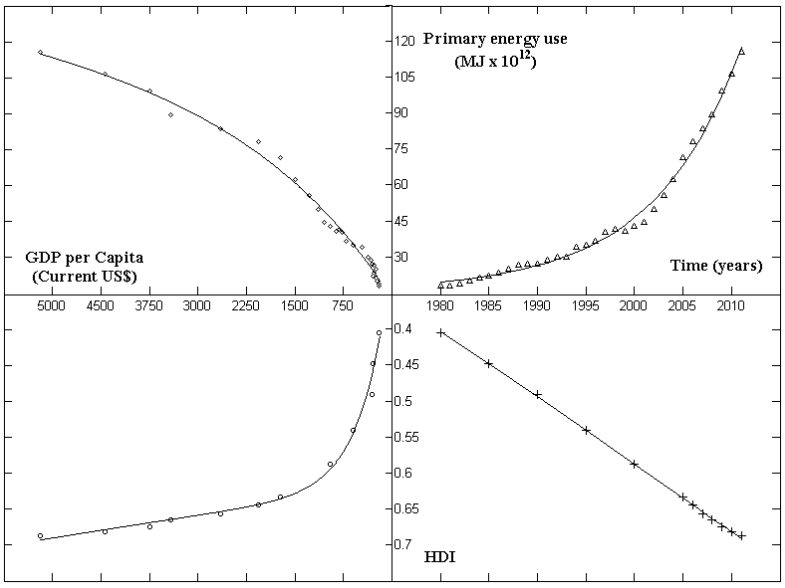

Figure 3-2: Metrics Quadrant sustainability Plot – China

For example, Figure 3-2 above presents the relationship between the metrics primary energy use (Energy aspect), GDP per capita (Economy aspect) and HDI (Societal aspect) for China from 1980 to 2010. Each quadrant a relationship between two metrics (out of three) as follows.

Quadrant 1 (Top-Right): This quadrant presents the Primary Energy Use (MJ x 10^{12}) for China as a function of time (years).

Quadrant 2 (Top-Left): This quadrant presents the GDP per capita (Current US$) as a function of Primary Energy use (MJ x 10^{12}), which in turn is presented as a function of time.

Quadrant 3 (Bottom-Left): This quadrant presents HDI as function of GDP per capita (Current US$), which in turn is presented as function of Primary energy use in quadrant 2

Quadrant 4 (Bottom-Right): This quadrant completes the plot by presenting the change in HDI as a function of time.

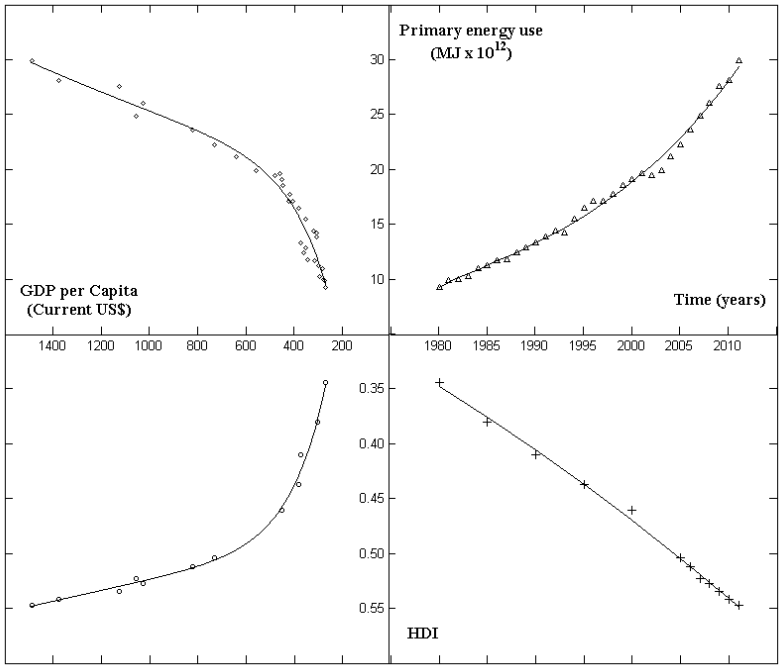

Figure 3-3: Metrics Quadrant sustainability Plot - India

Such representation has several advantages stemming for an easy identification of the rate of change of individual metrics in the context of changes of the other two metrics.

The plots presented in Figure 3-1, Figure 3-2 and Figure 3-3 were constructed by using the energy resources primary use[47], GDP per Capita[48] and HDI[49] metrics data for the past 30 years (1980-2010).

The nations selected for the study i.e. U.S.A, China and India were chosen after a preliminary evaluation of world economies and selecting an economy which has been considered as a developed economy for the period under consideration, viz. U.S.A; an economy which has developed rapidly over the last few decades and has recently made the transition to being termed as a developed economy, viz. China; and an economy which is currently in its early development stage and is aggressively moving towards economic/societal development, i.e. India.[50]

The trends indicate that for developing economies such as for India and China a steady rate of increase in HDI was observed which was supported by different rate of increase and different range of metric values for GDP per capita and Primary Energy use. The primary energy use indicates increase of the rate of change (while the rate of change of the GDP is decreasing). These trends indicate an importance of the energy resource use analysis simultaneously with the other important metrics of sustainability.

Note that the selection of metrics should be a subject of a rigorous sustainability analysis consideration and may differ from the ones presented. The metrics included were selected for the sake of simplicity because of their broad presence in such studies.

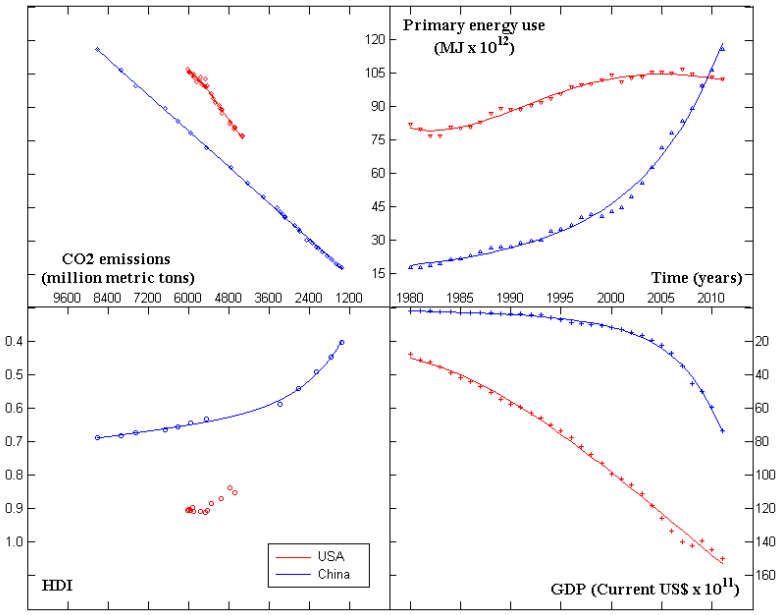

Figure 3-4: Metrics quadrant sustainability plot: USA and China Combined

Figure 3-4 presents a metrics quadrant plot modified to provide a comparison between the metrics for USA and China. Furthermore, the plot includes CO_2 emissions (Million metric tons) as an environmental metric, in addition to the metrics Primary Energy use, GDP and HDI. This provides an array of interdependent metrics information together

thus enabling further analysis of the state of sustainability. It is interesting to note that the primary energy use for China increased exponentially during the 30 year period considered, compared to primary energy use for USA, which is relatively lower rate of increase. Around 2010, the Primary energy use trend lines cross, indicating similar energy use for the two economies. However, comparing this with the CO2 emissions in quadrant 2, it is clear that the energy conversion processes for China seem to be more inefficient as the emissions are significantly more than those for USA.

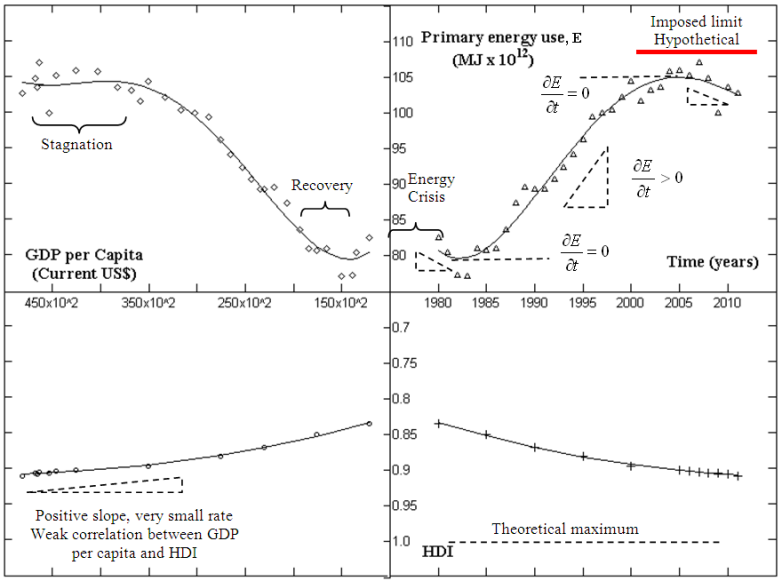

Figure 3-5: Metrics Quadrant Sustainability Plot – Trend analysis: USA

Figure 3-5 above shows the metrics quadrant plot for USA, indicating the trends of change in the metric variables. The slope of a selected graph, in any of the quadrants, indicates the rate of change of the given dependent variable in function of the corresponding independent variable. Moreover, if a metric is a differentiable function of the remaining metrics for $t \in T$ (what may not necessarily be the case for some systems), the chain rule implies:

Equation 3-1

$$\frac{\partial}{\partial t}(HDI) = \frac{\partial}{\partial t}\{f[GDP(E)]\} = \frac{\partial HDI}{\partial GDP}\frac{\partial GDP}{\partial E}\frac{\partial E}{\partial t}$$

The rate of change of the given metric in conjunction with the imposed limits define the sustainability state domain. For example:

Equation 3-2

$$\frac{\partial E}{\partial t}\begin{cases} = 0 & \text{steady} \\ < 0 & \text{reduction} \\ > 0 & \text{increase} \end{cases} \qquad \text{Subject to } E < E_{max}$$

Or

Equation 3-3

$$\frac{\partial HDI}{\partial GDP}\begin{cases} = 0 & \text{stagnation} \\ < 0 & \text{decline} \\ > 0 & \text{progress} \end{cases} \qquad \text{Subject to } HDI \leq 1$$

The implications of the metrics quadrant sustainability plot in terms of the equations above are beyond the scope of this study and may be a topic for future studies.

It can be observed that stagnation represented by one of the metric's rates leads to the diminishing rate of the compounded metric rate. Also a change in one metric may be neutralized with the change in another metric if the functional dependence can be identified between the metrics. Additional constraints can be imposed on the metrics change, for example, both increase in HDI and GDP per capita would be characterized as a progress, but a decrease in HDI with a decrease in GDP per capita may mean an onset

of a decline. From Figure 3-5 it is clear that a complex behavior of the considered metrics indicates a complex evolution of the resource use and economy development. A decline in energy resources use along with the stagnation in GDP per capita and a low rate of change in HDI indicate most likely an energy resources efficiency increase and/or energy intensity reduction in a well-developed economy. As presented in the plots earlier, the trends for various systems (USA, China, and India) are quite different. Developing economies such as China and India present a very strong correlation between HDI and GDP per capita; and GDP per capita and energy resources use. With no constraints imposed, the energy resources use will continue with a sharp increase and a large rate of change. With possible energy resources limits imposed, hypothetically through governmental regulations or external factors, stagnation if not a prosperity can be preserved only through an increase in energy efficiency. Alternately, technologies featuring dramatic reduction in energy resources use due to transformational technologies involvement may be introduced. Hence, with the limited rates of change of the energy efficiency of any well developed, state-of-the-art process, new transformational technologies are most likely the only solution in the long run.

Considering this requirement to assess how energy efficiency at lower levels affects the energy resource use at these higher levels, this global perspective must be extended with an analysis at sub-system levels. This study is focussed specifically in energy resources use in industry as it's one of the largest consumers of energy resources (Refer Energy flows for USA, China and India presented in Appendix 7). For illustration purposes, the study will focus on the sub-sector level related to manufacturing of heat exchangers (a hardware component of a vast number of systems). More specifically, on compact heat

exchangers for automotive industry. The state-of-the-art technology used in the net-shape manufacturing of these devices is Controlled Atmosphere Brazing (CAB). Figure 3-6 below provides an outlook of the cumulative nature of energy resources consumption, from a process level to a global level.

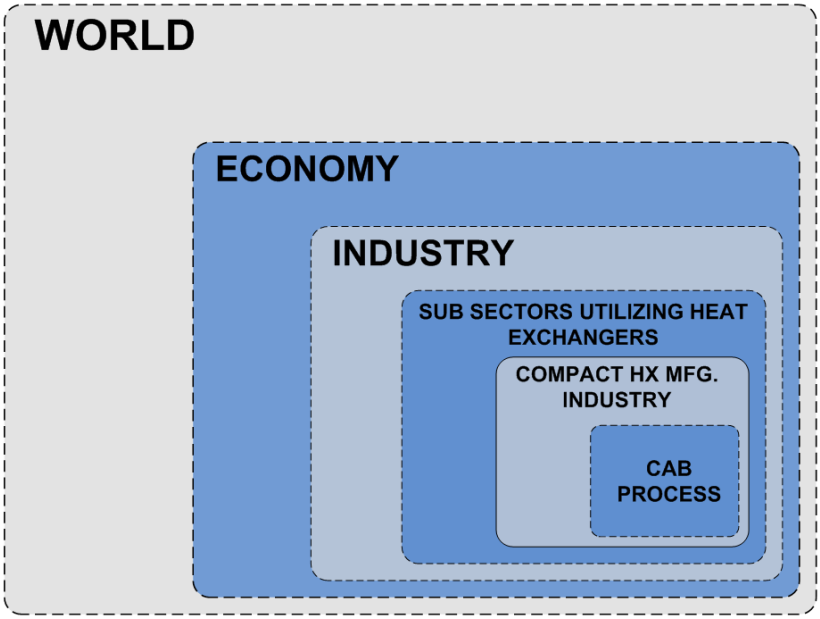

Figure 3-6: Energy resources consumption outlook

Data collected in Table 3-1 based on Figure 3-6 indicates that the energy resource use at the global scale must be influenced, in a final instance, by the rate of energy resources use at the process level, irrespective of the large difference in an order of magnitude of energy resources use for a single product vs. the industry sector, economy or a global impact.

Table 3-1: Energy resource consumption outlook

Domain	*Energy (GJ)*
World [36]	5.16×10^{11}
USA [51]	9.28×10^{10}
Industry [51]	2.12×10^{10}
Industry Subsector: Transportation equipment (NAICS:336) [51]	4.80×10^{08}
Industrial Controlled Atmosphere Brazing Facility [31]	8.58×10^{04}
Unit Compact heat exchanger [31]	7.80×10^{-3}

In the particular case of aluminum brazing of heat exchangers in automotive industry the unit energy resources use increases for many orders of magnitude at any of the upper levels. Total automobile production in U.S. (including passenger cars, commercial vehicles, trucks and busses) for 2010 was 7,762,544 units [52]. Considering (conservatively) that each manufactured vehicle has at least one aluminum compact heat exchanger (a typical automobile may have up to five or six heat exchangers) and each compact aluminum heat exchanger may require 7.8×10^{-3} GJ energy resources for its manufacturing using CAB; for all units, the energy resources need would be $\sim 6 \times 10^4$ GJ or $\sim 10^4$ barrels of oil equivalent. The world production is more than an order of magnitude larger.

Considering these statistics for application scale of controlled atmosphere brazing, it would be interesting to study the minimum amount of energy resources used use for executing a metal bonding process using Controlled Atmosphere Brazing technology.

This can provide insight into the margin of improvement possible in the existing process, and whether the margin of improvement is sufficient, or is there a need for a radical change in the way the process is carried out, to support the sustainability on a larger scale. The next chapter of the study focusses on understanding this aspect.

3.3 Summary

This chapter presented a summary of interrelated sustainability metrics through construction of a novel “metrics quadrant plot”. The metrics quadrant plots offer an interrelation between selected broadly accepted metrics such as: (i) Primary energy use (E), (ii) GDP per capita, and (iii) the human development index, HDI. The rate of change of these metrics and their interrelations can offer an insight into the state of sustainability of a global, regional, country, sector, etc., realm considered.

In the next chapter, a detailed study of an existing technology (Controlled Atmosphere Brazing) in terms of the actual energy resources use, and subsequently the minimum energy limit for performing the task is presented. The so established margin, identified across all the technologies, may offer an insight into the diminishing margins of the looming limits of energy resources use at the global scale.

Chapter 4: CASE STUDY: CONTROLLED ATMOSPHERE BRAZING

4.1 Introduction

A study of energy resources use for a manufacturing process must account for all the energy flows along the path of transforming input material streams into the products[21]. All the energy transformations along the path should be considered and the associated transformation losses must be accounted for. The case study presented herewith provides, for a controlled atmosphere brazing process, a comparison between actual energy use and the minimum (theoretical) energy required to accomplish the objective. The theoretical minimum work required for accomplishing a particular task can be used as an effective metric to study inherent second law inefficiencies associated with a process. Comparison between the theoretical minimum energy requirement and the actual energy use for a state of art manufacturing process can be used to highlight the energy intensiveness of the process. As a case study to elaborate this point, experiments were conducted on an experimental controlled atmosphere brazing furnace located in the advanced brazing facility at the University of Kentucky.

With an objective of finding the actual energy use for the process, a series of tests were performed to analyze the mass and energy flows into and out of an experimental controlled atmosphere brazing (CAB) furnace. The primary energy source for operation is electrical energy which is converted to heat utilizing joule heating. This is accompanied by mass flows associated with the nitrogen flow for maintaining a controlled atmosphere and quenching post experiment.

4.2 Experimental Setup

The controlled atmosphere brazing (CAB) furnace, manufactured by Centorr vacuum industries, is a resistively heated, hot-wall tube furnace. The experimental CAB furnace is presented in Figure 4-1. The equipment consists of a central cylindrical hot zone which is fabricated from clear fused quartz glass tubes. A proprietary high reflectance coating on the inner tube reflects majority of the radiation heat into the hot zone while simultaneously allowing visible light to pass through[53].

Figure 4-1: Experimental CAB furnace

This acts as a thermal insulation for the furnace while providing outstanding view of the process occurring within the hot zone. A clear fused quartz process chamber, located within the hot zone, provides a clean, dry, controlled atmosphere environment for the brazing process. The dimensions of the hot zone cylindrical volume are 4.5” inner diameter x 10” length. The furnace is equipped with a programmable temperature control and data recording capability.

The process chamber is equipped with a work platform on which the sample to be brazed is placed. The work platform can be retracted from process chamber by sliding it linearly to allow for changing and placement of sample, and thermocouple placement. The sample is heated using joule heating using electrical heater coils wound around the transparent inner quartz tube. Power supplied to the heater coil is a single phase 240V AC supply. In order to maintain the controlled atmosphere, nitrogen which is initially stored in a separate tank is supplied to the hot zone chamber. Flowrate for the nitrogen is controlled using the control panel on the furnace setup. The hot zone chamber is fitted with a work platform on which the sample to be brazed can be placed. Figure 4-2 shows the schematic for furnace setup.

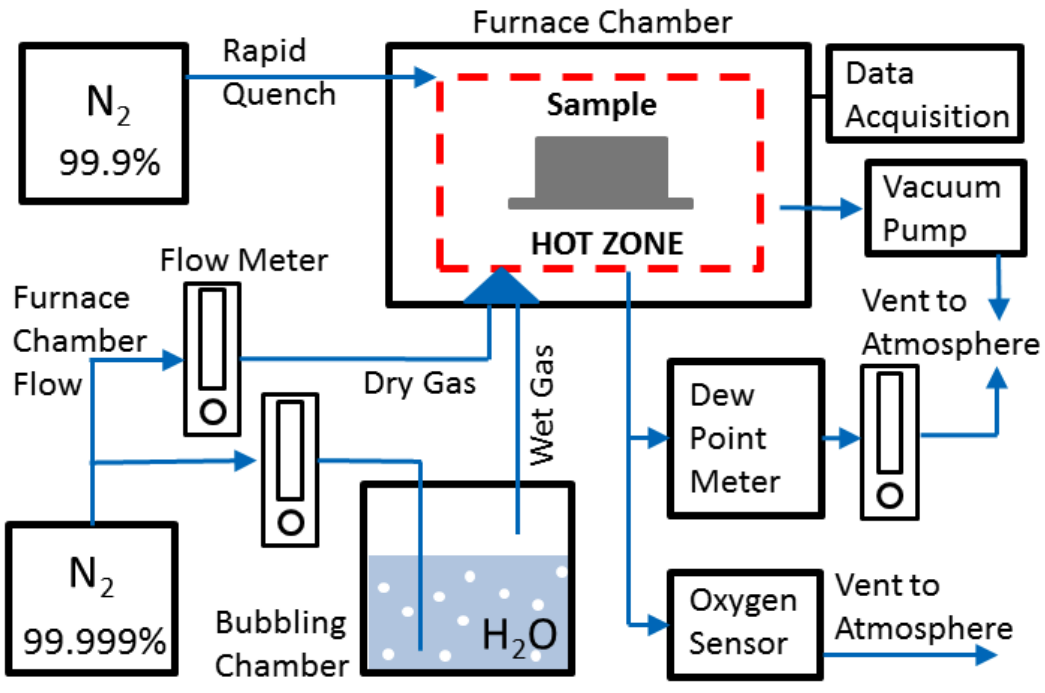

Figure 4-2: Schematic for CAB furnace (Adapted from [54])

With the objective of measuring the energy flows into and out of the furnace, it should be noted that the energy input into the system was preliminarily electrical work input. The electrical energy input was measured by installing Fluke 1735 Power logger to the electrical input supply of the furnace. Figure 4-3 depicts the block diagram for experimental setup. As shown, the system boundary was defined as the hot zone and other auxiliary equipment due to the constraints of attaching the power logger to the incoming power supply. Since the ultimate objective was to obtain energy flow into the hot zone of furnace, auxiliary equipment was initially operated without activating the CAB heater and these power readings were then set as baseline level.

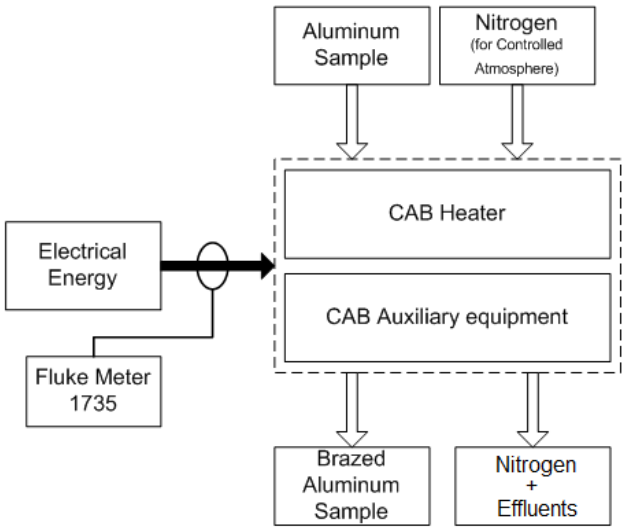

Figure 4-3: Experimental Setup Block Diagram

The Fluke 1735 Power logger is a power quality investigative tool which can be used to voltage, current, and power studies for determining loads[55]. For the purpose of this study, current and voltage probes for the logger equipment were installed on the supply power to furnace.

Schematic for single phase connections using the Fluke power logger is shown in Figure 4-4.

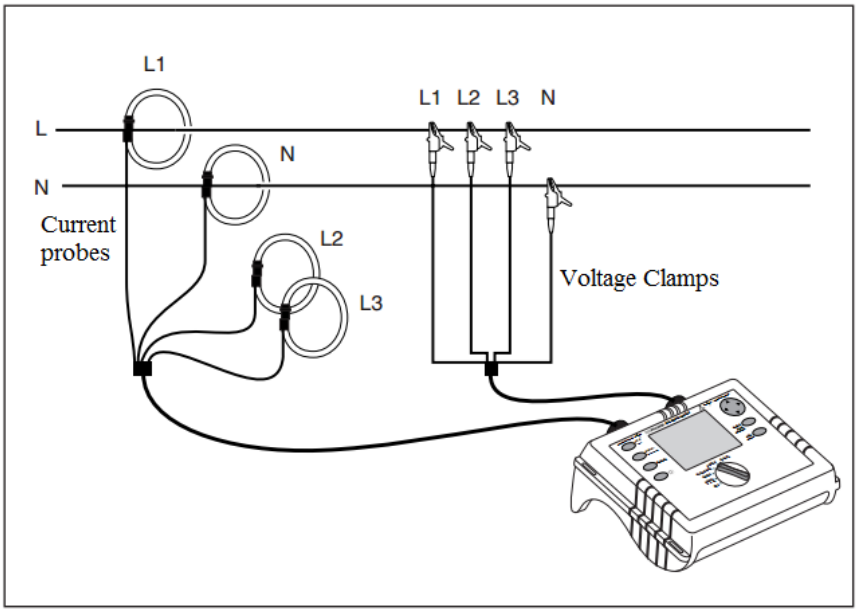

Figure 4-4: Power logger connections (Adapted from [55])

In order to quantify the energy interactions involved in the study, thermocouples were placed on the equipment to measure temperatures of flows entering and exiting the system boundary. Table 4-1 and Figure 4-7 provide details of locations for the thermocouples. Mass flow rates for the nitrogen flow during the experiment were adjusted based on the standard operating procedure for the CAB furnace [53] and were confirmed on the gauges on the setup.

Heater and work temperatures were measured using K type thermocouples (Omega KMQXL-032G-6) and data was recorded via the data acquisition system built into the furnace setup. Similarly, work piece temperatures were measured at two locations as indicated in Figure 4-7 (b) and recorded via the furnace data acquisition system.

Temperature of the outer shell of the furnace was recorded to calculate the convection and radiation losses from the furnace. This was achieved by installing four thermocouple probes (Omega KMQXL-032G-6) as shown in Figure 4-7 (a). The data for these thermocouples was recorded using National Instruments (NI 9211) thermocouple input modules. Data from the modules was logged on a PC using LabVIEW. Modules were connected to the PC via National Instrument USB chassis (NI cDAQ-9172). Block diagram for this setup is presented below in

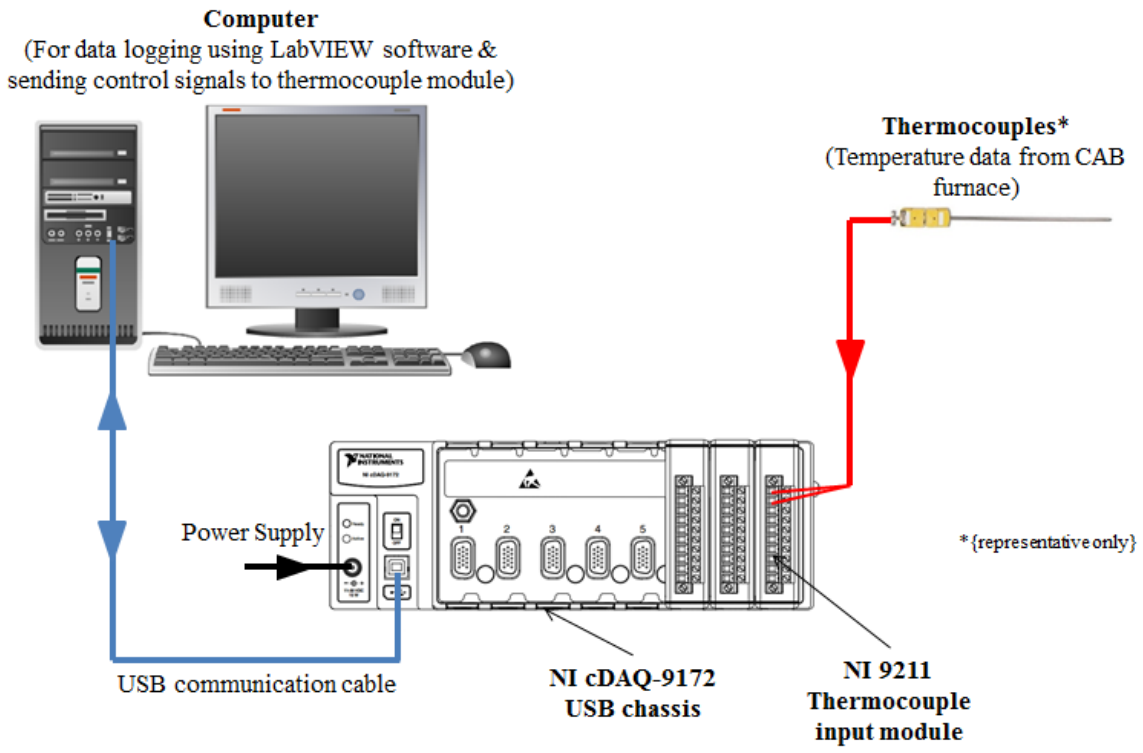

Figure 4-5: Block diagram – Thermocouple data logging setup (adapted from [56, 57])

Nitrogen outlet temperatures for chamber flow and quenching flow were measured using Omega TC-K-NPT-U-72, pipe plug thermocouple probes in order to obtain a direct contact with the gas flow and reduce the measurement error to the extent possible.

Additionally, temperature at the intersection of the horizontal galls tube and aluminum flanges holding the glass tubes was measured to account for heat transferred from the hot zone to the supports via conduction, and in turn lost to the atmosphere via convention and radiation from the flanges.

Ambient temperature for the duration of experiment was measured using Onset HOBO ambient temperature data logger. The logger position was chosen such that it was not affected by other sources and provided a true reading.

Further information on the measuring equipment mentioned in this section along with their uncertainties are provided in Appendix 5.

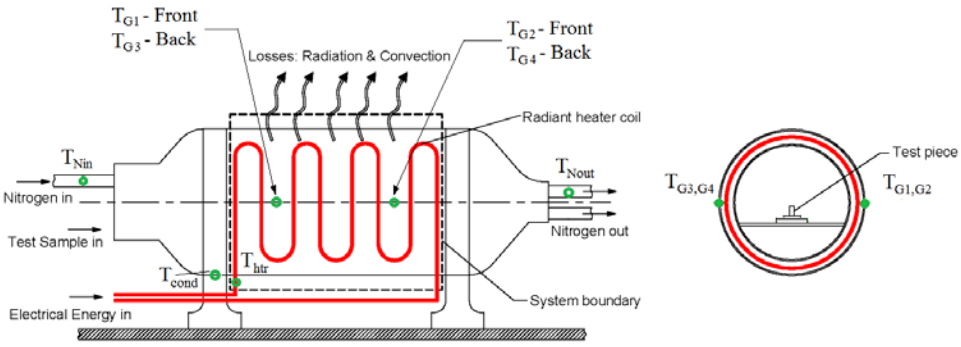

Figure 4-6: Thermocouple locations

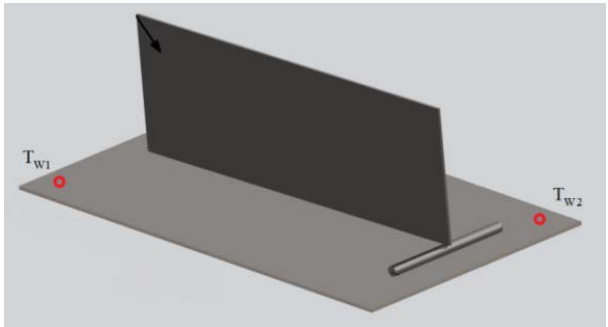

Figure 4-7: Work piece Thermocouple locations

Table 4-1: Thermocouple Locations

Nomenclature	Description	Thermocouple	Location	Data Acquisition
T_{htr}	Heater temperature	Omega KMQXL-032G-6	Refer Fig 4.5	Furnace Data Acquisition System
T_{W1}	Work piece temperature 1	Omega KMQXL-032G-6	Refer Fig 4.6	Furnace Data Acquisition System
T_{W2}	Work piece temperature 2	Omega KMQXL-032G-6	Refer Fig 4.6	Furnace Data Acquisition System
Ti_{N}	Nitrogen inlet temperature	N/A	Refer Fig 4.5	Data not logged. Single point readings.
To_{Nc}	Nitrogen outlet temperature for chamber flow	Omega TC-K-NPT-U-72	Refer Fig 4.5	Onset Hobo data logger #U12-014
To_{Nq}	Nitrogen outlet temperature for quenching flow	Omega TC-K-NPT-U-72	Refer Fig 4.5	Onset Hobo data logger #U12-014
T_{G1}	Outer glass temperature 1	Omega KMQXL-032G-6	Refer Fig 4.5	LabVIEW
T_{G2}	Outer glass temperature 2	Omega KMQXL-032G-6	Refer Fig 4.5	LabVIEW
T_{G3}	Outer glass temperature 3	Omega KMQXL-032G-6	Refer Fig 4.5	LabVIEW
T_{G4}	Outer glass temperature 4	Omega KMQXL-032G-6	Refer Fig 4.5	LabVIEW
T_{cond}	Temperature at intersection of glass and aluminum flange	Omega KMQXL-032G-6	Refer Fig 4.5	Onset Hobo data logger #U12-014
Ambient (T_{amb})	Ambient temperature	N/A	-	Onset Hobo data logger #U12-012

4.3 Sample Configuration

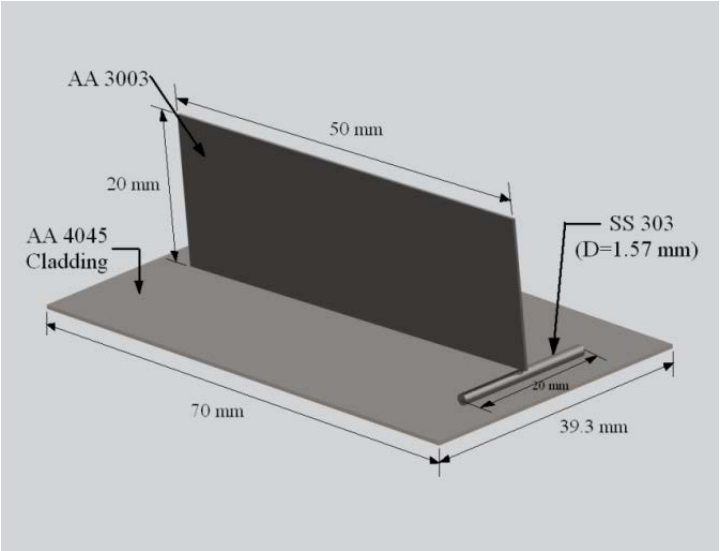

Figure 4-8: Sample Configuration

The sample, for which the brazing tests were conducted, was a T-joint specimen (Figure 4-8) which consisted of two sheets of Al-Si alloy held perpendicular to each other. The horizontal sheet selected was 70 x 39.3 mm and the vertical sheet was 20 x 50 mm. The vertical sheet was held at an angle with respect to the horizontal sheet. This was accomplished by balancing one end of the vertical sheet on a 1.57 mm diameter stainless steel rod. The arrangement was held in position using a stainless steel wire tied around the sample. The purpose of maintaining the vertical sheet at an angle was to obtain a variable clearance gap between the plates for the brazing joint formation. The length of travel of the filler metal was used for inferring the braze ability for a particular material composition and conditions inside the hot zone. Previous[58] and current research in the brazing laboratory focuses on the effects of changing conditions and material compositions on braze quality. These effects of change in the material composition and

the conditions are a part of separate studies and are beyond the scope of the work presented in this document.

The brazing sheet comprises of a core alloy over which a thin layer of cladding is bonded by roll bonding process[59]. Figure 4-9 shows a magnified image of the cross section for a typical brazing sheet. The core alloy and cladding composition are chosen such that the meting point range of cladding material is lower than that of the core alloy. The core provides structural integrity while the cladding melts during the controlled atmosphere brazing process to provide the joint.

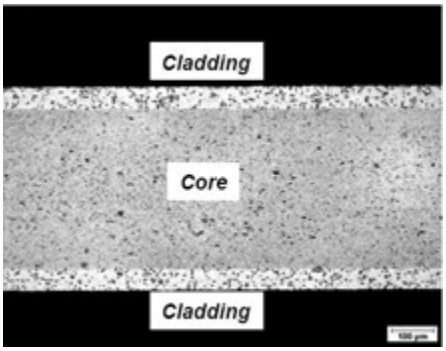

Figure 4-9: Typical Brazing sheet cross section(Adopted from [59])

The sample used for the experiments had AA 3003 as the core material and AA 4045 as the cladding. The brazing process to leads to melting of the clad (over the horizontal mating surface) and the molten phase driven by surface tension fills the gap forming the characteristic filet in the joint upon solidification. Hence the bonding of the two mating surfaces is accomplished by a phase change of a small quantity of clad. The solidus temperature of the clad is 577ºC. Chemical composition for AA 3003 and AA 4045 are provided in Appendix 4. Since the objective of this study is to analyze the energy flows, details for the sample preparation and brazing process are not provided. Details about the process of aluminum brazing using controlled atmosphere brazing are provided in [27]

4.4 Experimental Procedure

At the start of the experiment, vacuum is created in the system in order to allow for moisture particles and other eventual effluents to be removed. The next step is purging in order to flush the system and attain the required moisture/oxygen levels. In this case nitrogen is used for purging because of its inert nature which reduces oxidation. The experiments conducted for the case study involved a flow of high ultra-purity nitrogen gas (Specifications in Appendix 4) at 30± 2.5 psi and a flow rate of 2.0 x 10^{-5} m^3/s for approximately 3 hours. The system has an oxygen sensor to monitor the O_2 ppm. For the tests conducted, O_2 levels of 20±0.5 ppm were maintained to achieve the quality of joint desired.

After purging, the temperature profile for furnace was set using the control software. The temperature profile (set using software) used for the tests is divided into 5 phases as shown in Figure 4-10 below.

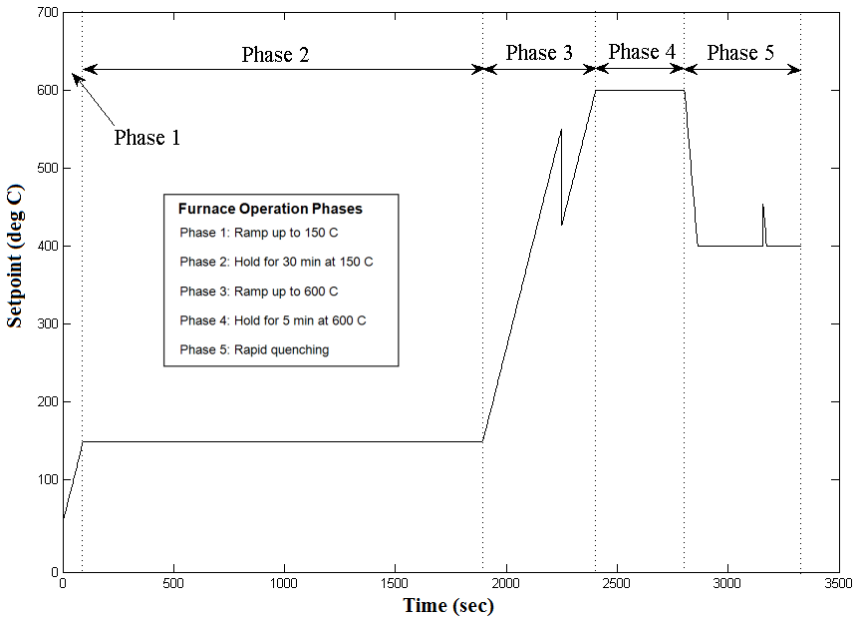

Figure 4-10: Set point profile - CAB testing

Table 4-2 presents the set point profile utilized for the experiments. In order to ease the analysis of the different profiles encountered to reach the temperature range to be maintained for melting of the clad alloy, the profile was subdivided into phases described in Figure 4-10. The setup houses a PID controller which controls the input power to the brazing chamber heating coil in order to achieve and maintain the temperature in the chamber in the melting point zone for the clad material.

Table 4-2: CAB set point profile - Phases

Phase	Description
Phase 1	Ramp up to 150°C at a rate of 100°C/min
Phase 2	Hold for 30 minutes at 150°C
Phase 3	Ramp up to 600°C at a rate of 50°C/min
Phase 4	Hold for 5 minutes at 150°C
Phase 5	Rapid quench to 400°C

Phase 1: Preheat Ramp up:

The initial phase for the brazing temperature profile consisted of ramp up of temperature to 150°C at a rate up to 100°C/min. This phase allows for the test sample to reach from room temperature to 150°C at a controlled specified ramp rate.

Phase 2: Soaking phase:

The second phase maintains the sample at 150°C for 30 min. This allows the furnace to preheat uniformly and to achieve a stable condition in the hot zone. High purity nitrogen is constantly circulated through the system at a flowrate of 2 SCFH (3.398 m^3/hr). The traces of oxygen are below 50 ppm.

Phase 3: Ramp up to brazing phase:

The third phase increases the temperature of the hot zone (area near the test piece) to 600°C at a rate of up to 50°C/min. The peak temperature is selected based on the alloy

composition of the cladding and base material. For the experiments conducted for this study the base material used was AA3003 and clad alloy was AA 4045. Properties for these alloys are provided in Appendix 4

Phase 4: Brazing phase:

In this phase the temperature of hot zone is maintained at 600°C for 5 min. This allows the PID controller to correct the actual temperature values and achieve a controlled work temperature. During this phase the clad material melts and the joint is formed by surface tension driven flow of metal into the joint.

Phase 5: Rapid quench:

During this segment the sample under test is cooled down from melting point temperature to 400°C by using industrial grade nitrogen; flow at rate of 20 SCFH (33.98 m^3/hr). After reaching 400 °C, the flow of nitrogen and power to the brazing setup is stopped and the sample is allowed to cool down to atmospheric temperature by natural convection.

The experimental approach started with a real time in situ data collection for determining the energy rates (electrical power and enthalpy rates of the main and auxiliary material flows) delivered to the hot zone. Furthermore, it involved a series of measurements of characteristic temperature histories (using temperature sensors as outlined in the experimental setup section), needed for determining enthalpy flows of outgoing material streams and heat transfers into the surroundings. Additionally, for qualitative analysis and depiction of heat transfers, thermal imaging of the hot zone was carried out for the entire duration of the experiment.

Appendix 7 provides thermal images of the setup at certain timestamps during the process. Note that due to the high reflectivity construction of the hot zone chamber, the thermal images were captured strictly for qualitative purposes only and temperature information from the thermal imaging was not used for any heat loss calculations.

4.5 Summary

The experimental setup and procedure described in this section were designed to measure the energy resource use for a Controlled Atmosphere brazing process. This is calculated by measuring the input and output parameters that could be used to assess energy inputs and outputs, and the losses to surroundings. The main objective of this study is to quantitatively compare the magnitude of energy consumed by a state of the art process and the minimum energy required for achieving the desired outcome, i.e. brazing of test piece joint in this case; and to understand the losses associated with the process in order to assess the sustainability of the process.

In the next chapter, results for the experiments are presented and a comprehensive evaluation regarding the various energy streams is provided. Furthermore, an energy mapping analysis is provided and comparison of energy use for controlled atmosphere brazing and other processes is discussed.

Chapter 5: RESULTS AND DISCUSSION

5.1 Experimental Result Analysis

The objective of this section is to discuss the experimental results for the controlled atmosphere brazing experiments. The first section of this chapter provides details of power and temperature measurements that were captured during the case study of Controlled Atmosphere Brazing.

Additionally, in order to compare the energy resources requirements into and out of the system for formation of a brazed joint with the theoretical minimum amount of energy required for the task, the second section will provide the basis for computing the theoretical minimum work.

This is followed by energy mapping represented by Sankey Diagram, which presents a pictorial quantitative analysis of energy flows into and out of the system under consideration (CAB Hot Zone) based on the measured values.

The chapter will conclude with the presentation of the case study results using the energy graph discussed in the previous sections of this document.

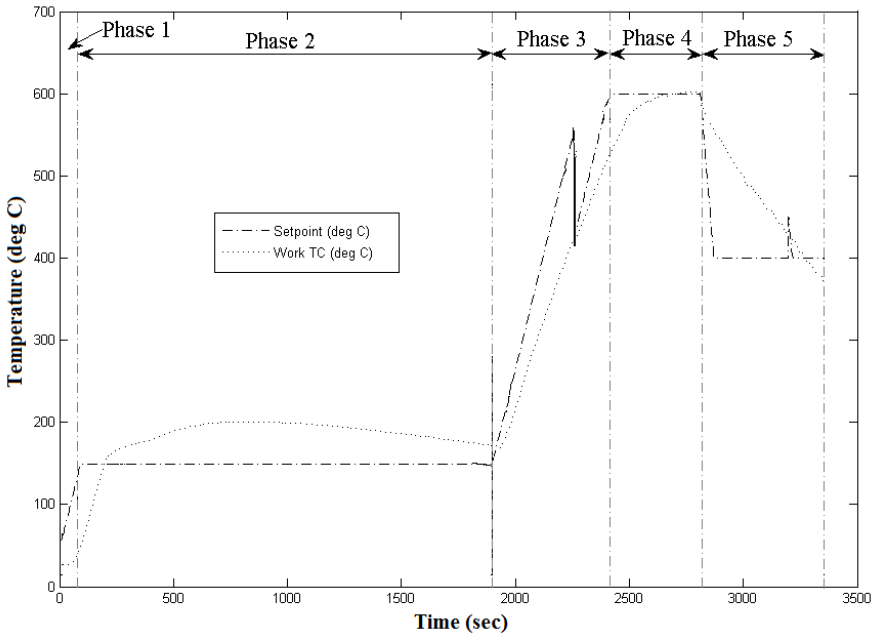

Figure 5-1: Comparison: Set point and Work temperature

Figure 5-1 presents the work temperature plotted along with the set point temperature. As it can be observed, with the PID control (as described in the earlier chapter), the system always tries to attain the work piece temperature close to the set point values. In doing so, we can observe that the work piece temperature overshoots during phase 2 and tries to converge to the set point of 150°C. However the main objective is to maintain the work temperature in the melting point range of the cladding alloy. This can be observed in Phase 4 where the work temperature in the final 2 minutes of the phase, converges to the set point value thus enabling to form the brazed joint. After completion of the brazing process, the rapid quench phase (Phase 5) begins and the work piece starts to cool down.

Input Electrical Energy

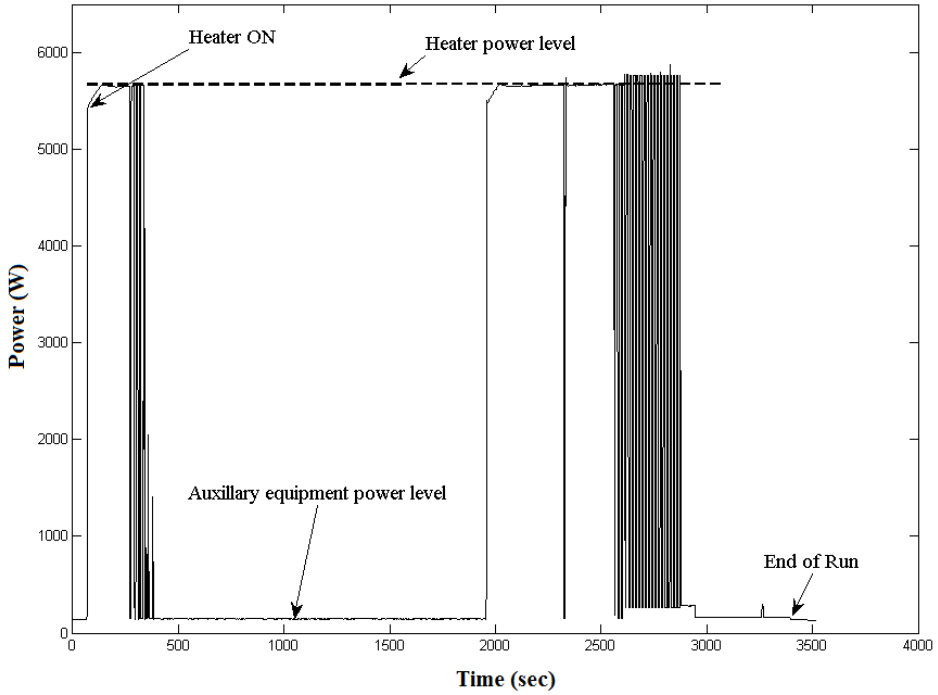

Figure 5-2: Power v/s Time plot for CAB furnace

In order to compare the magnitude of the Actual Energy Resource Use to the Theoretical Minimum Energy needed to complete the task, all energy inputs need to be quantified. As mentioned in the previous sections, the source of input to the system was electrical energy. To assess the magnitude of the electrical energy input, a power logger (Fluke 1735) was attached to the 240 V single phase input supply. Details of the setup are presented in the previous section. Measurement uncertainties are presented in Appendix 5. Figure 5-2 displays the plot for power data logged over the duration of the experiment. The power data (Watts) was recorded at 1 second intervals and the overall energy use (kJ) for the complete process (Transient in nature) was calculated employing numerical integration techniques using Microsoft Excel. Details of Energy use computation are provided in Appendix 2-b.

Energy data was measured for a total of 19 experimental runs. *Table 5-1* provides the measurement values for the final 7 experimental runs.

Table 5-1: CAB Energy consumption

Experiment #	Total setup Energy consumption (kJ)	Auxiliary equipment Energy Consumption (kJ)	Heater Energy Consumption(kJ)
13	5900	454	5546
14	6023	469	5554
15	6056	478	5578
16	5945	434	5511
17	6076	492	5484
18	6055	479	5576
19	6057	482	5575
Average	**6016**	**470**	**5546**
Std. Dev.	**67**	**20**	**51**

the repeatability of the experiments was confirmed by ensuring that the readings are within the acceptable limits, Standard Deviation of ±51 kJ (Based on the requirements of this study)[50]. Only one set of data (Experiment#19) at 10 second intervals is provided in Appendix 2-b for simplicity. However it should be noted that Power readings were captured at 1 second intervals and aggregated to energy use. Also, all the temperature and energy data presented in this document is for Experiment #19 which is ultimately used to create an energy balance for the system. Complete dataset is available in digital form in the file “Rahul Thesis Data”, stored in the Brazing laboratory.

The Auxiliary equipment power level indicated in Figure 5-2 consisted of power supply to all the equipment such as pumps, fans, control panel etc., i.e. equipment except the heating coil.

As mentioned in the previous sections, heat required for the brazing operation is generated using a resistance coil placed over the hot zone. It is evident from the comparison between the power consumption and heater temperature profile (Figure 5-3) that major portion of electrical power input is used by the heater coil. Also, since the objective of the study is to assess the energy inputs and outputs associated with the brazing operation, the system boundary was placed over the hot zone. Hence in order to calculate an accurate computation of the energy going into the system under consideration, power consumption by the auxiliary equipment was subtracted from the total power, so as to ensure that only the energy consumption of the heater coil is calculated.

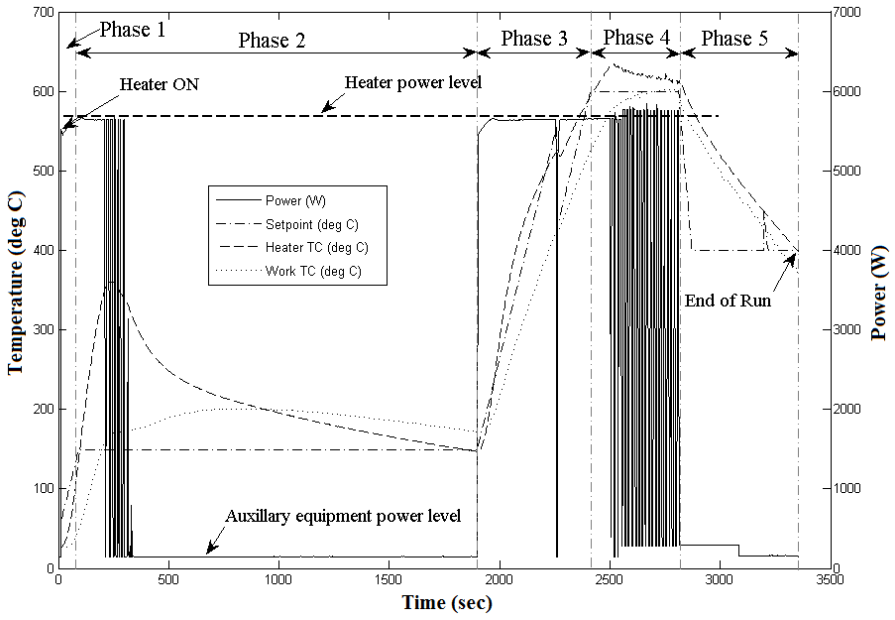

Figure 5-3: Power and temperature comparison for CAB furnace

The fluctuations in power levels in Phase 2 and Phase 4 are a result of the PID control which turns the power ON and OFF in order to converge and maintain the control value parameter close to the set point value.

The one fluctuation noticed in Phase 3 was observed in all the experiments. Upon further evaluation of the condition it was noted that this was due to the control logic set in the PID control. During Phase 1 and 2 the heater temperature is the control value and the PID control take the feedback from the heater temperature thermocouple to compare it to the setpoint. This is obvious from the fact that Phase 3 starts as soon as the heater temperature reaches setpoint value. This is acceptable since maintaining the work temperature is not very critical during the initial phases when the sample is just being heated up to the brazing temperature and helps in reducing the ramp up time and energy. However, in phase 4 it is of prime importance to maintain the work piece temperature within the clad melting range. Hence the control value switches from heater temperature to work piece temperature, during phase 3. This is indicated by the fluctuation noticed in phase 3.

Energy associated with Nitrogen Flow

As explained in the previous chapter, nitrogen was utilized during the experiments for two different purposes. The first was to provide a constant flow at 3.398 m^3/hr (2 SCFH) to maintain a controlled inert atmosphere during the brazing process. This is identified as “Chamber flow”. The other nitrogen flow was utilized for rapid cooling of the component post brazing. This is identified as “Quenching flow”. Quenching flow was 33.98 m^3/hr (20 SCFH)

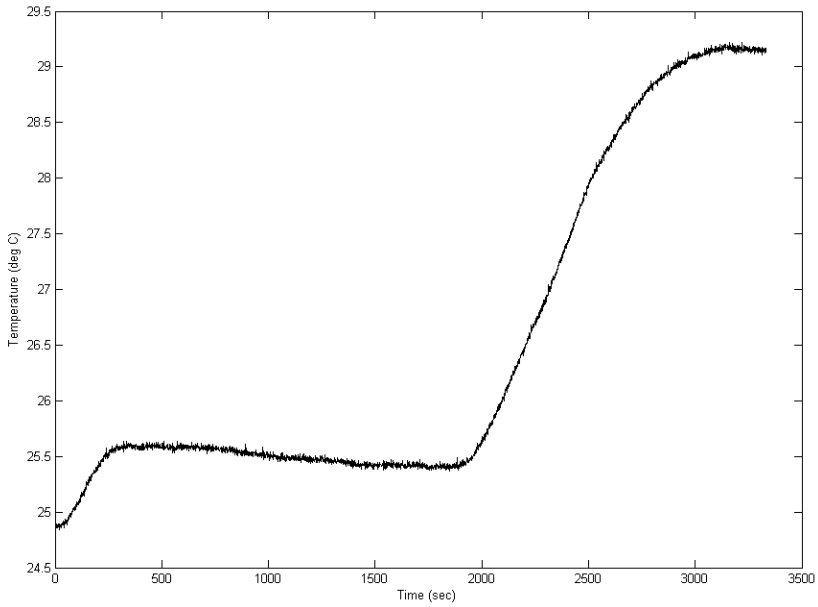

a: Chamber flow (Controlled atmosphere)

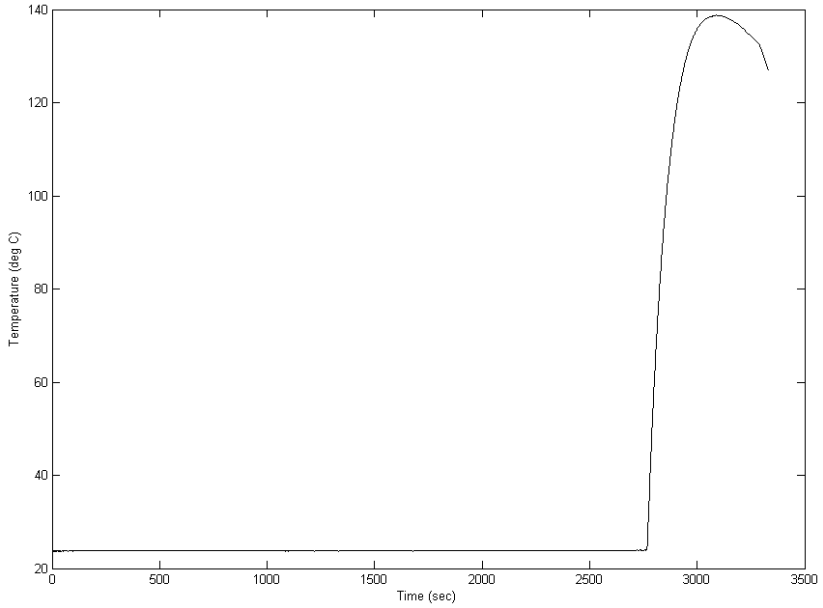

b: Quenching Flow

Figure 5-4 : Nitrogen flow

The figure above (Figure 5-4) presents the temperature data measured for the chamber flow and quenching flow. The temperature of nitrogen at the inlet to the system was assumed to be at ambient temperature, as the nitrogen cylinder was held at the ambient

conditions in the brazing laboratory and was separated from other equipment to eliminate the effects of heating or cooling due to process losses. The outlet temperatures were measured at location indicated in *Figure 4-6* and *Table 4-1*. As it can be expected, the chamber flow temperature profile follows a similar trend to the heating profile, while quenching flow shows a flat line with a spike in the later stage (Stage 5) since it only operates once the joint formation is complete. It can be noted that even though the chamber flow temperature readings follow the trends and profiles for the heater, sample, and hot zone outer surface temperature, the change in temperature is low compared to the other temperatures captured. This may be attributed primarily to the interplay between flow rate of the gas, design of the furnace for maximizing radiative heat transfer and a relatively low convective heat transfer when compared to the radiative transfer from the heater coil to the sample (Gas is non-participating in the radiation interaction). Additionally there were location constraints for placing the thermocouple further downstream due to the nature of construction of the furnace, resulting in complex heat transfer interactions within the experimental setup outside the hot zone.

Temperature for both the chamber flow and quenching flow was measured at one second intervals. With the mass flow rate controlled, and temperature data available, Enthalpy of nitrogen leaving the control volume was calculated for each interval and aggregated together to obtain values for Nitrogen enthalpies in the five different segments and the total process. Table below presents the aggregated inlet and outlet enthalpy values for the different segments for both the chamber flow and quenching flow.

Table 5-2: Nitrogen Inlet and outlet enthalpy (kJ)

N_2 Flow	Phase 1	Phase 2	Phase 3	Phase 4	Phase 5	Total (during Experiment)
Chamber Flow (H_{in})	0.51	10.19	4.53	0.68	2.94	**18.86**
Chamber Flow (H_{out})	0.51	10.26	4.58	0.69	3.00	**19.03**
Quenching Flow (H_{in})	-	-	-	-	29.45	**29.45**
Quenching Flow (H_{out})	-	-	-	-	38.95	**38.95**

Appendix 3-D provides the calculations and data for Chamber flow nitrogen and Appendix 3-E for Quenching flow. Again, as it was already noted for temperatures, the flowrate at which the chamber flow nitrogen is circulated (since it is needed only to maintain an inert atmosphere), and the change in temperature while Nitrogen passes through the hot zone, result in a very small amount of outgoing enthalpy values. Similar to electrical energy, the data presented in Appendix 3-D and 3-E are presented at 10 second intervals for simplistic representation. Also the data presented is for experiment #19 to aid in the construction of energy balance for the system. Complete data set is available in electronic format.

Energy losses to the surroundings

One of the objectives of the study was to assess the majority of losses associated with the CAB process to gain an insight into further areas of improvement. The main focus of the study was the control volume denoted as the Hot zone as described in the experimental setup section. For the cylindrical hot zone chamber, the means of heat transfer to the

surroundings are convection over the hot zone exterior, radiative heat transfer from the outer surface, and conduction from the hot zone to the aluminum flanges supporting the hot zone. The thermal energy that came into the CV in the mode of electrical input was obviously transferred to other parts of the equipment. This was quantified as remaining thermal energy for each phase which in turn is lost to the atmosphere as the equipment exchanges thermal energy with the surroundings post the experiment. Details of calculations for the convective, Radiative and Conductive (to the flanges) losses are provided herewith. In order to estimate the heat losses due to convection and radiation, four thermocouples were placed on the glass shell of the furnace as shown in Figure 4-6 and described in Table 4-1. Measurements were taken at 1 second intervals to get the external surface temperature profile.

Figure 5-5 below presents a comparison between the heater temperature, work temperature and hot zone external temperature through the experiment duration. This graph indicates the process of conversion of electrical energy to thermal energy and its dissipation to the surroundings.

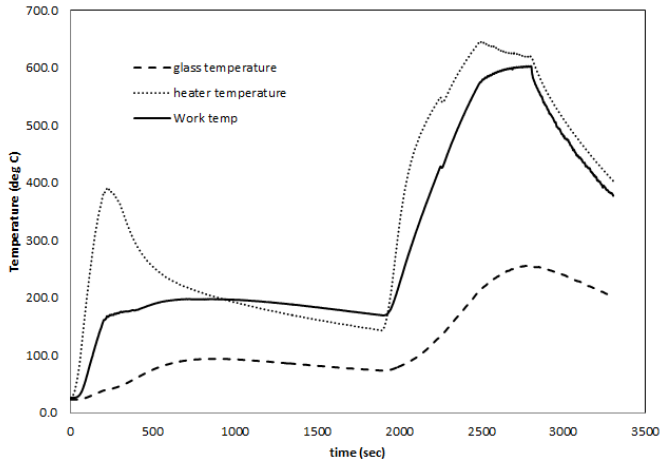

Figure 5-5: Hot zone temperature profiles

Figure 5-6 below presents the temperature profile for the average temperature of the hot zone outer surface during the experiments. The calculations for heat transfer to surroundings are based on this average temperature profile. Appendix 2-C provides the table with temperature values used for the calculations.

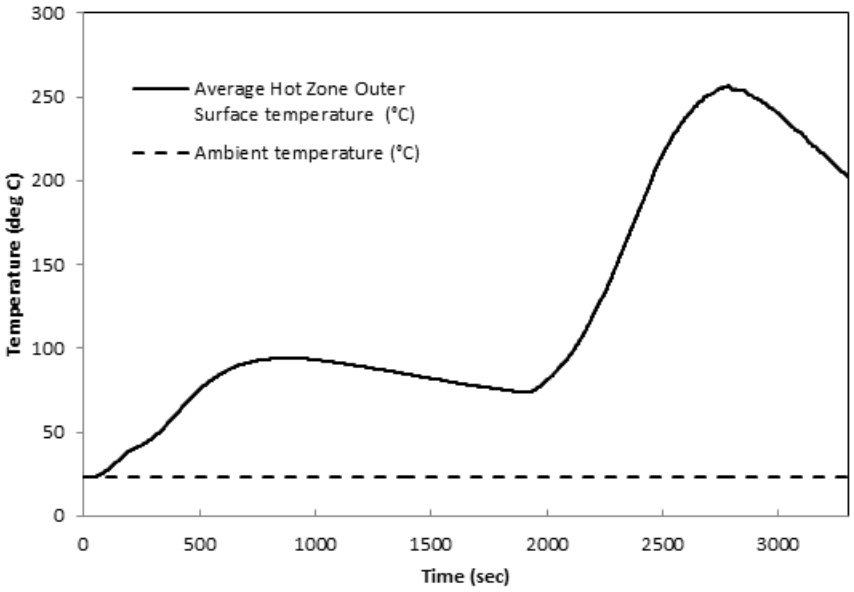

Figure 5-6: Hot Zone average outer surface temperatures – During Experiment

To quantify the possible heat loss mechanisms post the experiment duration, temperature data from the same 4 sets of thermocouples was recorded till the experimental setup reached equilibrium with the surroundings. (i.e. until the point at which the temperature of the setup and surroundings equalized). This was then utilized to compute the direct convective and radiative heat transfers to the surroundings post the experiment completion. Figure 5-7 below presents the average temperature profile based on the readings from these thermocouples. Appendix 2-D provides the values of the average temperature readings for hot zone outer surface post experiment. Note that the values presented in Appendix 2-C are provided at 10 second intervals, and the values provided in Appendix 2-D are presented at 1 min intervals. The actual measurements and

calculations were performed at 1 second intervals, detailed tables for which are available in the folder “Rahul Thesis Data” on the Brazing laboratory server.

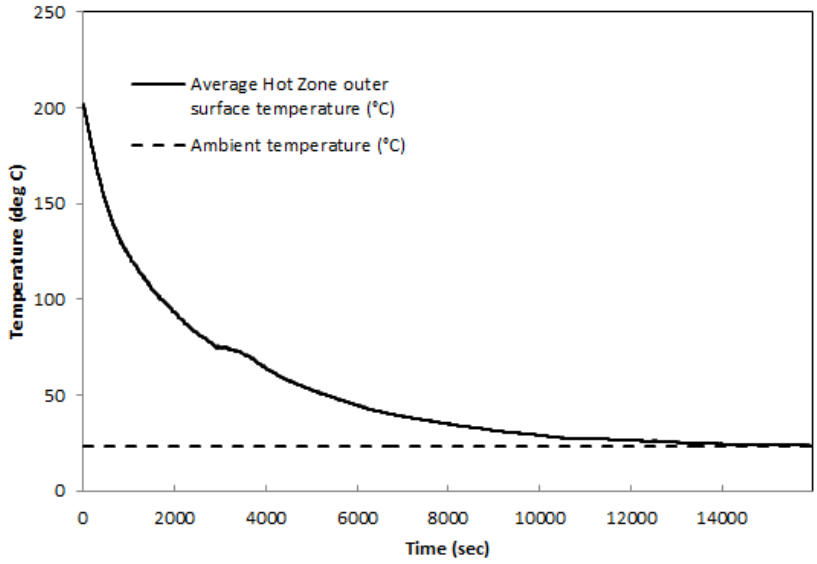

Figure 5-7: Average Hot Zone surface temperature – Post Experiment

Convection over hot zone

Convection losses over the furnace were calculated by considering the hot zone as a horizontal cylinder and assuming natural convection over a horizontal cylinder. For the purpose of this study, air was assumed as ideal gas. For calculating the convective heat transfer, it was assumed that the process is steady in the 1 sec duration. Hence, the Convective heat transfer to the surroundings was calculated for each second using the following formula

Equation 5-1

$$q_{conv} = h\,A\,(T_{ga} - T_{amb})$$

Where,

h = Convective heat transfer coefficient, W/m^2K

A = Exterior Surface area of Hot zone, m^2

T_{ga} = Average temperature of the hot zone exterior surface, °C

T_{amb} = Ambient temperature, °C

The Energy loss associated with the convective heat transfer was then calculated by integrating these values over the experimental timeframe. Similar calculations were also done for the direct convective heat loss post experiment. These values for each of the five phases and total during and post experiment are provided in *Table 5-3*

Table 5-3: Energy Loss due to convective heat transfer (kJ)

Phase 1	Phase 2	Phase 3	Phase 4	Phase 5	Total (during Experiment)	Total (Post Experiment)
0.03	108.3	125.2	40	164.6	**431.1**	**497**

Heat transfer coefficient was calculated as free convection over the hot zone. The hot zone was assumed as a horizontal isothermal cylinder. Details of the calculations and formulations associated with the heat transfer coefficient are provided in Appendix 3-A. Note that apart from the direct convective heat losses from the hot zone (which were

captured), there was convective heat transfer from the other parts of the setup which could not be captured due to the complexity of the other system components such as valves, pipes, solenoids, flanges etc. These losses have been accounted for in the term "Energy dissipation from the Equipment" in the energy balance as the "rest of the balance," which is presented in an upcoming section of this chapter.

Radiation over hot zone

Similar to the convection losses, the radiation heat transfer losses over the furnace were calculated by considering the hot zone as a horizontal cylinder. An emittance of 0.93 was assumed for the entire quartz glass surface[60]. Outer surface temperature readings were recorded at 1 sec intervals. For calculating the radiative heat transfer, it was assumed that the process is steady in the 1 sec duration. Hence, the radiative heat transfer to the surroundings was calculated for each second using the following formula

Equation 5-2

$$q_{rad} = \varepsilon \pi D L \sigma (T_{ga}^4 - T_s^4)$$

Where,

ε = Emittance for the hot zone surface

σ = Stefan Boltzmann's constant, W/m^2K^4

D = Diameter of hot zone outer surface, m

L = Length of hot zone, m

T_{ga} = Average temperature of the hot zone exterior surface, K

T_s = Temperature of surrounding objects, K

The Energy loss associated with the radiative heat transfer was then calculated by integrating these values over the experimental timeframe. Similar calculations were also done for the direct radiative heat loss post experiment. These values for each of the five phases and total during and post experiment are provided in *Table 5-4*

Table 5-4: Energy Loss due to radiative heat transfer (kJ)

Phase 1	Phase 2	Phase 3	Phase 4	Phase 5	Total (during Experiment)	Total (Post Experiment)
0.1	140.1	208	83	323.8	**755**	**706**

Details of the calculations related to the radiative heat transfer are provided in Appendix 3-B. Note that apart from the direct radiative heat losses from the hot zone (which were captured), there was radiative heat transfer from the other parts of the setup which could not be captured due to the complexity of the other system components such as valves, pipes, solenoids, flanges etc. These losses have been accounted in the term "Energy dissipation from the Equipment" in the energy balance which is presented in an upcoming section of this chapter.

Conduction from Hot Zone to Flanges.

As shown in Figure 4-1, the hot zone for the CAB setup is supported in place by two aluminum flanges on either ends. In order to reduce the heat transfer from the hot zone exterior to the aluminum flange, the setup has ceramic foam insulation between the glass

exterior and the aluminum flange. In order to quantify the amount of heat conducted to the aluminum flanges thermocouple was placed between the intersection of the insulating material and the aluminum flange and temperature data was recorded at 1 second intervals during the experiment and after the experiment till the assembly was in thermal equilibrium with the surroundings. Note that the heat conducted to the flanges is ultimately lost to the surroundings by means of convection and radiation.

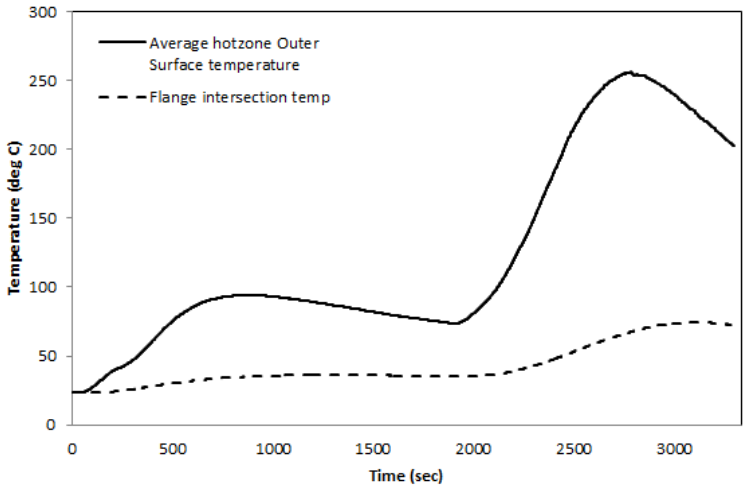

Figure 5-8: Flange intersection temperature

The figure above shows the temperature trends for the glass temperature and the flange intersection temperature during the experiment. At every instance, this then denotes the temperature on either side of the insulating material. The conductive heat transfer then is given by the 1 dimensional Fourier's law of heat conduction as follows:

Equation 5-3

$$q_{cond} = 2\,\frac{k\,A\,(T_{ga} - T_{int})}{x}$$

Where,

k = Coefficient of thermal conductivity for ceramic insulation material

A = Area of contact between flange and hot zone, m^2

x = Thickness of ceramic insulation, m

T_{ga} = Average temperature of the hot zone exterior surface, °C

T_{int} = Temperature at intersection of flange and ceramic insulation, °C

The Energy loss associated with this conductive heat transfer was then calculated by integrating these values over the experimental timeframe for two flanges (one on either end). Similar calculations were also done for the conduction heat loss post experiment. These values for each of the five phases and total during and post experiment are provided in *Table 5-5*

Table 5-5: Energy Loss due to conductive heat transfer (kJ)

Phase 1	Phase 2	Phase 3	Phase 4	Phase 5	Total (during Experiment)	Total (Post Experiment)
0.1	79.2	77.1	22.3	86.3	**265**	**268**

Details of the calculations related to the conductive heat transfer are provided in Appendix 3-C. Note that apart from this conductive heat transfer there was heat transfer to the other parts of the setup which could not be captured due to the complexity of the other system components such as valves, pipes, solenoids, flanges etc. These losses have been accounted in the term “Energy dissipation from the Equipment” in the energy balance which is presented in an upcoming section of this chapter.

5.2 Theoretical energy resource use

Theoretical energy resources use is defined as a thermodynamic limit needed to accomplish the phase change of an aluminum-silicon alloy treated in the experimental facility. The cross section of the bond is presented in *Figure 5-9.*

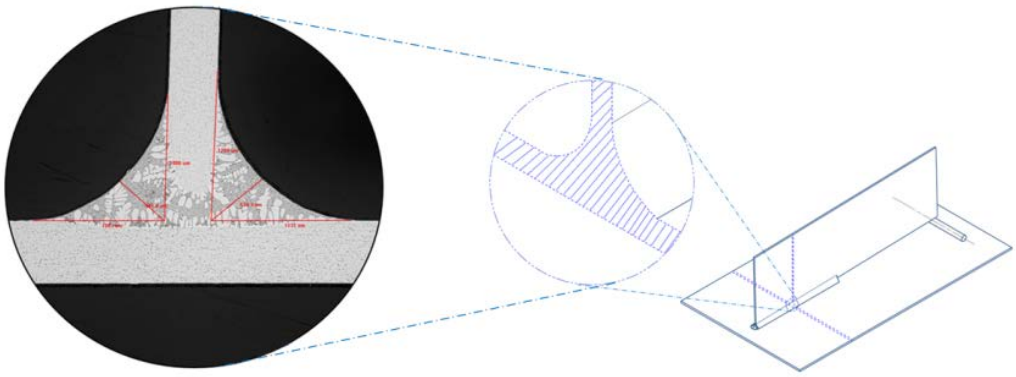

Figure 5-9: Brazed Joint

The brazing process leads to the melting of clad and the molten phase driven by surface tension fills the gap forming the characteristic fillet in the joint upon solidification. Hence the task of bonding two mating surfaces is accomplished by a phase change of a small quantity of clad.

The minimum energy resource use need for the Controlled Atmosphere Brazing case study was determined by considering the wedge shaped assembly as a solid state system heated up to the phase change point of the cladding material via convective, conductive and radiative heat transfer followed by the localized phase change of the clad.

Mass of brazing joint was calculated by firstly measuring the cross sectional area (indicated by red lines in Figure 5-9) along half the length of joint and multiplying it by length of joint and the density of cladding material. The brazing joint formed on the

sample is actually variable cross section, which was intentionally designed to facilitate a research study related to brazeability and joint formation. This joint formation effort was a part of parallel research and is out of scope as related to this thesis. For the purposes of this study, it was presumed that the joint is continuously variable with a constant taper. Hence, cross sectional area at the mid length of joint (as shown in the figure) was assumed to represent a uniform c/s along the entire length of the brazed joint.

Theoretical minimum amount of energy required to complete the brazed aluminum joint is defined as the energy that would be required for formation of joint irrespective of technology used.

Detail calculations are presented in Appendix 6. The amount of energy resources needed for performing the task by bringing mating parts to the peak temperature and melting the fillet material at the peak was ~3kJ (O 10^0 kJ) which indicates an margin three orders of magnitude less than the Energy input for the controlled atmosphere brazing process of 5575kJ (O 10^3 kJ).

If it's considered that the same task is performed with only local heating of the filet and melting the mass of aluminum alloy to form the joint, the energy resource use would be ~ $4x10^{-2}$ kJ (O 10^{-2} kJ), five orders of magnitude less. Apparently there is a very large margin for a reduction of the energy use in an actual process (that includes all the auxiliary energy resources need, as well as all the energy losses in the process) vs. the ideal process irrespective of technology of bonding based on the Controlled Atmosphere Brazing process.

5.3 Energy balance and assessment for CAB process

One of the primary objectives of this study was to map the energy interactions throughout the transient Controlled Atmosphere Brazing process. Based on the discussion provided in the earlier section of this chapter, an energy balance was created around the hot zone of the CAB furnace. This is presented below by employing a Sankey Diagram showing the energy inflows and outflows with the width of the arrows denoting the magnitude of each flow. As observed from *Figure 5-10* (Sankey diagram), there is a multiple orders of magnitude difference between the electrical energy that is supplied to the process and the amount of energy utilized by the sample for the mechanics of brazing joint formation, thus bolstering the claim for transformational technology development.

Note that in the diagram shown, to enable presenting the various flows at multiple orders of magnitude difference, energy flows with very low magnitude were represented by a minimum line width irrespective of their actual magnitude. The main system boundary for the study was the hot zone, and is denoted by the rectangle labeled “Furnace system boundary”. The electrical energy, nitrogen flows (chamber and quenching flow), Losses to surroundings, enthalpy of test piece are quantified. Furthermore, in order to present the transient nature of the process, the process was broken down into five phases, and the smaller system boundaries present the balance for each phase. Note that due to the transient nature, there is a residual energy component for each phase, which gets carried forward to the next phase. Eventually, only the energy that is either imparted into the brazing joint formation or utilized to maintain the non-reactive atmosphere using nitrogen is utilized, and all the other energy is lost to the surroundings as the system attains equilibrium with the atmosphere.

This type of analysis provides a guideline on areas of improvement in the existing process and/or a need for a completely different more efficient technology for completing the same task. For example, as it can be observed from the Sankey diagram, the most energy intensive step is the one in Phase 3, wherein it is required to raise the temperature of the entire assembly (base material + cladding) to a temperature higher than the melting point of the clad, and then allowing the cladding to melt to form the brazing joint. This infers that with a controlled atmosphere brazing process, if the process is carried out as per the current technology, i.e. heating of the entire part (not to include heating the surrounding hardware as well) and then melting the cladding, efficiency improvements for the existing process may not be sufficient to make a high impact. Hypothetically, if there would exist a technology (in the future) which could locally melt the cladding without expending tremendous amount of energy for heating the entire assembly and then cooling it back down, the resource use for completing the task would be much lower. The novelty here would not necessarily be localized heating (that can be done today by using tools like, e.g., laser or electron beam heating), but the ability to approach at the same time a myriad of locations in a complex assembly. This type of transformation technology development on all the processes would ultimately aggregate towards a more sustainable development on a larger global scale.

The table below presents the values of energy balance for each of the five phases for the CAB process.

Table 5-6 CAB process energy

Energy interaction (kJ)	Phase 1	Phase 2	Phase 3	Phase 4	Phase 5	Total
Electrical Energy	490	837	3941	288	19	5575
Convection losses over hot zone	0.03	108.3	125.2	40	164.6	438.1
Radiation losses over hot zone	0.1	140.1	208	83	323.8	755
Conduction to hot zone flanges	0.1	79.2	77.1	22.3	86.3	265
Chamber flow N2 – Inlet enthalpy	0.5	10.2	4.5	0.7	3.0	18.9
Chamber flow N2 – Outlet enthalpy	0.5	10.3	4.6	0.7	3.0	19.0
Quenching flow N2 – Inlet Enthalpy	-	-	-	-	29.4	29.4
Quenching flow N2 – Outlet Enthalpy	-	-	-	-	38.9	38.9
Al enthalpy (Experimental Estimation)	0.13	0.53	2.01	0.05	-1.06	2.71
End of phase residual thermal energy	489.6	998.5	4527.1	4669.8	4105.6	

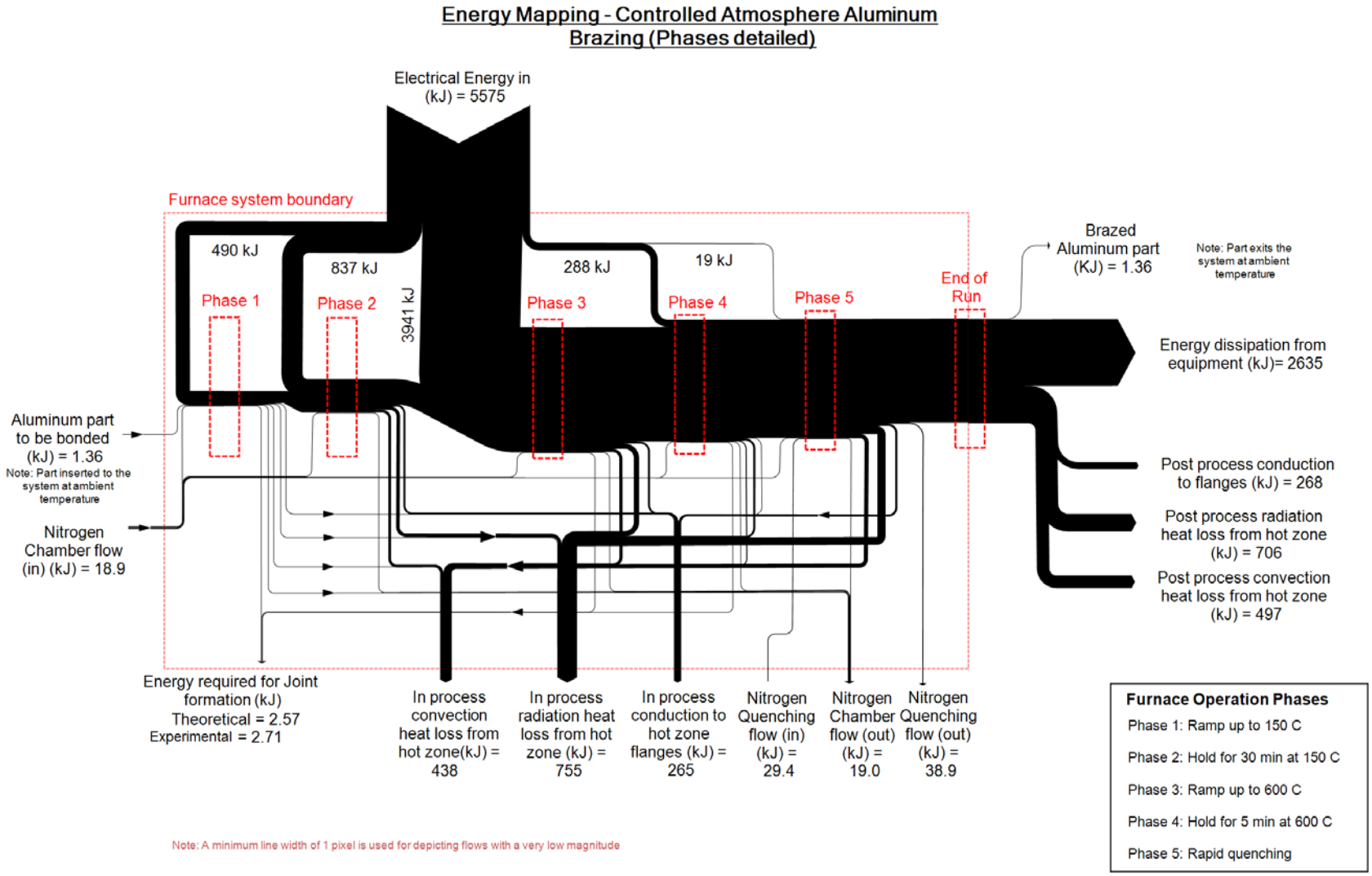

Figure 5-10: CAB furnace Sankey Diagram

Specific Energy Analysis

In the studies carried out by T. Gutowski and D. Sekulic[21], specific electrical energy use per unit of material processed have been analyzed and presented for 26 different manufacturing processes. The findings for different processes yielded specific power requirements in the range of 1-50kW. Figure 5-11 presents this data where the electrical requirements in joules/kg are plotted with respect to process rate in kg/hr. Each of the points or group of points on the plot represents specific electrical energy usage for a particular technology from a wide range of manufacturing processes. An interesting observation from the study was that even though the study considered multiple unrelated processes, the specific power requirements for these were constrained in a narrow band of 1 to 50 KW. This is represented by the two diagonal lines, with 1 kW being the lower diagonal, and 50 kW the upper diagonal on the log-log plot presented in Figure 5-11.

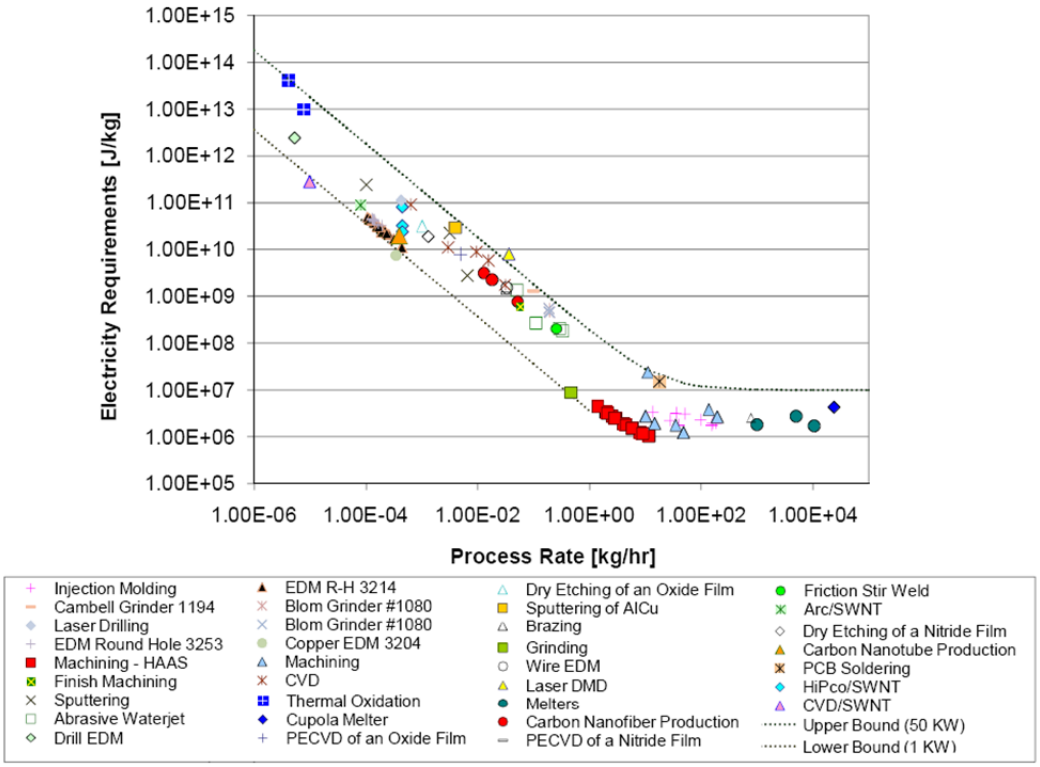

Figure 5-11: Specific Energy Requirements w.r.t Process Rate

Additionally, the lower horizontal boundary of 1 MJ/kg is approximately equal to the specific energy needed to melt solid aluminum. Likewise, the upper horizontal boundary of 100 MJ/kg is the approximate specific energy needed for the phase change of aluminum from a liquid to a vapor.

Another interesting thing to note is that the processes at the bottom right of the diagram in Figure 5-11, between the horizontal lines, are the older, more conventional manufacturing processes, such as metal melting for casting. At the very top left of the diagram are newer, more recently developed processes with very high values of electric work per unit of material processed.

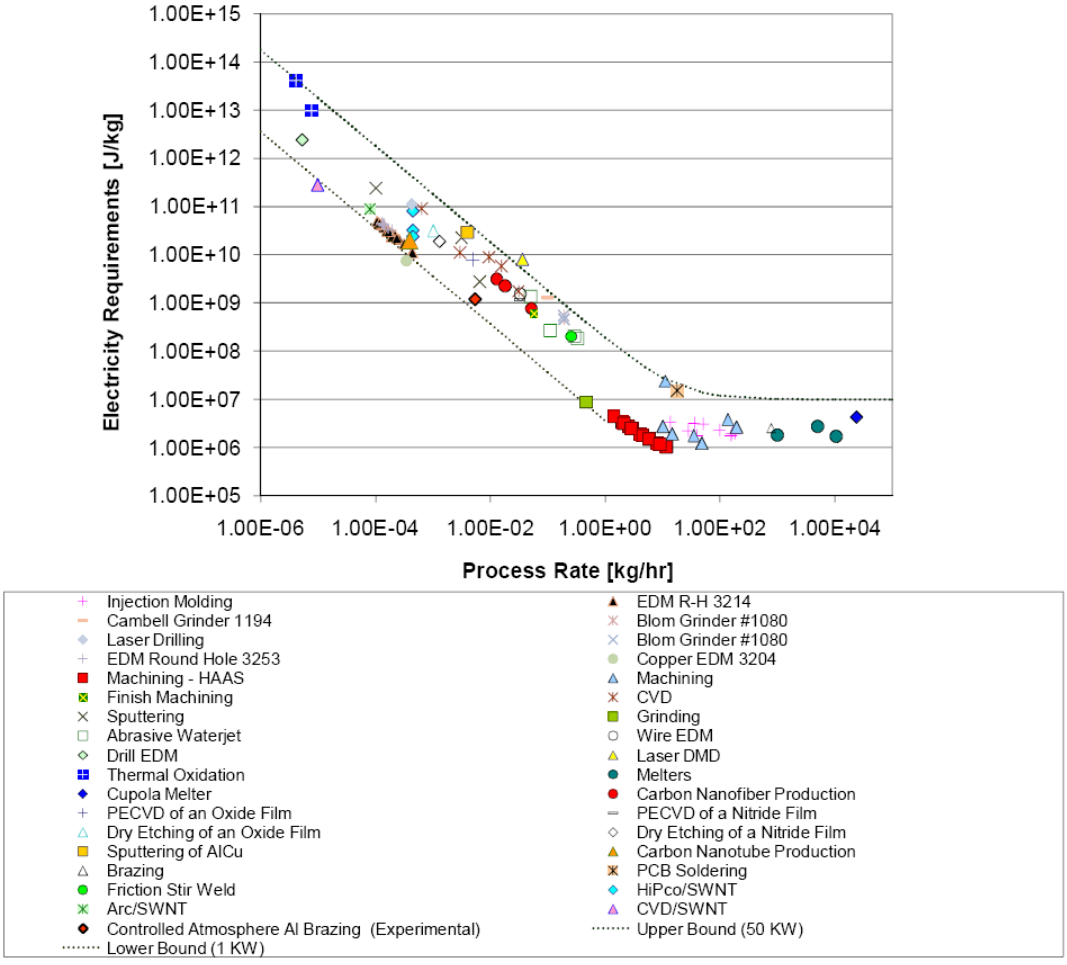

Figure 5-12: Specific Energy Requirements – Including CAB data point

Finally, Figure 5-12 offers the updated plot of specific energy used for a set of processes, with the CAB experimental study point included. It is interesting to note that the data point from this study follows the trend with the other technologies studied previously and falls in the narrow band between 1 KW and 50 KW (hockey plot).

Note the position of the CAB brazing (experimental). If multiple assemblies are brazed, the data point shifts deeper into the domain of other technologies. Also since the CAB experimental study carried out consisted of a “batch type” process, the point does not closely match with the point labelled “Brazing”. This is due to the fact that the “Brazing” data point was captured from a large scale industrial CAB process, and hence the process rate was significantly higher (and lower specific energy needs) than the one studied in this document.

Chapter 6: CONCLUSION AND FUTURE WORK

6.1 Conclusion

Energy resources use in various systems such as transformation of material flows into manufactured products has been a subject of an increased attention in the recent decades. Data related to global, regional, state, sector, industry etc. lack the means of assessing multiple sustainability metrics simultaneously in order to study the transdisciplinary aspects of sustainability on the various factors such as economic, environmental, social etc.

This study advocates a selection of metrics for energy resources use, starting with a process level and compounding the energy resources use up to the global level. Novel four quadrant sustainability metrics plots (4QSP) are constructed and presented to demonstrate mutual dependence of the rate of change of different sustainability metrics (environmental, economic, and societal).

Furthermore this study presents the metric in terms of a margin between the actual specific energy use and the theoretical minimum, irrespective of technology which is useful for evaluating a need for a transformational technology introduction vs. traditional technologies An in depth analysis of a brazing process is offered as an example of determining the margin between the theoretical minimum and the actual energy resources use by a state-of-the-art manufacturing process. This margin is a hypothetical energy resources savings domain irrespective of the technology used, as long as the bonding between two metal parts is achieved by adding liquid metal.

It has been demonstrated that the theoretical minimum energy requirement associated with a manufactured product for a particular material processing is a number of orders of magnitude smaller than the actual energy resources use for the actual process under consideration.

Hence, a significant reduction of energy resources use for a given production rate in manufacturing processes requires an introduction of transformational technologies at the process level, not just a gradual improvement of traditional technologies.

6.2 Future Work

The material presented in this thesis analyzes the energy resource utilization for Controlled Atmosphere Brazing process on an experimental basis. Further additions to this thesis work would be to explore the energy consumption of more metal joining technologies such as localized fusion processes (welding) etc. Also, an industrial CAB furnace will encounter some different dynamics as it would be a continuous process, as compared to the batch process presented in the study. It would be beneficial to explore the energy use for an industrial CAB furnace, quantify the sources of losses and compare the findings to the current study.

In terms of the evaluation of transdisciplinary aspects of various metrics on a larger scale (global, national), the 4 quadrant sustainability plots are presented considering commonly used metrics with the aim of providing the means of analysis. Further studies can build on this concept by

1. Extending the existing study by simply evaluating the metrics for other nations which provide unique characteristics in terms of sustainability, such as, Switzerland which is at the forefront of ecological sustainability, and/or Qatar, which is on the other side of the spectrum.
2. Presenting other specific metrics such as environmental footprint, wealth index etc. to gain insight into specific aspects of sustainability and their relationship to others. This approach would need much better synergy involvement between the diverse aspects of sustainability, all including ecological capacity vs. resources demand at a variety of scales of considered systems, ultimately at the global scale.[7]

APPENDICES

Appendix 1: Metrics data for key world economies

1-A: Primary Energy Consumption[47]

Time (Years)	Primary Energy Consumption (MJ x 10^{12})		
	USA	China	India
1980	82.36	18.24	4.26
1981	80.30	18.14	4.88
1982	77.12	18.92	5.00
1983	76.99	20.06	5.27
1984	80.85	21.58	5.97
1985	80.60	22.16	6.24
1986	80.87	23.46	6.71
1987	83.41	25.07	6.80
1988	87.26	26.85	7.43
1989	89.45	27.39	7.87
1990	89.14	27.43	8.31
1991	89.09	28.87	8.83
1992	90.51	30.04	9.34
1993	92.24	30.22	9.22
1994	94.00	34.27	10.50
1995	96.04	35.08	11.50
1996	99.20	36.92	12.07
1997	99.81	40.38	12.12
1998	100.25	41.72	12.69
1999	101.97	41.17	13.58
2000	104.25	43.19	14.07
2001	101.46	44.92	14.60
2002	103.02	49.90	14.42
2003	103.37	55.88	14.89
2004	105.68	62.75	16.16
2005	105.80	71.65	17.23
2006	105.11	78.37	18.60
2007	106.87	83.74	19.85
2008	104.74	89.62	21.00
2009	99.77	99.57	22.60
2010	103.44	106.44	23.13
2011	102.62	115.65	24.91

1-B: GDP per capita for key world economies[48]

Time (Years)	GDP per capita (Current US$)		
	USA	China	India
1980	12179.5	193	271.2
1981	13526.2	195.3	275.3
1982	13932.7	201.4	279.2
1983	15000.1	223.3	296.9
1984	16539.4	248.3	282.3
1985	17588.8	291.8	302.6
1986	18427.3	279.2	317.1
1987	19393.8	249.4	347.8
1988	20703.2	281	361.9
1989	22039.2	307.5	353.8
1990	23037.9	314.4	375.9
1991	23443.3	329.7	310.1
1992	24411.1	362.8	324.5
1993	25326.7	373.8	308.5
1994	26577.8	469.2	354.8
1995	27559.2	604.2	383.5
1996	28772.4	703.1	410.8
1997	30281.6	774.5	427.2
1998	31687.1	820.9	425.4
1999	33332.1	864.7	453.0
2000	35081.9	949.2	455.4
2001	35912.3	1041.6	464.7
2002	36819.4	1135.4	485.5
2003	38224.7	1273.6	564.6
2004	40292.3	1490.4	649.7
2005	42516.4	1731.1	740.1
2006	44622.6	2069.3	830.1
2007	46349.1	2651.3	1068.6
2008	46759.6	3413.6	1042.1
2009	45305.1	3748.9	1147.2
2010	46612	4433	1419.1
2011	48112	5444.8	1533.6

1-C: GDP for key world economies[61]

Time (Years)	GDP (Current US$)		
	USA	China	India
1980	2.767×10^{12}	1.894×10^{11}	1.895×10^{11}
1981	3.104×10^{12}	1.941×10^{11}	1.968×10^{11}
1982	3.227×10^{12}	2.032×10^{11}	2.042×10^{11}
1983	3.507×10^{12}	2.284×10^{11}	2.221×10^{11}
1984	3.900×10^{12}	2.574×10^{11}	2.158×10^{11}
1985	4.185×10^{12}	3.066×10^{11}	2.366×10^{11}
1986	4.425×10^{12}	2.978×10^{11}	2.533×10^{11}
1987	4.698×10^{12}	2.703×10^{11}	2.839×10^{11}
1988	5.061×10^{12}	3.095×10^{11}	3.018×10^{11}
1989	5.439×10^{12}	3.439×10^{11}	3.012×10^{11}
1990	5.750×10^{12}	3.569×10^{11}	3.266×10^{11}
1991	5.930×10^{12}	3.794×10^{11}	2.748×10^{11}
1992	6.262×10^{12}	4.226×10^{11}	2.932×10^{11}
1993	6.583×10^{12}	4.405×10^{11}	2.842×10^{11}
1994	6.993×10^{12}	5.592×10^{11}	3.330×10^{11}
1995	7.338×10^{12}	7.280×10^{11}	3.666×10^{11}
1996	7.751×10^{12}	8.561×10^{11}	3.998×10^{11}
1997	8.256×10^{12}	9.526×10^{11}	4.231×10^{11}
1998	8.741×10^{12}	1.019×10^{12}	4.287×10^{11}
1999	9.301×10^{12}	1.083×10^{12}	4.643×10^{11}
2000	9.898×10^{12}	1.198×10^{12}	4.747×10^{11}
2001	1.023×10^{13}	1.325×10^{12}	4.924×10^{11}
2002	1.059×10^{13}	1.453×10^{12}	5.228×10^{11}
2003	1.108×10^{13}	1.641×10^{12}	6.175×10^{11}
2004	1.179×10^{13}	1.931×10^{12}	7.215×10^{11}
2005	1.256×10^{13}	2.257×10^{12}	8.342×10^{11}
2006	1.331×10^{13}	2.713×10^{12}	9.491×10^{11}
2007	1.396×10^{13}	3.494×10^{12}	1.238×10^{12}
2008	1.422×10^{13}	4.522×10^{12}	1.224×10^{12}
2009	1.389×10^{13}	4.991×10^{12}	1.365×10^{12}
2010	1.442×10^{13}	5.931×10^{12}	1.711×10^{12}
2011	1.499×10^{13}	7.318×10^{12}	1.873×10^{12}

1-D: CO_2 emissions for key world economies[44]

Time (Years)	CO_2 emissions (million metric tons)		
	USA	China	India
1980	4776	1448	291
1981	4647	1440	338
1982	4411	1507	350
1983	4389	1593	367
1984	4619	1724	422
1985	4605	1766	447
1986	4613	1879	474
1987	4771	2011	487
1988	4991	2148	522
1989	5072	2183	553
1990	5040	2178	579
1991	4997	2296	621
1992	5093	2376	659
1993	5188	2499	691
1994	5261	2682	734
1995	5319	2723	870
1996	5504	2841	814
1997	5577	3130	856
1998	5617	3198	893
1999	5678	3116	951
2000	5863	3272	991
2001	5755	3354	1016
2002	5799	3777	1007
2003	5853	4236	1022
2004	5974	4745	1121
2005	5999	5464	1181
2006	5924	5936	1281
2007	6026	6326	1366
2008	5845	6685	1472
2009	5435	7573	1598
2010	5637	7997	1601
2011	5491	8715	1726

1-E: HDI for key world economies[49]

Time (Years)	USA	China	India
1980	0.837	0.404	0.345
1985	0.853	0.448	0.38
1990	0.87	0.49	0.41
1995	0.883	0.541	0.437
2000	0.897	0.588	0.463
2005	0.902	0.637	0.507
2006	0.904	0.65	0.515
2007	0.905	0.662	0.525
2008	0.907	0.672	0.533
2009	0.906	0.68	0.540
2010	0.908	0.689	0.547
2011	0.91	0.695	0.551

Appendix 2: Temperature data (CAB tests)

2-A: Furnace temperatures

The following table provides the furnace temperatures for experiment#19. This dataset was utilized for calculations related to the energy balance. Note that the readings presented are at approx. 1 minute intervals for simplicity. Complete dataset is available on the brazing laboratory server.

HTC – Heater temperature; WK1 – Work temperature 1; WK2 – Work temperature 2

t (sec)	S	SPT (ºC)	HTC (ºC)	WK 1 (ºC)	WK2 (ºC)	t (sec)	S	SPT (ºC)	HTC (ºC)	WK 1 (ºC)	WK2 (ºC)
0	1	26	26	26	26	1680.6	2	149	152	177	178
60.9	1	116	85	31	29	1739.5	2	149	149	174	176
119.9	2	149	237	79	75	1800.5	2	149	146	173	174
180.8	2	149	353	139	146	1861.5	2	149	144	170	172
239.8	2	149	389	170	181	1920.4	3	182	165	171	171
300.7	2	149	363	173	181	1981.4	3	251	292	208	207
359.7	2	149	322	175	179	2040.3	3	318	404	263	267
420.6	2	149	286	179	181	2101.3	3	387	468	316	321
479.6	2	149	262	185	185	2160.3	3	453	508	364	367
540.5	2	149	245	190	190	2221.2	3	522	539	409	411
601.5	2	149	233	194	194	2280.1	3	467	550	442	441
660.4	2	149	224	196	198	2341.1	3	536	585	487	486
721.4	2	149	216	197	200	2400	3	600	612	525	524
780.3	2	149	210	196	201	2461	3	600	636	560	559
841.3	2	149	204	197	202	2519.9	3	600	644	583	582
900.2	2	149	199	197	201	2580.9	3	600	637	592	589
961.2	2	149	194	196	201	2639.8	3	600	630	598	595
1020.1	2	149	190	196	200	2700.8	4	600	626	601	598
1081.1	2	149	186	195	198	2759.7	4	600	622	602	599
1140	2	149	182	194	197	2820.7	5	535	607	574	522
1201	2	149	178	192	195	2879.7	5	400	568	541	468
1259.9	2	149	174	190	193	2940.6	5	400	536	509	434
1320.9	2	149	170	188	191	2999.5	5	400	510	481	407
1381.9	2	149	167	187	189	3060.5	5	400	485	456	381
1440.8	2	149	164	185	187	3121.5	5	400	462	434	359
1501.8	2	149	161	183	185	3180.4	5	400	441	412	339
1560.7	2	149	158	181	183	3241.4	5	400	421	394	319
1621.7	2	149	155	179	181	3300.3	5	400	402	374	300

2-B: Power and Energy measurement data

t (sec)	P (kW)	E (kJ)	t (sec)	P (kW)	E (kJ)
60	5.64	339.7	1740	0.15	1581.6
120	5.65	679.8	1800	0.14	1590.4
180	5.65	1018.8	1860	0.15	1599.3
240	4.82	1287.2	1920	5.58	1771.5
300	0.15	1366.4	1980	5.66	2110.3
360	0.15	1377.8	2040	5.65	2449.7
420	0.15	1386.7	2100	5.66	2789.1
480	0.14	1395.6	2160	5.66	3128.7
540	0.15	1404.4	2220	5.66	3468.5
600	0.15	1413.4	2280	5.66	3765.6
660	0.15	1422.2	2340	5.67	4105.5
720	0.15	1431.1	2400	5.67	4445.7
780	0.15	1439.9	2460	5.67	4786.2
840	0.14	1448.8	2520	5.67	5086.9
900	0.14	1457.7	2580	0.27	5320.8
960	0.15	1466.6	2640	2.58	5525.9
1020	0.15	1475.4	2700	5.76	5697.8
1080	0.15	1484.2	2760	5.76	5849.7
1140	0.15	1493	2820	0.28	5970.7
1200	0.15	1502	2880	0.16	5987.3
1260	0.15	1510.8	2940	0.16	5997.1
1320	0.14	1519.7	3000	0.16	6007
1380	0.14	1528.6	3060	0.16	6016.8
1440	0.15	1537.5	3120	0.16	6026.6
1500	0.14	1546.3	3180	0.16	6036.5
1560	0.15	1555.1	3240	0.16	6047.2
1620	0.15	1563.9	3300	0.17	6057.1
1680	0.15	1572.7			

Auxiliary Equipment Energy consumption during Test duration = 481.1 kJ (Computed using a numerical integration of data recorded for area under the curve indicated as Auxiliary equipment power level (See Figure 5-2)

Hence the total energy consumption by the heater to form the joint = **5575 kJ**

2-C: Temperature for hot zone quartz glass (During experiments)

T_{g1} to T_{g4} are the measured values for temperatures for experiment # 19. T_{ga} is the average temperature which is used for calculations of losses to the surroundings.

T (sec)	T_{g1}(°C)	T_{g2}(°C)	T_{g3}(°C)	T_{g4}(°C)	T_{ga}(°C)
60	25.1	25.3	24.2	21.4	24
120	33.5	30.6	29.1	25.1	29.6
180	39.5	39.3	36.5	31.9	36.8
240	41.3	45	42.2	37.9	41.6
300	51	47	46.6	42.5	46.8
360	65.7	51.4	52.9	49.1	54.8
420	79.1	58.4	61.2	57.3	64
480	90.7	66	69.2	65.3	72.8
540	99.4	72.8	76.2	71.9	80.1
600	102.9	78.5	82	77.8	85.3
660	104.2	83.1	86.7	83.2	89.3
720	104	86.3	89.7	86.7	91.7
780	102.6	89	92.5	89.4	93.4
840	100.4	90.3	94.4	90.9	94
900	97.6	91	95.6	91.8	94
960	95	91.8	95.9	92	93.7
1020	92.5	92.6	95.6	91.3	93
1080	87.9	92.3	95.7	90.9	91.7
1140	85.2	91.5	95.2	90.1	90.5
1200	83.6	91	93.8	88.9	89.3
1260	81.1	89.4	93.3	87.4	87.8
1320	78	89	91.9	86	86.2
1380	75.7	88.1	90.8	85.4	85
1440	72.7	86.8	90.2	84.2	83.5
1500	70.8	86.2	88.8	82.6	82.1
1560	68.8	84.8	87.6	81.7	80.7
1620	68.3	83.6	86.2	78.7	79.2
1680	66.8	81.9	85.1	77.4	77.8
1740	65.7	81.3	84.4	75.8	76.8
1800	63.7	80.5	83.5	74.4	75.5
1860	61.4	79.5	82.8	73.5	74.3
1920	62.3	78.7	82.3	71.9	73.8
1980	71.7	82.3	85.3	75.1	78.6

T (sec)	T_{g1}(°C)	T_{g2}(°C)	T_{g3}(°C)	T_{g4}(°C)	T_{ga}(°C)
2040	81.9	89.7	91.4	82.1	86.3
2100	97.3	97	98.9	90	95.8
2160	122	107.3	108.7	97.6	108.9
2220	150.8	120.2	121.7	109.3	125.5
2280	176.7	133.4	135.8	123.3	142.3
2340	206.9	152.4	153.6	138.7	162.9
2400	232.3	170.5	171.7	157.5	183
2460	258.7	189.6	190	175.3	203.4
2520	275.2	207.6	207.1	192.5	220.6
2580	289.9	221	219	206.1	234
2640	299.3	232.6	226.4	217.6	244
2700	301.5	242.1	234.8	224.8	250.8
2760	304.9	248	239.3	228.6	255.2
2820	297.1	251.1	241.6	226.6	254.1
2880	285	250.9	239.6	228.9	251.1
2940	276.7	249	236.3	222.4	246.1
3000	267.7	243.7	233.3	216.6	240.3
3060	252.7	237.8	227.7	211	232.3
3120	243.3	231.8	222	203.3	225.1
3180	233.5	224	215	198	217.6
3240	224.2	215.8	210.4	190.8	210.3
3300	215	207.5	204.2	183.2	202.5

2-D: Post experiment temperature for hot zone quartz glass

The temperature data presented herewith is at 1 min duration for simplicity. The main dataset use for calculations consists of data recorded at 1 second intervals.

t (min)	T_{ga} (ºC)	t (min)	T_{ga} (ºC)	t (min)	T_{ga} (ºC)	t (min)	T_{ga} (ºC)
0	196.2	67	62.9	134	34.8	201	26.4
1	188.7	68	62.4	135	34.3	202	26.3
2	181.6	69	61.5	136	34.0	203	26.2
3	175.1	70	60.5	137	33.9	204	26.1
4	168.1	71	59.9	138	33.7	205	26.0
5	162.7	72	59.0	139	33.5	206	26.1
6	157.1	73	58.3	140	33.4	207	26.1
7	152.1	74	57.7	141	33.1	208	26.1
8	147.6	75	57.1	142	32.8	209	26.1
9	143.3	76	56.4	143	32.7	210	26.1
10	139.4	77	55.7	144	32.7	211	26.1
11	136.8	78	55.2	145	32.5	212	26.0
12	133.0	79	54.6	146	32.2	213	25.9
13	129.7	80	54.1	147	32.1	214	25.7
14	127.1	81	53.7	148	31.7	215	25.6
15	124.7	82	53.0	149	31.5	216	25.4
16	122.5	83	52.6	150	31.5	217	25.3
17	120.0	84	51.9	151	31.3	218	25.2
18	117.9	85	51.6	152	31.1	219	25.1
19	115.6	86	50.9	153	30.8	220	25.1
20	113.7	87	50.5	154	30.6	221	25.1
21	111.7	88	50.1	155	30.5	222	25.0
22	110.1	89	49.5	156	30.4	223	25.1
23	107.8	90	49.0	157	30.2	224	25.0
24	105.7	91	48.4	158	30.2	225	25.1
25	103.7	92	48.2	159	30.0	226	25.1
26	102.4	93	47.6	160	29.9	227	25.1
27	101.1	94	47.1	161	29.7	228	25.1
28	99.9	95	46.6	162	29.5	229	24.9
29	98.4	96	46.2	163	29.4	230	24.7
30	96.9	97	45.6	164	29.4	231	24.6
31	95.4	98	45.3	165	29.2	232	24.6
32	93.6	99	45.0	166	29.0	233	24.5
33	92.5	100	44.4	167	28.9	234	24.4
34	90.8	101	44.0	168	28.6	235	24.4
35	89.4	102	43.4	169	28.4	236	24.4

t (min)	T_{ga} (ºC)	t (min)	T_{ga} (ºC)	t (min)	T_{ga} (ºC)	t (min)	T_{ga} (ºC)
36	87.9	103	43.0	170	28.3	237	24.4
37	86.4	104	42.5	171	28.1	238	24.4
38	85.4	105	42.0	172	28.0	239	24.3
39	83.9	106	41.7	173	27.9	240	24.2
40	83.0	107	41.6	174	27.7	241	24.1
41	82.0	108	41.3	175	27.6	242	24.1
42	80.6	109	41.0	176	27.5	243	24.1
43	79.9	110	40.5	177	27.4	244	24.1
44	79.0	111	40.4	178	27.3	245	24.0
45	77.9	112	40.1	179	27.2	246	24.0
46	77.0	113	39.7	180	27.1	247	24.0
47	76.1	114	39.4	181	27.1	248	24.1
48	74.8	115	39.2	182	27.0	249	24.1
49	75.4	116	38.9	183	27.2	250	24.1
50	75.2	117	38.7	184	27.2	251	24.2
51	75.0	118	38.4	185	27.3	252	24.2
52	74.1	119	38.1	186	27.3	253	24.1
53	73.8	120	37.9	187	27.2	254	24.1
54	73.4	121	37.7	188	27.3	255	24.0
55	73.3	122	37.5	189	27.2	256	24.0
56	72.9	123	37.2	190	27.1	257	24.0
57	72.0	124	37.0	191	27.0	258	24.0
58	71.3	125	36.8	192	26.8	259	24.0
59	70.7	126	36.5	193	26.7	260	23.9
60	70.0	127	36.2	194	26.8	261	23.9
61	69.1	128	36.0	195	26.7	262	23.8
62	67.8	129	35.8	196	26.6	263	23.8
63	66.5	130	35.5	197	26.5	264	23.7
64	65.7	131	35.3	198	26.5	265	23.7
65	64.9	132	35.0	199	26.4		
66	63.9	133	34.9	200	26.3		

Appendix 3: Energy flow calculations

3-A: Convection over Hot zone

The convective heat transfer coefficient was calculated using the following formula:

$$h = \frac{k}{D} Nu_D$$

Where,

H = Convective heat transfer coefficient, $W/m^2.K$

k = thermal conductivity, W/m.K

D = Diameter of the furnace, m

Nu_D = Nusselt number based on the diameter

The Nusselt number was calculated using the Churchill and Chu correlation [62] for free convection assuming laminar flow as follows

$$Nu_D = \left\{ 0.6 + 0.387 \frac{Ra_D^{1/6}}{\left[1 + (0.559/Pr)^{\frac{9}{16}}\right]^{8/27}} \right\}^2 \qquad Ra_D \leq 10^{12}$$

Where,

Ra_D = Rayleigh number

Pr = Prandtl number

The Rayleigh number was calculated using the following equation

$$Ra_D = \left(\frac{g\beta}{\nu\alpha}\right)\Delta T D^3$$

Where,

g = Gravitational Acceleration, m/s^2

β = Expansion coefficient

α = Thermal diffusivity, m^2/s

ΔT = Temperature difference, °C

The term$\left(\frac{g\beta}{\nu\alpha}\right)$ and thermal conductivity (required for calculations of Nusselt number and convective heat transfer coefficient) were calculated using the following correlations[63]:

$$\frac{g\beta}{\nu\alpha} = \frac{1}{[6.8568 \times 10^{-3} - 1.5079 \times 10^{-4}T + 1.5715 \times 10^{-6}T^2]^2}\left[\frac{10^6}{m^3K}\right]$$

$$\kappa = \frac{2.3340 \times 10^{-3}T^{\frac{3}{2}}}{164.54 + T}\left[\frac{W}{mK}\right]$$

In order to assess the transient nature of the process, it was assumed that the process is steady over 1 second duration. Properties were then calculated for each second and integrated together to get the final value of convective heat transfer.

t (sec)	T_{ga} (ºC)	Nu	h (W/m^2 . ºC)	$\dot{Q}_{conv}$ (J/s)	t (sec)	T_{ga} (ºC)	Nu	h (W/m^2 . ºC)	$\dot{Q}_{conv}$ (J/s)
60	24	13	1.77	0.35	1740	76.8	37	5.41	58.33
120	29.6	22	3.02	3.98	1800	75.5	36.8	5.37	56.5
180	36.8	26.9	3.73	10.3	1860	74.3	36.7	5.34	54.97
240	41.6	29.1	4.06	15.11	1920	73.8	36.6	5.33	54.25
300	46.8	30.9	4.35	20.7	1980	78.6	37.2	5.45	60.69
360	54.8	33.1	4.71	29.97	2040	86.3	38.1	5.63	71.41
420	64	35.1	5.04	41.44	2100	95.8	38.9	5.83	85.08
480	72.8	36.4	5.3	52.85	2160	108.9	39.8	6.06	104.32
540	80.1	37.4	5.49	62.75	2220	125.5	40.6	6.31	129.51
600	85.3	38	5.61	69.99	2280	142.3	41.1	6.52	155.74
660	89.3	38.4	5.7	75.66	2340	162.9	41.5	6.73	188.55
720	91.7	38.6	5.75	79.1	2400	183	41.6	6.9	221.17
780	93.4	38.7	5.78	81.49	2460	203.4	41.6	7.05	254.67
840	94	38.8	5.79	82.37	2520	220.6	41.5	7.15	283.14
900	94	38.8	5.8	82.46	2580	234	41.4	7.23	305.45
960	93.7	38.7	5.79	81.93	2640	244	41.3	7.28	322.17
1020	93	38.7	5.77	80.95	2700	250.8	41.2	7.31	333.58
1080	91.7	38.6	5.75	79.08	2760	255.2	41.1	7.33	340.87
1140	90.5	38.5	5.72	77.37	2820	254.1	41.1	7.32	339.08
1200	89.3	38.3	5.7	75.63	2880	251.1	41.2	7.31	334.13
1260	87.8	38.2	5.67	73.59	2940	246.1	41.3	7.29	325.65
1320	86.2	38.1	5.63	71.27	3000	240.3	41.3	7.26	315.94
1380	85	37.9	5.61	69.6	3060	232.3	41.4	7.22	302.71
1440	83.5	37.8	5.57	67.59	3120	225.1	41.5	7.18	290.7
1500	82.1	37.6	5.54	65.54	3180	217.6	41.5	7.14	278.19
1560	80.7	37.5	5.51	63.68	3240	210.3	41.6	7.09	266.05
1620	79.2	37.3	5.47	61.57	3300	202.5	41.6	7.04	253.21
1680	77.8	37.1	5.44	59.72					

3-B: Radiation over Hot zone (during experiment)

Ambient temperature (T_{amb}) = 23 ºC; Emissivity for quartz glass (ε) = 0.93[60]

Diameter of outer quartz glass = 0.19 m; Length of hot zone = 0.3356 m [53][53]

Stefan Boltzmann constant (σ) = $5.67e^{-8}$ $W/m^2.K^4$;

Segment	$\dot{Q}_{rad}$ (kJ)
1	0.1
2	140.1
3	208.0
4	83.0
5	323.8
Total	**755.05**

t (sec)	T_{ga} (ºC)	$\dot{Q}_{rad}$ (J/s)	t (sec)	T_{ga} (ºC)	$\dot{Q}_{rad}$ (J/s)	t (sec)	T_{ga} (ºC)	$\dot{Q}_{rad}$ (J/s)
60	24	1.06	1380	85	89.42	2700	250.8	691.1
120	29.6	7.21	1440	83.5	86.74	2760	255.2	717
180	36.8	15.67	1500	82.1	84.02	2820	254.1	710.58
240	41.6	21.64	1560	80.7	81.57	2880	251.1	693.04
300	46.8	28.41	1620	79.2	78.82	2940	246.1	663.65
360	54.8	39.53	1680	77.8	76.42	3000	240.3	630.97
420	64	53.43	1740	76.8	74.62	3060	232.3	588.18
480	72.8	67.64	1800	75.5	72.28	3120	225.1	550.94
540	80.1	80.35	1860	74.3	70.32	3180	217.6	513.76
600	85.3	89.94	1920	73.8	69.41	3240	210.3	479.17
660	89.3	97.62	1980	78.6	77.67	3300	202.5	444.19
720	91.7	102.35	2040	86.3	91.85			
780	93.4	105.67	2100	95.8	110.72			
840	94	106.9	2160	108.9	138.99			
900	94	107.04	2220	125.5	179.29			
960	93.7	106.29	2280	142.3	225.66			
1020	93	104.92	2340	162.9	290.6			
1080	91.7	102.32	2400	183	363.55			
1140	90.5	99.96	2460	203.4	448.09			
1200	89.3	97.57	2520	220.6	528.26			
1260	87.8	94.8	2580	234	596.88			
1320	86.2	91.66	2640	244	651.83			

3-C: Conduction to the flanges of Hot zone

Coefficient of Thermal Conductivity for Ceramic foam insulation (k) = 0.41[64]

Diameter of outer quartz glass = 0.19 m

Width of aluminum flanges = 0.02 m

Thickness of insulation (x) = 0.01 m

t (sec)	T_{ga} (°C)	T_{hf} (°C)	$\dot{Q}_{cond}$ (J/s)	t (sec)	T_{ga} (°C)	T_{hf} (°C)	$\dot{Q}_{cond}$ (J/s)
60	24	25.6	0	1740	76.8	38.1	40.9
120	29.6	25.7	6.3	1800	75.5	38	39.7
180	36.8	26.2	13	1860	74.3	37.8	38.7
240	41.6	27.1	16.8	1920	73.8	37.7	38.3
300	46.8	28.3	20.8	1980	78.6	37.7	43
360	54.8	29.6	27.4	2040	86.3	38.1	50.3
420	64	31	35.3	2100	95.8	39	58.9
480	72.8	32.2	42.7	2160	108.9	40.2	70.6
540	80.1	33.4	48.8	2220	125.5	42.1	85.2
600	85.3	34.4	52.9	2280	142.3	44.4	99.6
660	89.3	35.4	56	2340	162.9	47.1	117.3
720	91.7	36.1	57.6	2400	183	50.1	134.3
780	93.4	36.7	58.6	2460	203.4	53.3	151.4
840	94	37.2	58.8	2520	220.6	56.8	164.9
900	94	37.6	58.4	2580	234	60.2	174.9
960	93.7	37.9	57.7	2640	244	63.4	181.6
1020	93	38.2	56.8	2700	250.8	66.2	185.5
1080	91.7	38.3	55.4	2760	255.2	69	187.2
1140	90.5	38.5	54	2820	254.1	71.4	183.7
1200	89.3	38.6	52.7	2880	251.1	73.4	178.7
1260	87.8	38.6	51.3	2940	246.1	75	172.2
1320	86.2	38.6	49.6	3000	240.3	75.9	165.5
1380	85	38.6	48.5	3060	232.3	76.5	157.1
1440	83.5	38.6	47.1	3120	225.1	76.7	149.7
1500	82.1	38.5	45.7	3180	217.6	76.5	142.4
1560	80.7	38.4	44.4	3240	210.3	75.8	135.9
1620	79.2	38.3	43.1	3300	202.5	75.1	128.8
1680	77.8	38.2	41.8				

3-D: Nitrogen Chamber flow

Nitrogen inlet temperature (T_{in}) = 24.1 ºC; Volume flow rate = 3.398 m^3/hr (2 SCFH);[53]

Density for N_2 (ρ) = 1.165 kg/m^3;[65]; Specific heat for N_2 (C_P) = 1.04 kJ/kg K;[65]

N_2 mass flow rate ($\dot{m}$) = 1.83e^{-5} kg/s;

$$\dot{H}_{in} = \dot{m} \times C_P \times T_{in} = 0.00566 \text{ kJ/s}$$

Segment	H_{in} (kJ)	H_{out} (kJ)
1	0.51	0.51
2	10.19	10.26
3	4.53	4.58
4	0.68	0.69
5	2.94	3.00
Total	**18.86**	**19.03**

t (sec)	T_{out} (ºC)	$\dot{H}_{out}$ (kJ)	t (sec)	T_{out} (ºC)	$\dot{H}_{out}$ (kJ)
0	25.3	0.0057	1680	26	0.0057
60	25.3	0.0057	1740	26	0.0057
120	25.3	0.0057	1800	26	0.0057
180	25.5	0.0057	1860	26	0.0057
240	25.7	0.0057	1920	26	0.0057
300	25.9	0.0057	1980	26	0.0057
360	25.9	0.0057	2040	26.2	0.0057
420	26	0.0057	2100	26.4	0.0057
480	26	0.0057	2160	26.6	0.0057
540	26	0.0057	2220	26.9	0.0057
600	26	0.0057	2280	27.1	0.0057
660	26	0.0057	2340	27.4	0.0057
720	26	0.0057	2400	27.7	0.0057
780	26	0.0057	2460	28	0.0057
840	25.9	0.0057	2520	28.3	0.0057
900	25.9	0.0057	2580	28.5	0.0057
960	26	0.0057	2640	28.8	0.0058

t (sec)	T_{out} (°C)	$\dot{H}_{out}$ (kJ)	t (sec)	T_{out} (°C)	$\dot{H}_{out}$ (kJ)
1020	26	0.0057	2700	29	0.0058
1080	26	0.0057	2760	29.1	0.0058
1140	25.9	0.0057	2820	29.3	0.0058
1200	26	0.0057	2880	29.4	0.0058
1260	26	0.0057	2940	29.5	0.0058
1320	26	0.0057	3000	29.6	0.0058
1380	26	0.0057	3060	29.6	0.0058
1440	26	0.0057	3120	29.7	0.0058
1500	26	0.0057	3180	29.7	0.0058
1560	26	0.0057	3240	29.7	0.0058
1620	26	0.0057	3300	29.8	0.0058

3-E: Nitrogen Quenching flow

Nitrogen inlet temperature (T_{in}) = 24.1 ºC;

Volume flow rate = 33.98 m^3/hr(20 SCFH) [53]

Density for N_2 (ρ) = 1.165 kg/m^3;[65]; Specific heat for N_2 (C_P) = 1.04 kJ/kg K;[65]

N_2 mass flow rate ($\dot{m}$) = 1.83e^{-4} kg/s;

$$\dot{H}_{in} = \dot{m} \times C_P \times T_{in} = 0.0566 \text{ kJ/s}$$

Segment	H_{in} (kJ)	H_{out} (kJ)
1	-	-
2	-	-
3	-	-
4	-	-
5	29.45	38.95
Total	**29.45**	**38.95**

t (sec)	T_{out} (ºC)	$\dot{H}_{out}$(kJ)	t (sec)	T_{out} (ºC)	$\dot{H}_{out}$ (kJ)	t (sec)	T_{out} (ºC)	$\dot{H}_{out}$ (kJ)
2810	24.5	0.0567	2990	128.5	0.0765	3170	139.8	0.0787
2820	24.9	0.0568	3000	130.4	0.0769	3180	139.7	0.0787
2830	35.3	0.0588	3010	132.1	0.0772	3190	139.6	0.0786
2840	47.2	0.0610	3020	133.6	0.0775	3200	139.4	0.0786
2850	57.5	0.0630	3030	134.9	0.0777	3210	139.1	0.0785
2860	66.5	0.0647	3040	136.0	0.0779	3220	138.7	0.0785
2870	75.0	0.0663	3050	136.9	0.0781	3230	138.4	0.0784
2880	82.5	0.0678	3060	137.8	0.0783	3240	138.1	0.0783
2890	89.5	0.0691	3070	138.4	0.0784	3250	137.8	0.0783
2900	95.5	0.0702	3080	139.0	0.0785	3260	137.4	0.0782
2910	101.1	0.0713	3090	139.3	0.0786	3270	136.9	0.0781
2920	106.1	0.0723	3100	139.7	0.0787	3280	136.5	0.0780
2930	110.5	0.0731	3110	139.9	0.0787	3290	136.0	0.0779
2940	114.4	0.0738	3120	140.0	0.0787	3300	135.5	0.0779
2950	117.9	0.0745	3130	140.1	0.0787	3310	135.0	0.0778
2960	121.0	0.0751	3140	140.0	0.0787	3320	134.6	0.0777
2970	123.8	0.0756	3150	140.0	0.0787	3330	134.1	0.0776
2980	126.3	0.0761	3160	139.9	0.0787			

Appendix 4: Material Compositions and Gas Properties

Nitrogen[66]

- For Quenching post brazing

  Product: PurityPlus Extra Dry (Industrial Grade)

  Specifications: Moisture <8 ppm

  Oxygen 19.5% to 23.5%

- For controlled atmosphere

  Product: PurityPlus 5.0 (Ultra High Purity)

  Specifications: Purity 99.999%

  Moisture <3 ppm

  Oxygen <2 ppm

Aluminum Alloys (Weight %) [67]

Alloy	Si	Fe	Cu	Mn	Mg	Zn	Ti	Others (Total)	Al
AA 3003	0.6	0.7	0.05 – 0.20	1.0-1.5	-	0.10	-	0.15	Remainder
AA 4045	9.0-11.0	0.8	0.30	0.05	0.05	0.10	0.20	0.15	Remainder

Appendix 5: Equipment/Tools Used and Uncertainties

This appendix provides the descriptions of the equipment and tools used for experimentation and analysis in this document.

Fluke 1735 Power Logger

The Fluke 1735 Power logger is a versatile multipurpose power and energy analyzer which measures and records voltage, current, and power data. The power logger has both voltage clamps and current probes which attach to all three legs of an AC connection. For the CAB experiments conducted as a part of this study, the logger measured the input power from 240V, single phase connection. The Fluke Power Log Software (Ver. 2.9.2) was used to transfer and evaluate the active power data from the logger, for the CAB experiments. Power data was then exported to excel and numerically integrated to compute the energy consumption.

The specifications and errors associated with this equipment are as follows[68]:

Voltage range: 100-830 V AC

Intrinsic error: ± (0.2% of measured value + 5 digits)

Operating error: ± (0.5% of measured value + 10 digits)

Resolution: 0.1 V

Current range: 0-3000 A

Intrinsic error: ± (0.5% of measured value + 10 digits)

Operating error: ± (1% of measured value + 10 digits)

Flexi set measuring error: ± (2% of measured value + 10 digits)

Position influence: ± (3% of measured value + 10 digits)

e! Sankey (Version 3.2.0.424)[20]

The e! Sankey software was used for creating the Sankey diagrams used to present the energy flows for different nations and the Energy flow diagram for the Controlled Atmosphere Brazing process.

Hobo U 12 Temperature/ RH Data logger[69]

The Hobo U 12 Temperature logger was used for logging the ambient temperature during the experiments.

Temperature Range: -20°C to 70°C

Accuracy: ± 0.35°C from 0C to 50C (See plot below)

Resolution: 0.03°C at 25°C

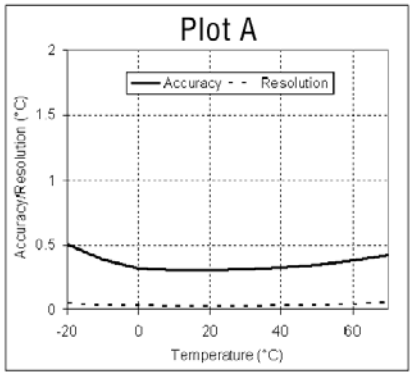

Hobo U 12-014 (J,K,S,T Thermocouple Data Logger)[70]

The Hobo U12-014 Thermocouple data logger was used for logging the Nitrogen Chamber flow and Quenching Flow Outlet temperatures as well as the temperature at the intersection of flanges holding the hot zone, during the experiments using K-Type thermocouples.

Temperature Range (K-Type): 0°C to 1250°C

Accuracy: ± 4°C or 0.5% of reading, whichever is greater

Resolution: 0.32°C at 625°C

NI 9211 thermocouple input module[71]

The NI 9211 is a thermocouple input module used with NI CompactDAQ chassis (cDAQ-9172). It includes a 24-bit delta-sigma analog-to-digital converter, anti-aliasing filters, open-thermocouple detection, and cold-junction compensation for high-accuracy thermocouple measurements. The NI 9211 features NIST-traceable calibration and a channel-to-earth ground double isolation barrier for safety, noise immunity, and high common-mode voltage range.

The four channels on this module were used for the CAB experiments in order to log the temperatures of the Hot zone Outer surface.

NI cDAQ-9172 USB Chassis[72]

The NI cDAQ-9172 is an eight-slot USB chassis designed for use with C Series I/O modules. It is capable of measuring a broad range of analog and digital I/O signals and sensors using a Hi-Speed USB 2.0 interface. This was used along with the NI 9211 to record temperature data with time for the hot zone external surface temperatures during and after the experiment. A LabVIEW program was designed to measure and record temperature from this chassis.

Analog Input

Maximum sample rate: 3.2 MS/s

Timing accuracy: 50 ppm of sample rate

Timing resolution: 50 ns

Analog Output

Maximum update rate: 1.6 MS/s

Timing accuracy: 50 ppm of sample rate

Timing resolution: 50 ns

Pipe plug thermocouple – TC-K-NPT U 72[73]

The TC-K-NPT U 72 pipe plug thermocouple probes are plug type sensors utilized for measurement of temperature inside a pipe through which fluid flows. Two of these types of thermocouples were used during the experiments to record the Nitrogen Chamber flow and Quenching flow outlet temperatures.

The K type thermocouple has a maximum range of -200°C to 1250°C. The standard error is 2.2°C or 0.75% (whichever is greater) above 0°C and 2.2°C or 2% whichever is greater for temperatures below 0°C

Super OMEGACLAD® Thermocouple Probes - KMQXL-032G-6[74]

The Super Omegaclad probes are wire type thermocouples used for high temperature measurement. For the experimentation conducted in this study, four such probes were utilized to measure the temperature of the hot zone outer surface.

The K type thermocouple has a maximum range of -200°C to 1250°C. The standard error is 2.2°C or 0.75% (whichever is greater) above 0°C and 2.2°C or 2% whichever is greater for temperatures below 0°C

Appendix 6: Theoretical Minimum Energy Calculations

Calculations for the minimum actual and theoretical energy required for the joint formation are provided herewith. The basis for calculations is that the entire assembly (Base of A3003 + clad of A4045) is heated till the melting point and then the cladding material melts. In the actual case scenario which happens during the test, the entire cladding material is melted. In a theoretical sense, the joint may be formed just by melting the cladding material in the area close to the joint.

Sample mass:

1. Vertical Sheet (AA 3003)
    a. Size: 20 mm x 50 mm x 0.4m thk
    b. Volume: 0.4 cm^3
    c. Density: 2.73 g/cm^3 [75]
    d. Mass = Volume x Density = 1.092 g
2. Horizontal Sheet (AA3003 with 5% A4045 Cladding)
    a. Size: 70 mm x 39.3 mm x 0.53 mm thk
    b. Volume (A3003) = 7 x 3.93 x 0.053 x 95% = 1.385 cm^3
    c. Volume (A4045) = 7 x 3.93 x 0.053 x 5% = 0.073 cm^3
    d. Density (A4045) = 2.67 g/cm^3 [76]
    e. Mass (A3003) = 3.78 g
    f. Mass (A4045) = 0.194 g

3. Fillet mass

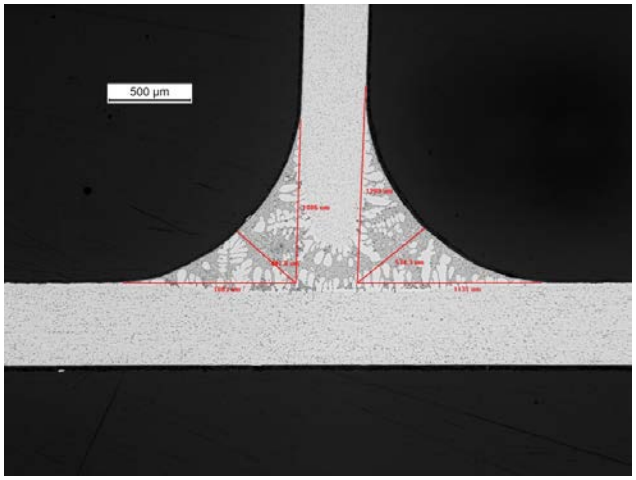

a. C/S Area of Joint (RHS) = 0.353 mm^2 (Calculated for the geometry shown in the figure above)

b. C/S Area of Joint (LHS) = 0.286 mm^2 (Calculated for the geometry shown in the figure above)

c. Total C/S area = 0.639 mm^2

d. Length of Joint = 26.67 mm (Average Measured value for test piece)

e. Volume of joint (both sides) = 17.04 mm^3 = 0.01704 cm^3

f. Mass of joint (m_{fillet}) = 0.046 gm

Energy required for raising the temperature of A3003 mass of assembly:

a. Total A3003 mass (m_{3003})= 4.87 g

b. Melting point of Cladding material (T_m)= 599°C [76]

c. Initial temperature of Sample (T_i)= 24°C

d. Specific heat (Cp) = 902 J/kg°C

e. Heat requirement to raise temperature of A3003 mass of assembly (H_{3003})

$= m_{3003} \times Cp \times (T_m - T_i)$ = 2.53 kJ

Energy required for raising the temperature and melting of A4045 cladding mass of assembly:

a. Total A4045 mass (m_{4045})= 0.195 g

b. Heat requirement to raise temperature of A3003 mass of assembly

= m_{4045} x Cp x (T_m-T_i) = 0.1 kJ

c. Latent heat of fusion for Cladding material (L_f)= 397 J/g [77]

d. Heat required for melting of cladding material (considering melting of entire cladding material – Actual - H_{act}) = m_{4045} x L_f = 0.18 kJ

e. Heat required for melting of cladding material to form the fillet (considering melting of entire cladding material – Theoretical - H_{theo}) = m_{fillet} x L_f = 0.04 kJ

Theoretical minimum Energy required = H_{3003} + H_{theo} = 2.57 kJ

Energy use calculated using experimental data = H_{3003} + H_{act} = 2.71 kJ

Appendix 7: Thermal Images for Experimental CAB Study

Instantaneous snapshots of the thermal imaging for case study are provided herewith for qualitative/visual purposes. Complete set of thermal imaging data is available in the folder “Rahul Thesis Data” stored on the brazing laboratory server. Note that the thermal imaging information was captured for qualitative analysis only, and not for inferring any quantitative information.

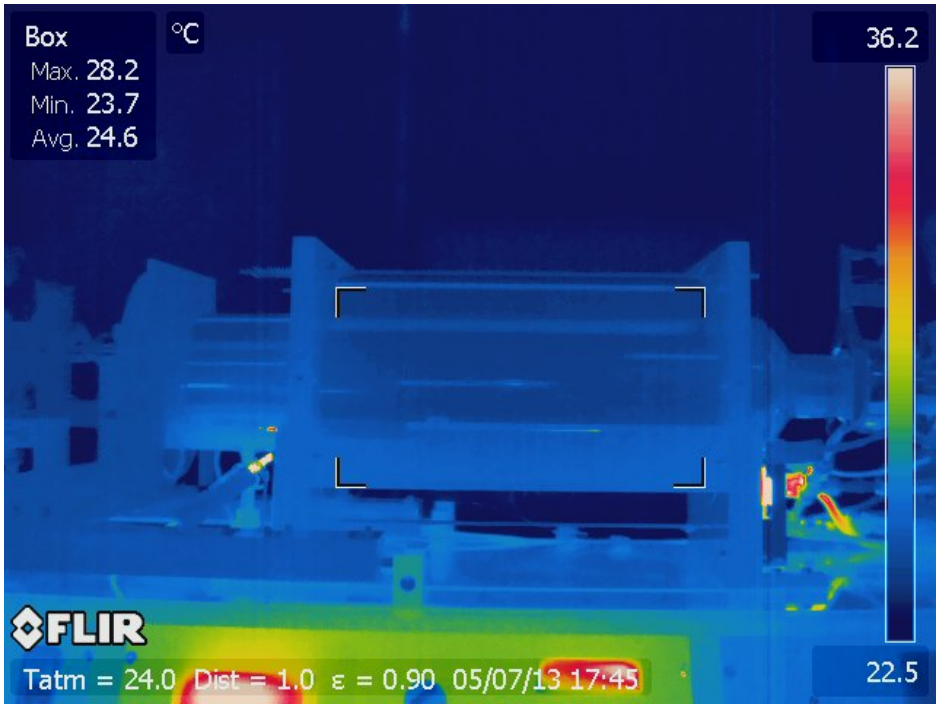

Setup at atmospheric conditions prior to start of experiment

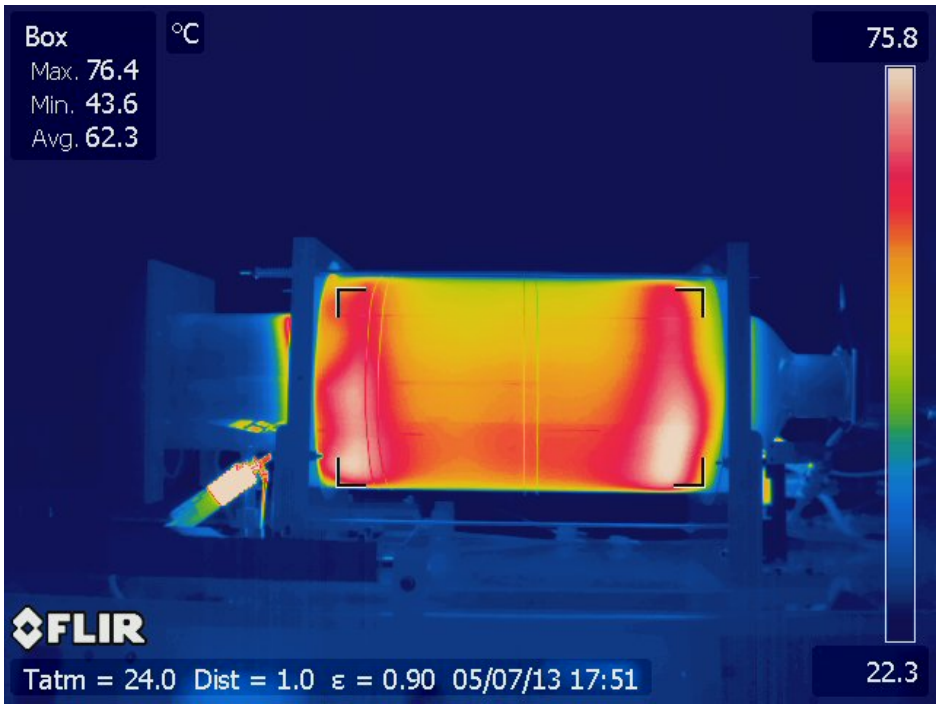

Phase 1 – Ramp up phase to 150°C (instantaneous timestamp)

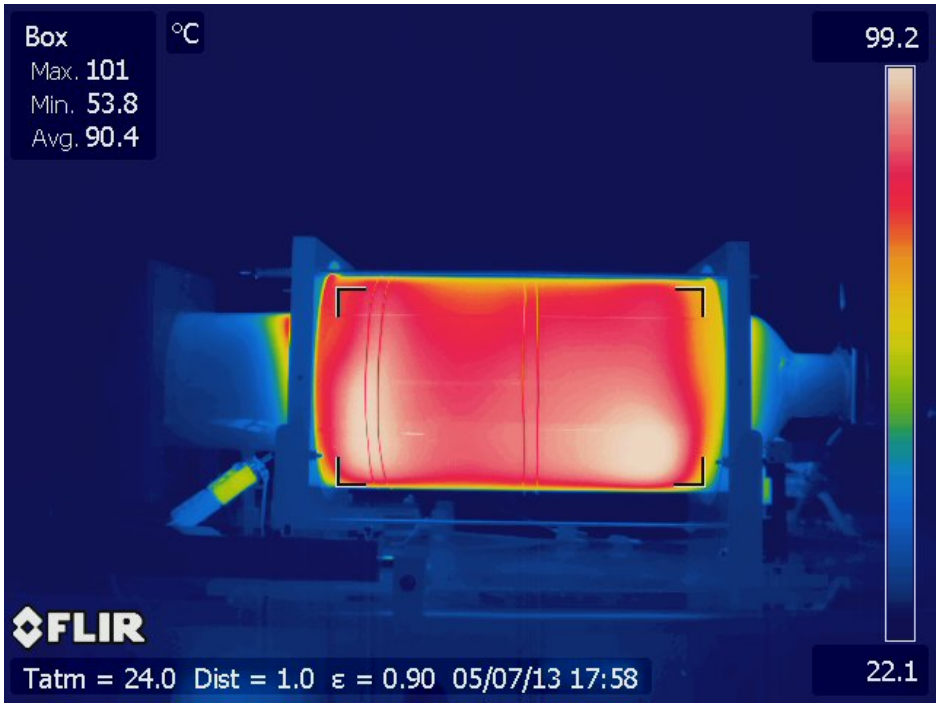

Phase 2 – Hold at 150°C for 30 min

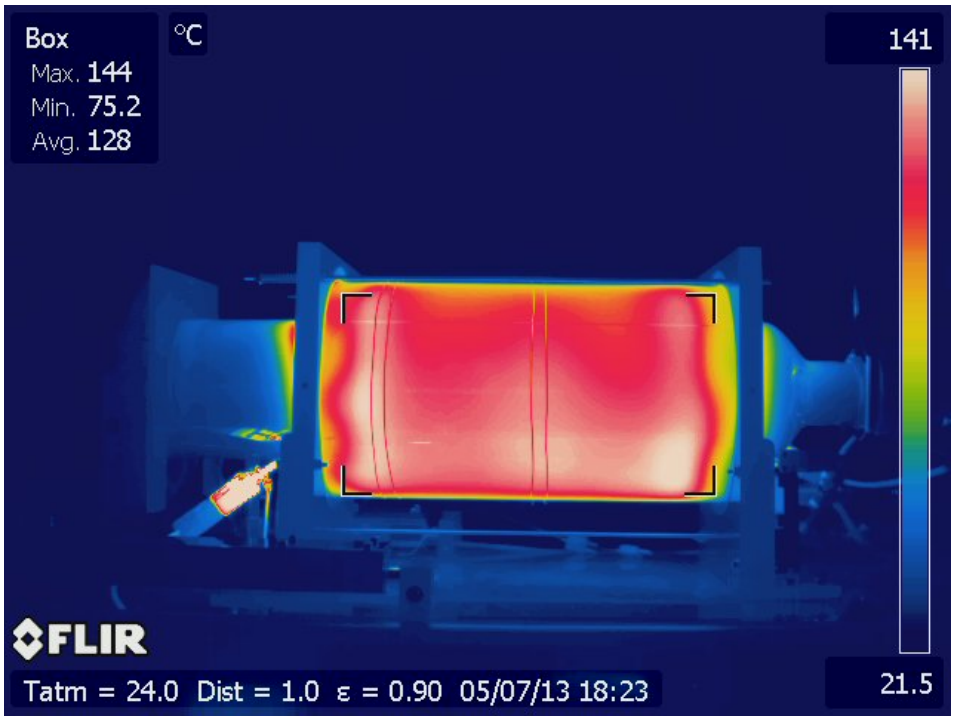

Phase 3 – Ramp up to 600C (Instantaneous timestamp)

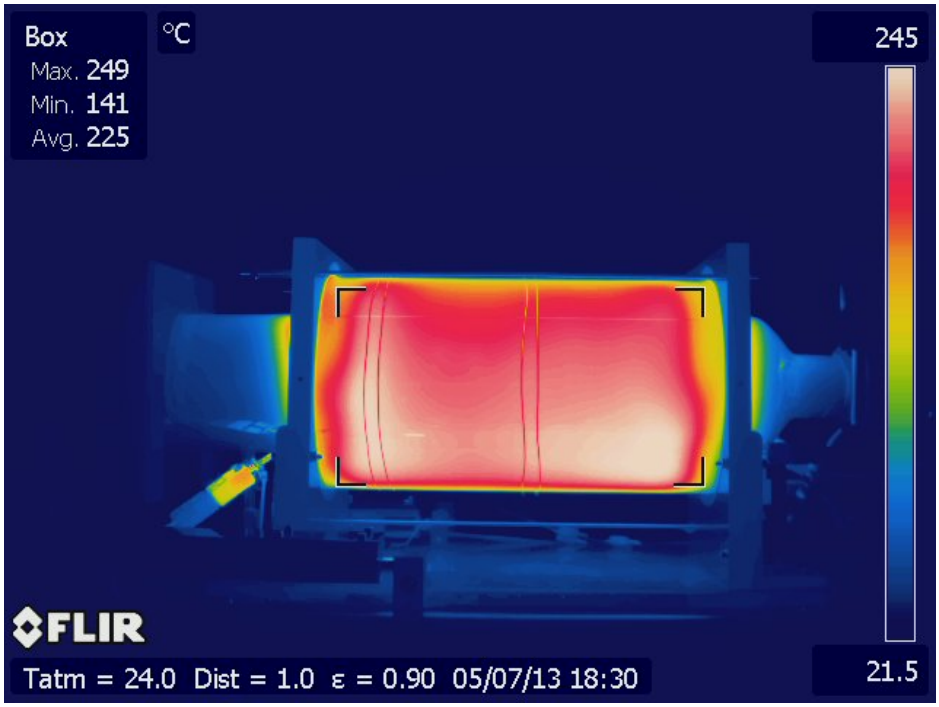

Phase 4 – Ultimate temperature during melting of cladding material

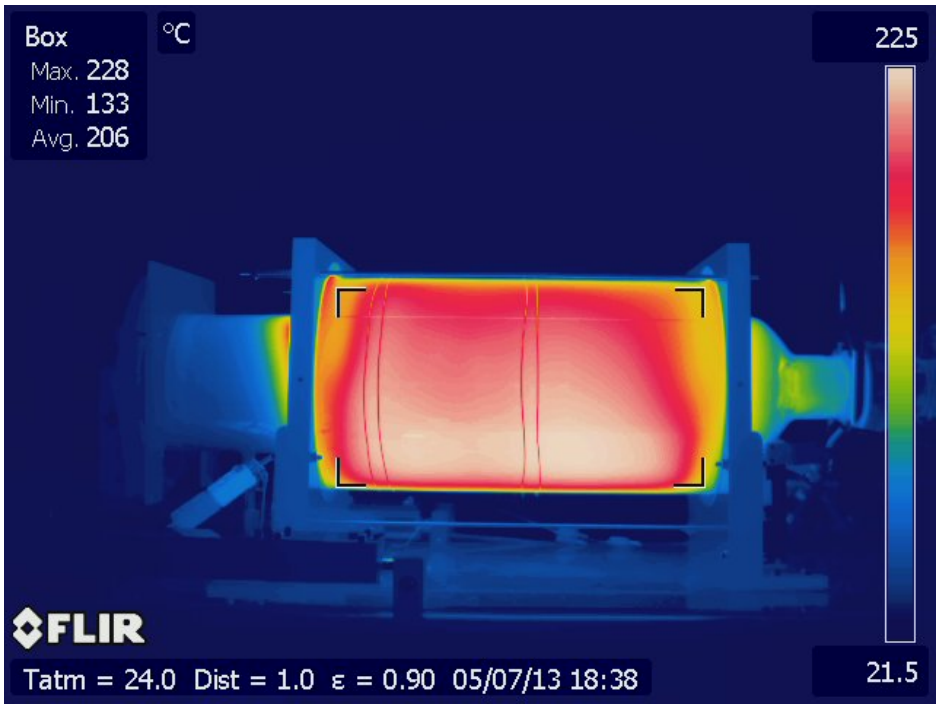

Phase 5 – Rapid quench

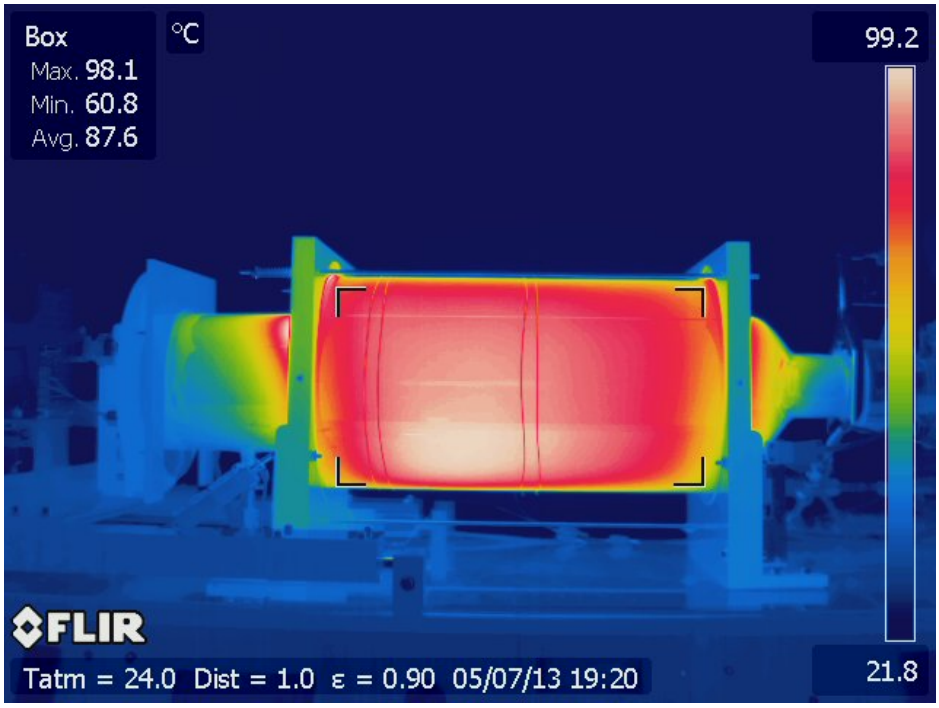

Cooling of setup post experiment

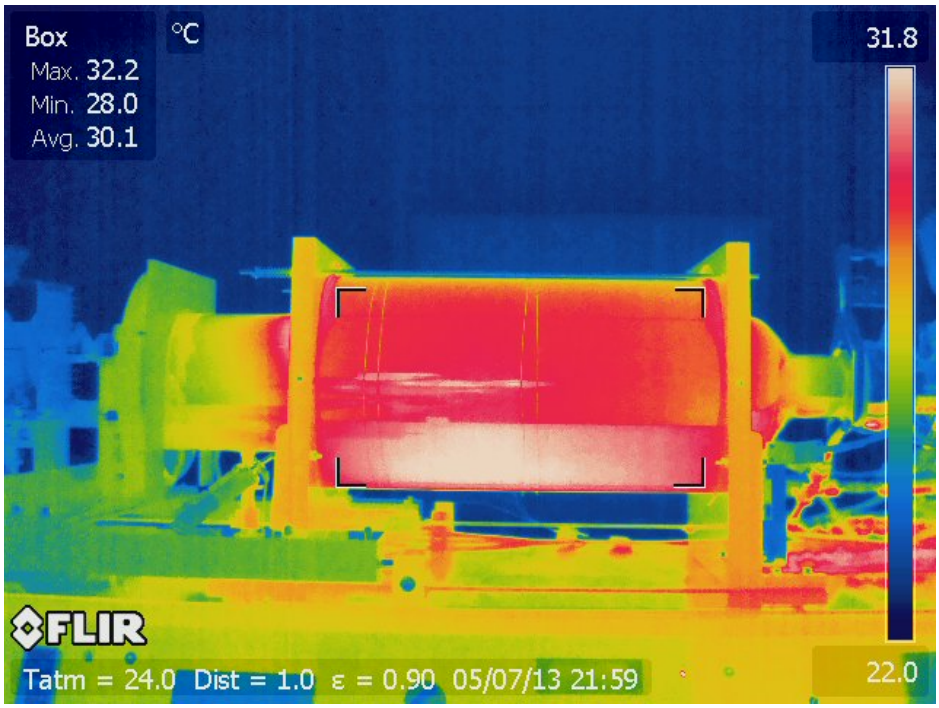

Setup at equilibrium with the surroundings post experiment

REFERENCES

1. Cobb, K., "the price of Oil is rising and may never fall: The Energy Slaves," Le Monde Diplomatique, English version, available at http://mondediplo.com/2006/05/08energyslaves [Accessed February 10 2013]. 2006.
2. Ghomshei Mory, Villecco Francesco ; Energy Metrics and Sustainability. 2009.
3. Ghomshei Mory ; Postmodern Sustainability. International journal of engineering and interdisciplinary mathematics, 2009. **1**: p. 103-106.
4. Global Footprint network - Home page, Available at http://www.footprintnetwork.org/, Accessed on 03/24/2013.
5. United Nations Development Programme - Human Development Reports, Available at http://hdr.undp.org/en/content/human-development-index-hdi.
6. Environmental Performance Index (EPI), Available at http://epi.yale.edu/.
7. “Sekulic, D.P., Personal Communication, University of Kentucky D.P. Sekulic, Editor. 2016: University of Kentucky, Lexington.
8. Brundtland GH; Our common future : report of the World Commission on Environment and Development, ed. E. World Commission on and Development. 1987: Oxford University.
9. Rodriguez Sandra, Roman Matthew, Sturhahn Samantha, Terry Elizabeth; Sustainability Assessment and Reporting for the University of Michigan's Ann Arbor Campus; pp 3-8. 2002, Center for Sustainable Systems.
10. Three Pillars of Sustainability, Available at http://www.thwink.org/sustain/glossary/ThreePillarsOfSustainability.htm#F1, Accessed on 08/18/2015.
11. Uniter Nations Environment Programme, Available at www.unep.org, Accessed on 07/20/2013.
12. United States Environmental Protection Agency, http://www3.epa.gov/, accessed on 07/18/2013.
13. World Trade Organization, available at https://www.wto.org/, accessed on 07/20/2013.
14. Organization for economic co-operation and development, available at http://www.oecd.org/, accessed on 07/21/2013.
15. United Nations, available at http://www.un.org/, accessed on 07/25/2013.
16. Arrow Kenneth, Dasgupta Partha, Goulder Lawrence, Daily Gretchen; Are We Consuming Too Much?; pp 147-172. The Journal of Economic Perspectives, 2004. **18**(3).
17. MacKay David; Sustainable Energy - Without the hot air. 2009, Cambridge, England: UIT.
18. BP Statistical Review of World Energy, pp. 42, Accessed on February 12, 2012, Available at bp.com/statisticalreview. June 2010.
19. IEA Statistical Energy Balance, Accessed on April 16, 2012,Available at https://www.iea.org/statistics/statisticssearch/report/?country=CHINAREG&product=Balances&year=2009. 2009.
20. e!Sankey Software, Available at http://www.e-sankey.com/en/.

21. Gutowski Timothy, Branham Matthew, Dahmus Jeffrey, Jones Alissa, Thiriez Alexandre, Sekulic, Dusan; Thermodynamic analysis of resources used in manufacturing processes; pp 1584-1590. Environmental Science and Technology, 2009. **43**(5).
22. Branham Matthew, Gutowski Timothy, Jones Alissa, Sekulic Dusan; A thermodynamic framework for analyzing and improving manufacturing processes. in 2008 16th IEEE International Symposium on Electronics and the Environment, ISEE, May 19, 2008 - May 22, 2008. 2008. San Francisco, CA, United states: Institute of Electrical and Electronics Engineers Inc.
23. Bakshi Bhavik, Gutowski Timothy, Sekulic Dusan; Thermodynamics and the Destruction of Resources. 2011: Cambridge University Press.
24. Szargut J. , Morris D., and Steward F.; Exergy Analysis of Thermal Chemical and Metallurgical processes. 1988.
25. Sekulic Dusan, An Entropy-based metric for a transformational technology development; pp 133-162, in Thermodynamics and the destruction of resources. 2011, The Cambridge University press.: Cambridge UK.
26. Sekulic Dusan P., Nehete Rahul, Yu Cheng-Nien, Fu Hi; An energy sustainability metric. Energy, 2014. **74**(C).
27. Sekulic Dusan; Advances in Brazing 1ed. 2013, Oxford-Cambridge, UK: Woodhead Publishing.
28. NOCOLOK flux brazing process applications, Solvay Chemicals. 08/12/2013]; Available from: http://www.solvaychemicals.com/EN/products/Fluor/Aluminium_Brazing_Fluxes/Nocolok_Flux_Bindermixture.aspx.
29. Controlled atmosphere aluminum brazing system catalogue - Seco Warwick.
30. The NOCOLOCK Flux Brazing process report, available at http://www.solvay.com/en/binaries/NOCOLOK_Brazing_Process-en-de-179520.pdf, accessed on 01/27/2016.
31. Sankara, Jayashankar; Exergy based method for sustainable energy utilization analysis of a Net Shape Manufacturing system. 2005, University of Kentucky.
32. Renduchintala, A.B., Experimental study and quantification of emmisions in Control Atmosphere Brazing process, in Manufacturing Systems Engineering. 2006, University of Kentucky.
33. Glasby, G.P., Sustainable Development: The need for a new paradigm; pp 333-345. Environment, Development and Sustainability, 2002. **4**.
34. Overgaard, S., Definition of primary and secondary energy. International Recommendation on Energy Statistics (IRES), 2008.
35. EIA Annual Energy Review 2011, available at http://www.eia.gov/totalenergy/data/annual/pdf/aer.pdf,. 2012.
36. World Bank Database; available at http://data.worldbank.org,. [accessed 02/20/2013].
37. Measures of well-being: There is more to it than GDP, Deustsche Bank Research, available athttp://www.dbresearch.com/PROD/DBR_INTERNET_EN-PROD/PROD0000000000202587.pdf, accessed on 01/27/2016. 2006.

38. Costanza Robert , Hart Maureen , Posner Stephen , Talberth John ; Beyond GDP: The need for new measures of Progress. The Pardee Papers, University of Boston, 2009.
39. Jones Charles , Klenow Peter; Beyond GDP? Welfare across Countries and Time. 2015.
40. Genuine Progress Indicator, available at http://rprogress.org/sustainability_indicators/genuine_progress_indicator.htm, accessed on 01/29/2016.
41. Hasan Al-Hilani; HDI as a Measure of Human Development: A Better Index than the Income Approach?; pp 24-28. IOSR Journal of Business and Management, 2012. **2**(5).
42. Social Progress Index, available at http://www.socialprogressimperative.org/data/spi, accessed on 01/28/2016.
43. Happy planet index, available at http://www.happyplanetindex.org/, accessed on 01/29/2016.
44. World Bank Database, CO2 emmisions, Accessed on March 7 2013, Available at http://data.worldbank.org/indicator/NY.GDP.MKTP.CD.
45. Carbon Capture & Sequestration Technologies @ MIT, available at https://sequestration.mit.edu/, accessed on 01/25/2016.
46. Cleveland, C.J., Encyclopedia of Energy. 2005: Elsevier academic press.
47. U.S E.I.A. International Energy Statistics. Accessed on March 7, 2013.
48. World Bank database, GDP per capita (current US$). Accessed on March 7, 2013.
49. HDI (2008) Human Development Indices, UNDP Report. Accessed on April 5, 2013.
50. "Sekulic, D.P., Personal Communication, University of Kentucky D.P. Sekulic, Editor. 2013: University of Kentucky, Lexington.
51. US EIA / Annual energy review 2011 (DOE/EIA-0384(2011), Table 2.1a and 2.2, pp 40, 47. 2011.
52. OICA (International Organization of Motor Vehicle Manufacturers), report available at http://oica.net/category/production-statistics/2010-statistics/. [accessed 20.2.2013].
53. Controlled Atmosphere Brazing Instruction Manual, Centorr Vacuum Industries.
54. Yu, CN, Hawksworth, D, Liu, W, Sekulic, DP; Al brazing under severe alterations of the background atmosphere: A new vs. traditional brazing sheet. Brazing and Soldering 2012, IBSC Proceedings of 5th Intl. Conference, 2012: p. 347.
55. User Manual_Fluke 1735 Power Logger, F. Corporation, Editor. 2006. p. 22.
56. Omega OMEGACLAD XL Thermocouple Probes, available at http://www.omega.com/pptst/KQXL_NQXL.html, accessed on 01/28/2016.
57. National Instruments NI cDAQ-9172 Manual, Available at http://libr2.com/get/national_instruments-ni-cdaq-9172-27755, accessed on 01/28/2016.
58. Renduchintala, A.B., Experimental study and quantification of emmisions in control atmosphere brazing process. 2006, University of Kentucky.

59. Metallographic Sample Preparation and Examination of Brazed Heat Exchangers. 2012 05/13/2013]; Available from: http://www.aluminium-brazing.com/tag/metallurgy/.
60. Table of Emmisivity of Various Surfaces for Infrared Thermometry, Available at http://www-eng.lbl.gov/~dw/projects/DW4229_LHC_detector_analysis/calculations/emissivity2.pdf.
61. World Bank Database, GDP (current US$), Accessed on March 7 2013, Available at http://data.worldbank.org/indicator/NY.GDP.MKTP.CD.
62. Bergman Theodore, Lavine Adrienne, Incropera Frank, Dewitt David; Fundamentals of Heat and Mass Transfer, Seventh Edition, p 613.
63. F.J. McQuillan, J.R.C.a.M.M.Y., Properties of Dry Air at one atmosphere. 1984, University of Waterloo: Waterloo, Ontario.
64. Ceramic Foam Insulation Specifications - Industrial Ceramics; available at http://www.induceramic.com/industrial-ceramic-product/ceramic-foam-insulation, Accessed on March 26 2013.
65. Cengel Yunus and Boles Michael ;Thermodynamics - An Engineering Approach.
66. Purity plus Speciality Gases Specification Sheet, Available at www.purityplusgas.com,.
67. International Alloy Designations and Chemical Composition Limits for Wrought Aluminum and Wrought Aluminum Alloys, T.A. Association, Editor. 2009. p. 4,6.
68. Fluke 1735 Equipment Specifications, Available at http://en-us.fluke.com/products/power-quality-analyzers/fluke-1735-power-quality.html#techspecs.
69. Onset Hobo U 12 data logger specifications, available at http://www.onsetcomp.com/products/data-loggers/u12-012.
70. Onset Hobo U12-014 Thermocouple data logger specifications, avaialble at http://www.onsetcomp.com/products/data-loggers/u12-014.
71. NI 9211 Thermocouple module specifications, available at http://sine.ni.com/nips/cds/view/p/lang/en/nid/208787.
72. NI cDAQ-9174 CompactDAQ 4-slot USB Chassis Specifications, available at http://sine.ni.com/nips/cds/view/p/lang/en/nid/207535.
73. Omega TC-K-NPT U 72 Pipe plug thermocouple specifications, available at http://www.omega.com/pptst/TC-NPT.html.
74. Super OMEGACLAD Thermocouple probes Specifications, available at http://www.omega.com/pptst/KMQXL_NMQXL.html.
75. Material Datasheet for Aluminum 3003-H14, Matweb, available at http://www.matweb.com/search/datasheet.aspx?matguid=09c63ea8e10e4eea8398256801bb8514&ckck=1.
76. Material Datasheet for Aluminum 4045, Matweb, available at http://www.matweb.com/search/datasheet.aspx?matguid=01e63ba5b064416c94eb5f8ed8bbf50c.
77. http://physics.info/heat-latent/.

VITA

Name: Nehete Rahul Yashwant

Education:

- B.E, Mechanical Engineering, University of Pune, India, 2006

Professional Positions Held:

- Deputy Manager, Godrej and Boyce mfg. co. ltd., India, 2006-2011
- Graduate Research Assistant, University of Kentucky, 2012-2013

Educational Institutions attended:

- University of Pune, 2003-2006
- University of Kentucky, 2011-2016

Publications:

- Rahul Nehete, Cheng-Nien Yu, and Dusan P. Sekulic,
  "Limits of Energy Resources Use in Traditional Technological Processes – A General Approach and a Metal Bonding Case Study",
  Proceedings of the International Symposium on Sustainable Systems & Technologies, May 15-17 2013 Cincinnati, OH, USA.
- Rahul Nehete, Cheng-Nien Yu, Hai Fu, and Dusan P. Sekulic,
  "Energy Resource Use: Sustainability Metric of a Manufacturing Process", International Conference on Efficiency, Cost, Optimization, Simulation and Environmental Impact of Energy System, July 16-19 2013 Guilin, China. [Session: Energy and manufacturing: new routes to sustainability, Paper PO12]
- Dusan P. Sekulic, Rahul Nehete, Cheng-Nien Yu, Hai Fu,
  "An energy sustainability metric",
  Energy, v.74, pp.37-44, 2014.